The Thesis Committee for Christopher Hing Lu
Certifies that this is the approved version of the following thesis:

Determination of Fission Product Yields of ^{235}U Using Gamma Ray Spectroscopy

APPROVED BY

SUPERVISING COMMITTEE:

Steven Biegalski, Supervisor

Sheldon Landsberger

Determination of Fission Product Yields of ^{235}U Using Gamma Ray Spectroscopy

by

Christopher Hing Lu, B.S.Phy.

THESIS

Presented to the Faculty of the Graduate School of

The University of Texas at Austin

in Partial Fulfillment

of the Requirements

for the Degree of

MASTER OF SCIENCE IN ENGINEERING

THE UNIVERSITY OF TEXAS AT AUSTIN

December 2012

This work is dedicated to the men and women of the United States Armed Forces who have given some or all of their lives to maintain the freedom that most take for granted.

The LORD bless you and keep you; the LORD make his face to shine on you and be gracious to you; the LORD turn his face toward you and give you peace.

- Numbers 6:24-26

Acknowledgments

As I reflect on the short time I spent in graduate school, I realize that there are many people deserving of recognition for what has ultimately become a Master's Degree in Nuclear and Radiation Engineering.

First and foremost, I wish to acknowledge my God, His Son, the Lord Jesus Christ, and the Holy Spirit, the triune being that has made me all that I am. Without their compassion, their conviction, and their mercy, I would be nothing. Yet, they have loved when I did not deserve it and blessed me with a peace in my most trying times. Without their grace, none of this would have been possible.

> The LORD is righteous in all his ways and kind in all his works. The LORD is near to all who call on him, to all who call on him in truth. He fulfills the desire of those who fear him; he also hears their cry and saves them. The LORD preserves all who love him, but all the wicked he will destroy. My mouth will speak the praise of the LORD, and let all flesh bless his holy name forever and ever.
> **- Psalm 145: 17-21**

I must give thanks to my adviser, Professor Steven Biegalski, for all the technical assistance and funding that he has given. Throughout the time I've been in graduate school, he has shown patience with me and with my work. He always seemed to have an answer or something new to try to get things to work out.

I would also like to acknowledge Professor Sheldon Landsberger for his continued guidance throughout my undergraduate and graduate careers. His professional advice and technical knowledge have been invaluable. He was never one to hold back in correcting, criticizing, and motivating me when I needed it. I cannot thank him enough for that. I also wish to extend my thanks to him for his role as one of my supervising committee members and readers.

I would like to recognize the staff at the Nuclear Engineering Teaching Laboratory: Tracy Tipping, who helped me greatly when it came to the standards used; Mike Whaley, who spent hours acquainting me with OrigenArp; Larry Welch, who always seemed to know why the detectors weren't behaving properly; Dana Judson, who was always on top of administrative matters; and all of the reactor operators who spent more time starting up the reactor and preparing the pneumatic tube for my samples than I spent doing the actual runs. I give thanks to all of them.

I would also like to give thanks to Admiral Bobby Ray Inman, who was willing to take time out of his schedule to provide career counseling and professional advice. He was a great inspiration to me during my final semester.

I must also give many thanks to those who have given immense technical advice, as well as their friendship: Bonnie Canion, Robert Chin, Ph.D., Kenny Dayman, Christie Egnatuk, Ph.D., Alex Fay, Joseph Graham, Steven Horne, Franziska Klingberg, Donald Millsap, Carlos Rios-Perez, and Joshua J. Yi, Ph.D., Esq. Each one provided a unique inspiration, reassurance, and, above all, friendship to me while I've been in graduate school.

Finally, I give my great thanks to my family. To my parents, David and Hazel Lu, my sister, Desiree Alvarado, and to my brothers and sisters in Christ, thank you from the bottom of my heart. Your encouragement, prayers, and confidence in me have kept me going through the many long hours. Thank you for your love.

Christopher H. Lu
December 2012
Austin, Texas

The grace of the Lord Jesus Christ be with all. Amen.

Determination of Fission Product Yields of ^{235}U Using Gamma Ray Spectroscopy

Christopher Hing Lu, M.S.E.
The University of Texas at Austin, 2012

Supervisor: Steven Biegalski

It is important to have a method of experimentally calculating fission product yields. Statistical calculations and simulations produce very large uncertainties. Experimental calculations, depending on the methods used, tend to produce lower uncertainties. This work set up a method to calculate fission product yields using gamma ray spectroscopy. In order to produce a method that was theoretically sound, a simulation was set up using OrigenArp to calculate theoretical concentrations of fission products from the irradiation of natural uranium. From these concentrations, the fission product yields were calculated to verify that they would agree with expected values. Moving forward in the work, the total flux at the point of irradiation, in the pneumatic transfer system, was calculated and determined to be 3.9070E+11 ± 6.9570E+10 $\frac{n}{cm^2 s}$ at 100 kW. Once the flux was calculated, the method for calculating fission product yields was implemented and yields were calculated for 10 fission products. The yields calculated were in very good agreement (within 10.04%) with expected values taken from the ENDF-349 library. This method has strong potential in nuclear forensics as it can provide a means for developing a library of experimentally-determined fission product yields, as well as rapid post-nuclear detonation analysis.

Table of Contents

List of Tables

List of Figures

Chapter 1

Introduction

1.1 Background of Nuclear Terrorism

Terrorists have never been shy about revealing their ambitions to the world. After the attacks on September 11, 2001, the notion of nuclear terrorism has made its way into political debate, particularly when Osama bin Laden received a *fatwa* stating that the use of a nuclear weapon against American civilians would be permissible, nay mandatory, if it stopped United States actions against Muslims [1].

During the Cold War, there was a steady proliferation of fissile material throughout the world, particularly highly enriched uranium (HEU). Since the first critical mass quantities of HEU were created, there has been a theoretical risk of nuclear terrorism or clandestine attack. Terrorist organizations, or even nation states intending to proliferate, would require approximately 50 kilograms of HEU to be able to improvise a nuclear weapon [2]. HEU is of particular concern since many facilities containing HEU, mostly in former Soviet states, are believed to lack adequate security [3]. Since the 1950s, there have been warnings by U.S. national intelligence agencies that have considered the possibility of clandestine transfer of nuclear weapons by foreign nuclear states [2].

Former U.S. Defense Secretaries Robert Gates, Donald Rumsfeld, William Perry, and Robert McNamara, as well as former Vice President Dick Cheney have warned that the risk of a nuclear weapon detonation on U.S. targets is at

50% within the next decade [2]. Current U.S. policy is "to hold fully accountable any state, terrorist group, or other non-state actor that supports or enables terrorist efforts to obtain or use weapons of mass destruction, whether by facilitating, financing, or providing expertise or safe haven for such efforts" [4]. In the extremely unfortunate event that a nuclear device detonation does occur, it is important to swiftly and accurately determine the source of the weapon [5–7]. For this reason, Congress passed the Nuclear Forensics and Attribution Act and several U.S. agencies, national laboratories, and universities have been rapidly expanding their capacities to study and enhance the field of nuclear forensics and hasten the attribution process [2, 5, 8, 9].

1.2 Nuclear Forensics

Nuclear forensics dates back to at least 1949 when high-altitude, airborne debris collected off the coast of China was analyzed to determine that the Soviet Union had, in fact, detonated their first nuclear weapon [10]. This specialized subset of forensic science is the comprehensive analysis and characterization of pre- and post-detonation nuclear and radiological materials, devices, and debris, as well as prompt effects from nuclear detonation [11–13]. The analysis and characterization is used to determine the physical, chemical, elemental, and isotopic characteristics of the nuclear and radiological material in question [14]. The general process is to acquire samples, analyze them, and characterize the signatures by comparing analysis results against samples of known material from reactors, weapons, and enrichment facilities, as well as from medical, academic, commercial, and other facilities that contain such materials, throughout the world [8]. Acquisition and analysis of samples must be completed rapidly (within hours to days) [11, 15]. Nuclear forensics provides the technical and scientific analysis that provides the basis for prevention, mitigation, and attribution of a nuclear or radiological incident [13, 16, 17]. Attribution is the identification of the nature, source, perpetrator, and pathway of a nuclear or radiological attack, whether attempted or realized [13, 18]. Attribution includes the rapid and comprehensive coordination of law enforcement, intelligence, and forensics, along with other relevant information, to evaluate a nuclear adversary's capabilities, resources, supporters, and method of operation [13].

1.2.1 Acquisition

The first step in the nuclear forensics process is to acquire samples. In a predetonation interception of nuclear material, the acquisition process is done through the confiscation of the material itself. The process differs for post-detonation nuclear forensics. Under this constraint, acquisition involves collecting debris in the immediate and downwind regions of the detonation point, as well as samples from the radioactive cloud drifting with the prevailing winds [15]. It is important to note that isotopes will transport through the environment differently, whether they are solid, liquid, or gas [19]. These samples can then be moved through to the next step in the nuclear forensics process [15].

1.2.2 Analysis

When nuclear weapons were first introduced into the world almost 70 years ago, nuclear and radiochemistry techniques were used to characterize nuclear weapons developed by the United States and other countries [15, 20]. The characterization included weapon yield, materials used, and weapon design. These techniques of analyzing samples can still be used today, but those techniques, primarily radiochemical techniques, take weeks to complete [15]. New techniques, such as gamma ray spectroscopy are required to reduce the analysis timeline down to hours or days [15, 21]. In the case of a post-detonation analysis, debris collected will contain fission products representative of the fuel used in the device. Analyzing the sample will provide signatures characteristic to the device that can be compared with those of known samples [15, 22, 23].

1.2.3 Characterization

Comparing the signatures of a device with those of known samples through databases, sample archives, and device modeling allows for the characterization of the device [15, 22]. Characterization of the material provides the material "fingerprint" that allows intelligence agencies to determine the material's origin, production process, and weapon design [24]. The characterization leads to attribution which allows an explosion to be traced back to its originators [15, 25].

Assuming a nuclear device detonation event, following the acquisition, analysis, and characterization method, it should be possible to answer the following questions [15]:

What was the yield?

What was the isotopic composition of the fuel used?

Was the device crude or sophisticated?

Does the debris match that from known weapons tests?

What was the most probable device design, and does it match any existing designs?

What other materials were used in the construction of the device that may suggest a place of origin?

1.3 Importance of Determining Fission Product Yields

Fission products (FPs) are the stable and radioactive isotopes produced by the fission of heavy nuclides, e.g., ^{235}U, ^{239}Pu, etc. Each fissionable isotope contains a unique pattern of FP production that depends on the incident neutron energy, as Figures 1.1 and 1.2 demonstrate [18]. The FP yield is the probability of a particular isotope being formed per thermal neutron fission [26].

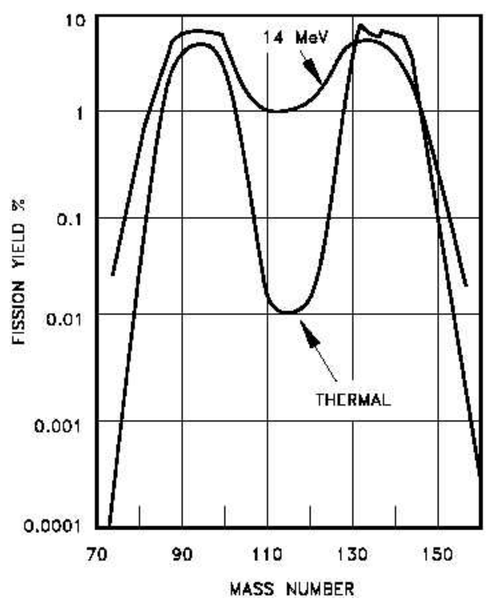

Figure 1.1: The fission product yield curve for ^{235}U with thermal and 14 MeV incident neutrons. Adapted without permission [27].

While all fissile nuclides generally follow similar double-peak curves for thermal neutron-induced fission, yielding the same FPs, the concentrations will vary depending on the fuel used [29, 30]. Therefore, the concentration of a given FP within a sample of fissioned fuel is very unique to the composition of the fuel

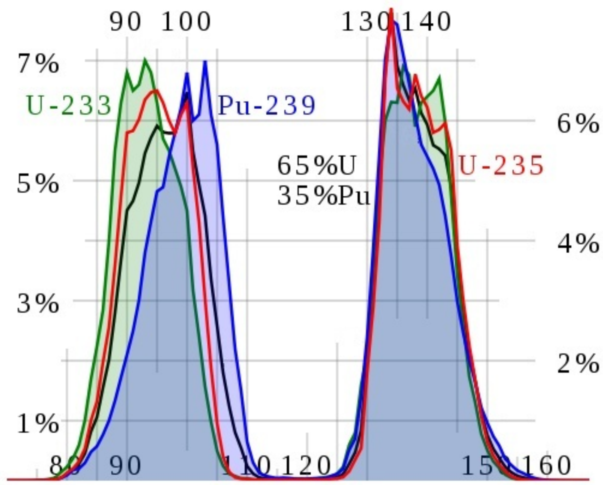

Figure 1.2: The fission product yield curve for various fissile isotopes. Adapted without permission [28].

itself [30]. In other words, determining what FPs and how much of each were produced can give the previously mentioned characteristic "fingerprint" for various properties of the fuel, i.e., age and composition [7, 31]. Previously, during the era of U.S. nuclear testing, it was considered a security concern that classified information could be revealed through the isotopic ratios of released fission products [32].

Many FPs that are produced are far from the line of stability (see Figure 1.3), and generally decay either through beta emission or delayed neutron emission [31]. Upon emission of a beta particle, the daughter nuclide is usually unstable and will emit a gamma ray unique to the particular isotope to stabilize itself [33–35]. Thus, by measuring the gamma rays from a sample, the bulk composition and relative abundances of FPs present can be determined [21]. As FPs undergo beta decay, they set up a decay chain of FPs that follow a general trend of increasing half lives as they approach stability [36]. Gamma ray spectroscopy following irradiation can determine which FPs are present in the sample [37].

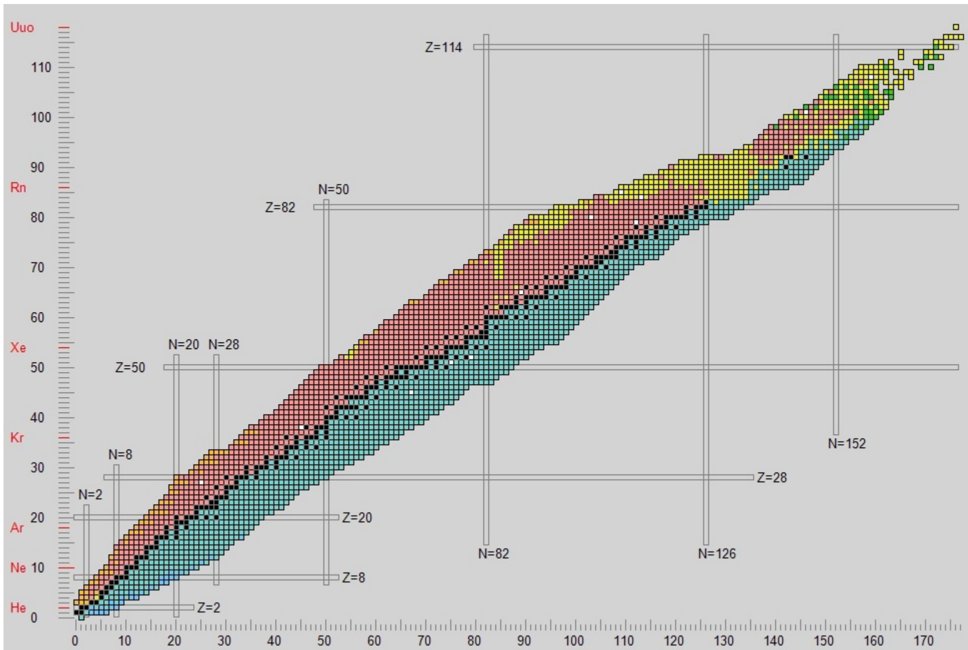

Figure 1.3: Black squares represent stable nuclides. The general trend line that follows the black squares up the chart of nuclides is known as the line of stability. Adapted without permission [38].

Through gamma ray spectroscopy and sample preparation and measurement techniques, a database of empirically-derived FP yields can be developed [10, 16]. Through coordination of databases, ensuring continuity of data, these can be important tools used to attribute the fuel [10, 16, 39]. If this database were to be used, it would be important to have the necessary sample preparation and measurement equipment functioning, calibrated, and ready to use [16]. This work is concerned with measuring the gamma rays associated with those FPs that decay through beta emission using gamma ray spectroscopy.

1.4 Goals of This Work

This work was conducted with the following three goals in mind:

1. To test the theoretical validity of this method of calculating FP yields using OrigenArp.

2. To determine the flux in the pneumatic transfer system of the TRIGA Mark II research reactor at The University of Texas J.J. Pickle Research Campus.

3. To set up a method of determining FP yields by using gamma ray spectroscopy. Calculated FP yields will be compared with the ENDF-349 FP yield library.

Chapter 2

Theory

2.1 Fission

2.1.1 Process

Fission is a process by which a heavy nucleus splits into two or more smaller nuclei. The fission of interest in this work is the thermal fission of ^{235}U. That is, fission induced by neutrons of thermal energy (0.0253 eV) [40].

^{235}U is considered a fissile nuclide, which means a ^{235}U nucleus can fission with any incident neutron energy [40].

2.1.2 Cross-Section

The extent to which a specific reaction will occur when a neutron interacts with a nucleus is known as the cross-section. The cross-section can be thought of as the probability of interaction per effective cross-sectional area of the target nucleus. Thus, the cross-section has units of $\left[\frac{1}{cm^2}\right]$ [40]. In the case of thermal fission of ^{235}U, the target is a ^{235}U nucleus.

2.1.3 FP Yield

Upon fission of ^{235}U, the remaining nuclei formed from the fission are called fission products (FPs). All FPs have a unique probability of being produced from the fission process [30].

Nearly all FPs produced are neutron-rich, and therefore undergo beta decay in an effort to stabilize themselves [41]. That is, a down quark is converted to an up quark through via the weak interaction which results in an electron and electron antineutrino being ejected from the nucleus [33].

2.2 Gamma Ray Interactions

As the FPs undergo beta decay, it is likely that they will decay to an energetic state of the daughter nucleus. Therefore, they will emit one or more gamma rays to bring the daughter nucleus down to the ground state, as Figure 2.1 demonstrates [34, 42]. The energies of these gamma rays tend to be specific to the given nuclide emitting them. These gamma rays can be measured using a high-purity germanium (HPGe) detector [42].

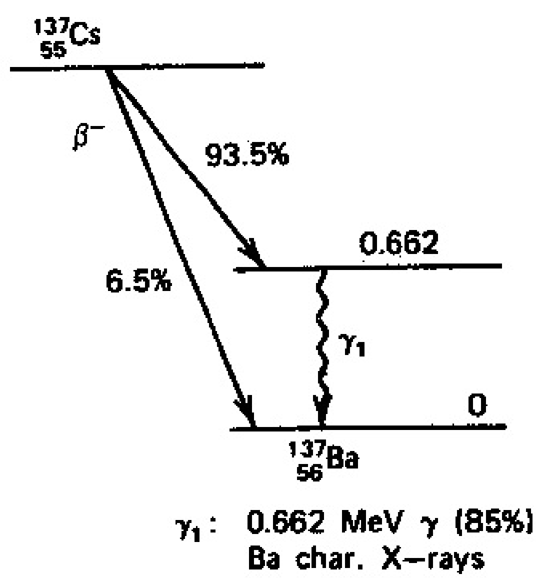

Figure 2.1: A decay scheme that shows the gamma ray emitted following the beta decay of the FP ^{137}Cs. Adapted without permission [34].

2.2.1 Photoelectric Effect

When a photon strikes an electron bound to an atom, that photon may impart all of its energy and momentum to the electron, thus releasing the electron from the atom. The ejected photoelectron has a kinetic energy equal to the energy of the incident photon less the binding energy of the electron. This is known as the photoelectric effect (PEE) [40]. Note that the PEE is dominant at low photon energy in high Z materials, as can be seen in Figure 2.2 [42].

2.2.2 Compton Scattering

When a photon of higher energy strikes an unbound electron, it may undergo an elastic scattering event by which part of the photon energy and momentum is transferred to the electron. The lower energy photon may continue on to undergo another Compton scattering (CS) or PEE event [40]. CS is dominant for moderate energies [42].

2.2.3 Pair Production

When a photon of sufficiently high energy (>1.022 MeV) travels through a Coulomb field (usually that of a nucleus), there is a possibility that the photon will transform into an electron-positron pair, conserving energy and momentum. This is known as pair production (PP). The energy threshold is due to the mass-energy relationship, where the rest-mass energy of one electron or positron is 0.511 MeV [40]. PP is the dominant effect for high energy photons and high Z absorbing materials [42].

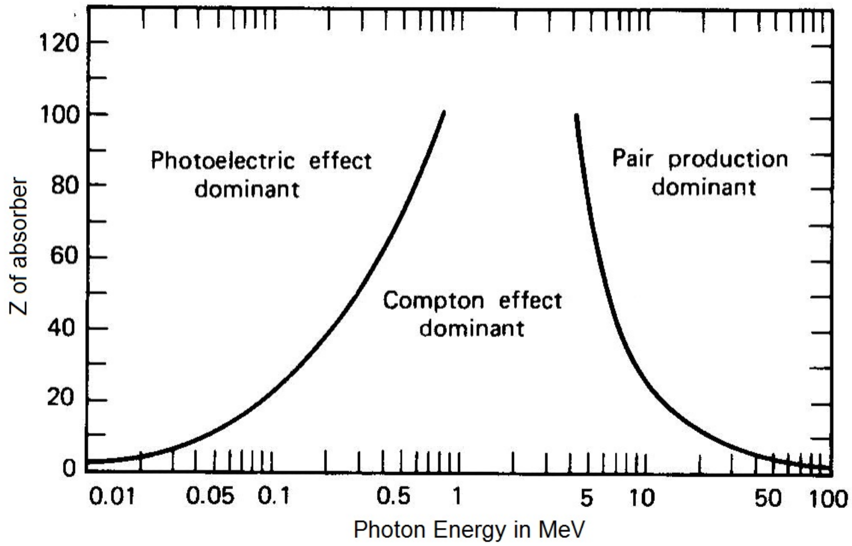

Figure 2.2: A graph that depicts PEE, CS, and PP regions in a material. Note that the energy is the photon energy and the Z is for the absorbing material. Adapted without permission [42].

2.3 High-Purity Germanium Detectors

For this experiment, semiconductor detectors were used, where the detection material is manufactured from ultrapure germanium crystals. These detectors, known as high-purity germanium (HPGe) detectors, have impurity levels as low as $10^9\ \frac{atoms}{cm^3}$. The HPGe detector type was chosen because it has excellent energy resolution [42]. When photons (specifically gamma rays and X-rays) interact with the HPGe crystal, they will undergo PEE, CS, or PP. All of these interactions produce free electrons, also known as charge carriers. When a high voltage is applied across the coaxial configuration of the detector, as shown in Figure 2.3, the charge carriers are accelerated to the electronic system to be counted as a pulse at a given channel. The program used to count these pulses can be calibrated such that each channel will correspond to a particular energy [34, 42].

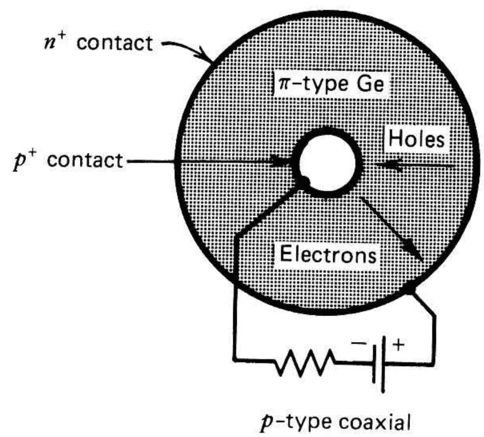

Figure 2.3: A cross-section of the HPGe detector. Adapted without permission [34].

2.3.1 Detector Efficiency

Since gamma rays are emitted from the source isotropically, only a fraction of those emitted will ever reach the detector (see Figure 2.4). The gamma rays that reach the detector must undergo PEE, CS, or PP with the detector before detection is possible. Some gamma rays must travel long distances before they interact. This fact, coupled with geometry restrictions, restrict detectors to often being less than 100% efficient. The absolute efficiency of the detector can be calculated using Equation 2.1. It is necessary to note that the solid angle subtended by the detector from the source position is an implicit factor in the calculation [34].

$$\varepsilon_{abs} = \frac{\text{number of pulses recorded by the detector}}{\text{number of radiation quanta emitted by the source}} \tag{2.1}$$

where ε_{abs} is the absolute efficiency of the detector.

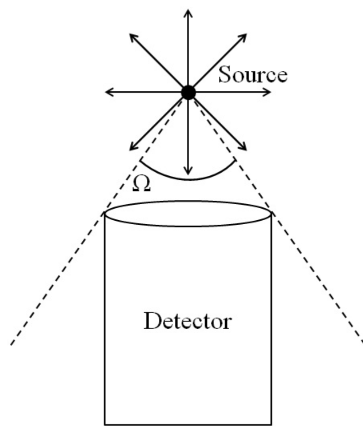

Figure 2.4: The solid angle subtended by the detector.

2.4 Setting up the Problem

2.4.1 Equations for Fission Product Yield Determination

Once spectra are collected, equations can be set up to calculate the FP yields. The following three assumptions and restrictions are used for these calculations:

1. An overwhelming majority of fissions were thermal neutron-induced fission of ^{235}U.
2. Neutron absorption by FPs is negligible.
3. A series of three nuclides in the decay chain and, where appropriate, their respective metastable states are used in this model, as shown in Figure 2.5.

To describe the system during production, the following coupled differential equations are used:

$$\frac{dN_1(t)}{dt} = \phi\sigma_f N_{25}\chi_1 - \lambda_1 N_1(t) \tag{2.2}$$

$$\frac{dN_2(t)}{dt} = \phi\sigma_f N_{25}\chi_2 + \lambda_1 N_1(t) - \lambda_2 N_2(t) \tag{2.3}$$

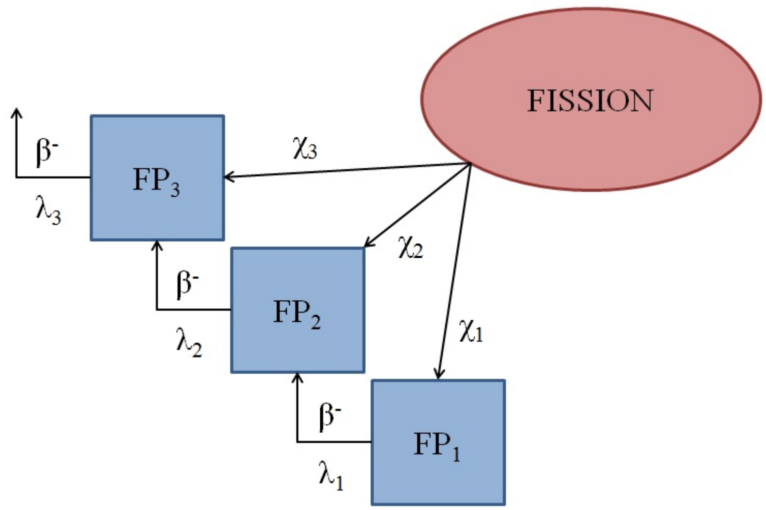

Figure 2.5: A model of the series of three nuclides in a decay chain produced from fission.

$$\frac{dN_3(t)}{dt} = \phi\sigma_f N_{25}\chi_3 + \lambda_2 N_2(t) - \lambda_3 N_3(t) \tag{2.4}$$

where the following apply:

N_1, N_2, N_3 refer to the fission product atom numbers

ϕ is the neutron flux $\left[\frac{n}{cm^2 s}\right]$

σ_f is the cross-section for the thermal fission of ^{235}U

N_{25} is the atom number of ^{235}U in the sample

χ_1, χ_2, χ_3 are the cumulative FP yields

λ_1, λ_2, λ_3 are the decay constants for each FP $[s^{-1}]$

Converting to the LaPlace domain and rearranging to solve for N_1, N_2, N_3, noting that initial concentrations of FPs are 0:

$$N_1(s) = \frac{\phi\sigma_f N_{25}\chi_1}{s(s+\lambda_1)} \tag{2.5}$$

$$N_2(s) = \frac{\phi\sigma_f N_{25}\chi_2}{s(s+\lambda_2)} + \frac{\lambda_1 N_1(s)}{(s+\lambda_2)} \tag{2.6}$$

$$N_3(s) = \frac{\phi\sigma_f N_{25}\chi_3}{s(s+\lambda_3)} + \frac{\lambda_2 N_2(s)}{(s+\lambda_3)} \tag{2.7}$$

Now converting back to the time domain:

$$N_1(t) = \frac{\phi\,\sigma_f N_{25}\chi_1\left(1-\mathrm{e}^{-\lambda_1 t}\right)}{\lambda_1} \tag{2.8}$$

$$\begin{aligned} N_2(t) =& \frac{\phi\,\sigma_f N_{25}}{\lambda_2\left(\lambda_1-\lambda_2\right)}\left(\left(-\chi_2\lambda_1+\chi_2\lambda_2-\lambda_1\chi_1\right)\mathrm{e}^{-\lambda_2 t}-\lambda_2\left(\chi_2+\chi_1\left(1-\mathrm{e}^{-\lambda_1 t}\right)\right)\right) \\ &+\frac{\phi\,\sigma_f N_{25}}{\lambda_2\left(\lambda_1-\lambda_2\right)}\left(\lambda_1\left(\chi_2+\chi_1\right)\right) \end{aligned} \tag{2.9}$$

$$\begin{aligned} N_3(t) =& \frac{\phi\,\sigma_f N_{25}}{\left(\lambda_1-\lambda_3\right)\left(\lambda_1-\lambda_2\right)\left(\lambda_2-\lambda_3\right)\lambda_3}\left(A+B+C\right) \\ A =& \left(-\chi_3\lambda_1\lambda_2+\chi_3\lambda_1\lambda_3-\chi_1\lambda_2\lambda_1+\chi_3\lambda_3\lambda_2+\chi_2\lambda_2\lambda_3-\chi_3\lambda_3^2-\chi_2\lambda_2\lambda_1\right) \\ &\mathrm{e}^{-\lambda_3 t}\left(\lambda_1-\lambda_2\right) \\ B =& \lambda_3\left(\chi_1\lambda_2\left(\lambda_3-\lambda_2\right)\mathrm{e}^{-\lambda_1 t}+\left(\lambda_1-\lambda_3\right)\left(\chi_1\lambda_1-\chi_2\lambda_2+\chi_2\lambda_1\right)\mathrm{e}^{-\lambda_2 t}\right) \\ C =& \left(\chi_1+\chi_2+\chi_3\right)\left(\lambda_1-\lambda_3\right)\left(\lambda_2-\lambda_3\right)\left(\lambda_1-\lambda_2\right) \end{aligned} \tag{2.10}$$

Similarly, after irradiation, the following equations describe the decay of the FPs that have been produced (note that t_i is the irradiation time):

$$\frac{dN_1(t)}{dt} = -\lambda_1 N_1(t) \tag{2.11}$$

$$\frac{dN_2(t)}{dt} = \lambda_1 N_1(t) - \lambda_2 N_2(t) \tag{2.12}$$

$$\frac{dN_3(t)}{dt} = \lambda_2 N_2(t) - \lambda_3 N_3(t) \tag{2.13}$$

Again, converting to the LaPlace domain, rearranging to solve for the concentrations, and converting back to the time domain, the following equations give the FP concentrations as a function of time:

$$N_1(t) = \frac{\phi \sigma_f N_{25}\left(1-\mathrm{e}^{-\lambda_1 ti}\right)\mathrm{e}^{-\lambda_1 t}\chi_1}{\lambda_1} \tag{2.14}$$

$$N_2(t) = \phi\, \sigma_f N_{25}\left(\frac{\left(1-\mathrm{e}^{-\lambda_2 ti}\right)\mathrm{e}^{-\lambda_2 t}\left(\lambda_1\chi_1 - \chi_2\lambda_2 + \chi_2\lambda_1\right)}{\lambda_2\left(\lambda_1-\lambda_2\right)} + \frac{\left(1-\mathrm{e}^{-\lambda_1 ti}\right)\mathrm{e}^{-\lambda_1 t}\chi_1}{\lambda_2-\lambda_1}\right) \tag{2.15}$$

$$\begin{aligned}
N_3(t) =& \frac{\phi\, \sigma_f N_{25}}{\lambda_3}\left(A+B+C\right)\\
A =& \chi_3\mathrm{e}^{-\lambda_3 t}\left(1-\mathrm{e}^{-\lambda_3 t}\right)\\
B =& \frac{\lambda_2\mathrm{e}^{-\lambda_3 t}\left(\lambda_1-\lambda_2\right)\left(\chi_2\lambda_1+\chi_1\lambda_1-\chi_2\lambda_3\right)\left(1-\mathrm{e}^{-\lambda_3 t_i}\right)}{\left(\lambda_1-\lambda_3\right)\left(\lambda_1-\lambda_2\right)\left(\lambda_2-\lambda_3\right)}\\
C =& \frac{\lambda_3\lambda_2\left(\lambda_2-\lambda_3\right)\chi_1\mathrm{e}^{-\lambda_1 t}\left(1-\mathrm{e}^{-\lambda_1 t_i}\right)}{\left(\lambda_1-\lambda_3\right)\left(\lambda_1-\lambda_2\right)\left(\lambda_2-\lambda_3\right)}\\
&+\frac{\lambda_3\left(\lambda_1-\lambda_3\right)\mathrm{e}^{-\lambda_2 t}\left(\chi_2\lambda_2-\chi_2\lambda_1-\chi_1\lambda_1\right)\left(1-\mathrm{e}^{-\lambda_2 t_i}\right)}{\left(\lambda_1-\lambda_3\right)\left(\lambda_1-\lambda_2\right)\left(\lambda_2-\lambda_3\right)}
\end{aligned} \tag{2.16}$$

It is assumed that FPs N_1 and N_2 are too short-lived to measure. Therefore, their FP yields (χ_1 and χ_2) are taken from the ENDF library, leaving FP N_3 as the only one to be measured [43].

The number of decays during an acquisition period can be calculated by integrating the activity ($A = \lambda N$) over the acquisition time (from the end of the decay time, t_d, to the end of the acquisition time, $t_d + t_a$). The decay time is defined as the time after irradiation until the beginning of acquisition.

$$Decays_3(t) = \int_{t_d}^{t_d+t_a} \lambda_3 N_3(t)\,\mathrm{d}t \tag{2.17}$$

The number of counts to be measured by the detector is determined by multiplying the decays by the detector efficiency and gamma ray yield at the particular energy being measured.

$$Counts_3(t) = \varepsilon_3\gamma_3 Decays_3(t) \tag{2.18}$$

Note that the $Decays_3(t)$ term contains the FP yield variable χ_3. Therefore, inserting the detector efficiency (ε_3), gamma ray yield γ_3, and counts at the measured peak energy, Equation 2.18 can be rearranged to solve for χ_3.

2.4.2 Equations for Activation and Neutron Flux Calculation

Knowing the neutron flux at the point of irradiation is vital to the FP yield calculations. In general, a neutron density monitor wire can be used to determine the flux. The National Institute of Standards and Technology (NIST) uses Standard Reference Material (SRM) 953 that is composed of ^{27}Al and ^{59}C [44]. Both of these nuclides, while under irradiation, will undergo radiative capture reactions to produce ^{28}Al and ^{60}Co, respectively. The gamma radiation emitted from both of these products can be measured to determine the neutron flux. The following procedure uses the Al component, but the same procedure can be used with Co to determine the flux.

During irradiation:

$$\frac{dN_{28}}{dt} = \phi\sigma_c N_{27} - \lambda_{28} N_{28}(t) \tag{2.19}$$

where:

N_{27} is the original number of ^{27}Al atoms

N_{28} is the atom number of ^{28}Al

ϕ is the neutron flux $\left[\frac{n}{cm^2 s}\right]$

σ_c is the radiative capture cross-section of ^{27}Al $[cm^2]$ weighted for the flux of the reactor used

λ_{28} is the decay constant of ^{28}Al $[s^{-1}]$

Converting to the LaPlace domain, rearranging to solve for the $N_{28}(s)$, and then converting back to the time domain:

$$N_{28}(t) = \frac{\phi \sigma_c N_{27} \left(1 - \mathrm{e}^{-\lambda_{28} t}\right)}{\lambda_{28}} \tag{2.20}$$

After irradiation, $t = t_i$:

$$N_{28}(0) = \frac{\phi \sigma_c N_{27} \left(1 - \mathrm{e}^{-\lambda_{28} t_i}\right)}{\lambda_{28}} \tag{2.21}$$

$$\frac{dN_{28}(t)}{dt} = -\lambda_{28} N_{28}(t) \tag{2.22}$$

Therefore, at time t, the number of ^{28}Al atoms in the sample are:

$$N_{28}(t) = \frac{\phi \sigma_c N_{27} \left(1 - \mathrm{e}^{-\lambda_{28} t_i}\right) \mathrm{e}^{-\lambda_{28} t}}{\lambda_{28}} \tag{2.23}$$

The decays can be calculated by integrating the activity over the acquisition period:

$$Decays_{28}(t) = \frac{\phi \sigma_c N_{27}}{\lambda_{28}} \left(1 - \mathrm{e}^{-\lambda_{28} t_i}\right) \left(\mathrm{e}^{-\lambda_{28} t_d}\right) \left(1 - \mathrm{e}^{-\lambda_{28} t_a}\right) \tag{2.24}$$

The number of counts can then be calculated:

$$Counts_{28} = \frac{\varepsilon_{28} \gamma_{28} \phi \sigma_c N_{27}}{\lambda_{28}} \left(1 - \mathrm{e}^{-\lambda_{28} t_i}\right) \left(\mathrm{e}^{-\lambda_{28} t_d}\right) \left(1 - \mathrm{e}^{-\lambda_{28} t_a}\right) \tag{2.25}$$

Rearranging and solving for the neutron flux:

$$\phi = \frac{\lambda_{28} Counts_{28}}{\varepsilon_{28} \gamma_{28} \sigma_c N_{27}} \frac{1}{\left(1 - \mathrm{e}^{-\lambda_{28} t_i}\right) \left(\mathrm{e}^{-\lambda_{28} t_d}\right) \left(1 - \mathrm{e}^{-\lambda_{28} t_a}\right)} \tag{2.26}$$

2.5 OrigenArp Analysis

To test the theoretical integrity of this method of experimentation, an analysis was conducted using OrigenArp. A sample pressurized water reactor (PWR) core was simulated in a 14x14 geometry using the composition given in Table 2.1.

Table 2.1: Composition of uranium for analysis using OrigenArp.

Mass (g)	^{234}U Concentration	^{235}U Concentration	^{238}U Concentration	Irradiation Time (s)
0.09988	5.4934E-06	7.1914E-04	9.9155E-02	10

The program was set to simulate irradiation for 10 seconds and decay for 3,000,000 seconds. FP concentrations were reported at the following intervals (in seconds) after irradiation: 0, 0.001, 0.003, 0.01, 0.03, 0.1, 0.3, 1, 3, 10, 30, 100, 150, 300, 750, 1000, 1250, 1500, 3000, 7500, 10000, 12500, 15000, 30000, 75000, 100000, 125000, 150000, 300000, 750000, 1000000, 1250000, 1500000, 3000000. The output of the code gives the mass of each FP nuclide at each given time step. The mass can then be converted to number of atoms using Equation 2.27. From here, the calculations given above can be used to determine the FP yield. This will be explained in more detail in Section 4.1. The OrigenArp code used for this analysis is given in Appendix B.

$$N = \frac{m}{A} N_A \tag{2.27}$$

where the following apply:

N is the number of atoms of a particular nuclide

m is the mass in grams of the nuclide within the sample as given in the output of OrigenArp

A is the atomic mass of the nuclide

N_A is Avogadro's number (6.022E+23 $\frac{atoms}{mole}$).

2.6 Evaluated Nuclear Data File Library

Calculated FP yields will be compared to those given in the Evaluated Nuclear Data File (ENDF)-349 library as compiled by the Lawrence Berkeley National Laboratory. Literature values for cumulative FP yields for nuclides calculated in this experiment are given in Table 2.2. Note that the uncertainties could not be found for these values [43].

Table 2.2: FP yields for nuclides calculated in this experiment [43].

Fission Product	Cumulative Yield
^{95}Zr	0.0650
^{97}Zr	0.0598
^{99}Mo	0.0611
^{103}Ru	0.0303
^{131}I	0.0289
^{140}Ba	0.0621
^{143}Ce	0.0596
^{144}Ce	0.0550
^{145}Pr	0.0393
^{147}Nd	0.0225

Chapter 3

Experiment

3.1 Sample Preparation

A small vial (0.20 cm^3) was cut in half to hold the sample. Samples used were prepared from Certified Reference Material (CRM) 129-A, shown in Figure 3.1. CRM 129-A has a certified composition of 0.72087 ± 0.00039% ^{235}U and 99.27382 ± 0.00039% ^{238}U [45]. 0.1005 grams of CRM 129-A was placed in the small vial and the lid was heat-sealed on, as depicted in Figures 3.2 and 3.3, to prevent FP gases from escaping. The small vial containing the sample was then placed in the center of a medium vial (1.57 cm^3) using halves of a small vial as spacers, shown in Figure 3.4, to center the sample and prevent movement within the vial. The medium vial's lid was then heat-sealed on.

Figure 3.1: CRM 129-A.

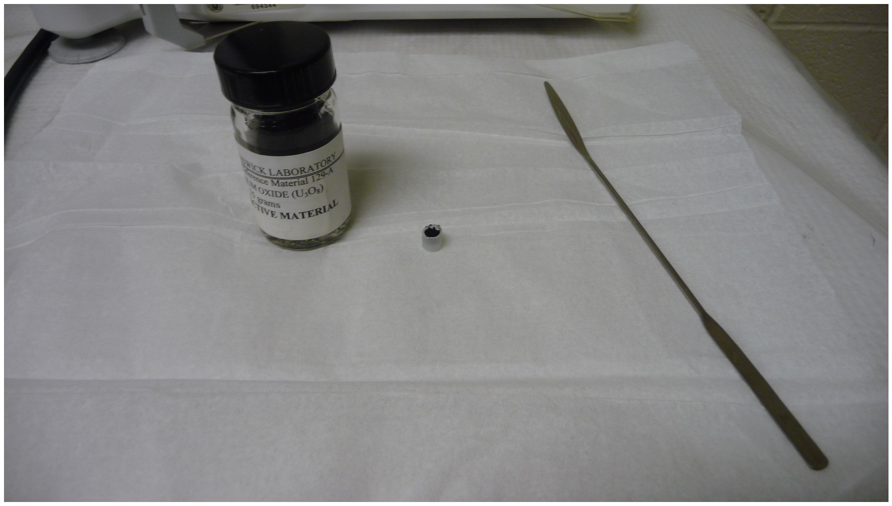

Figure 3.2: A small vial cut in half and filled with 0.1005 g of CRM 129-A.

Figure 3.3: Heat sealing the small vial with CRM 129-A inside.

After heat-sealing the medium vial, the NIST SRM 953 neutron density monitor wire, shown in Figure 3.5, was taped to the outside of the medium vial, shown in Figure 3.6. The composition of the wire was certified to be 99.884±0.002% ^{27}Al and 0.116±0.002% ^{59}Co [44]. Upon irradiation, the ^{27}Al and ^{59}Co will undergo radiative capture reactions to form ^{28}Al and ^{60}Co with half lives of 2.2414 minutes and 1925.1 days, respectively. ^{27}Al can also undergo an

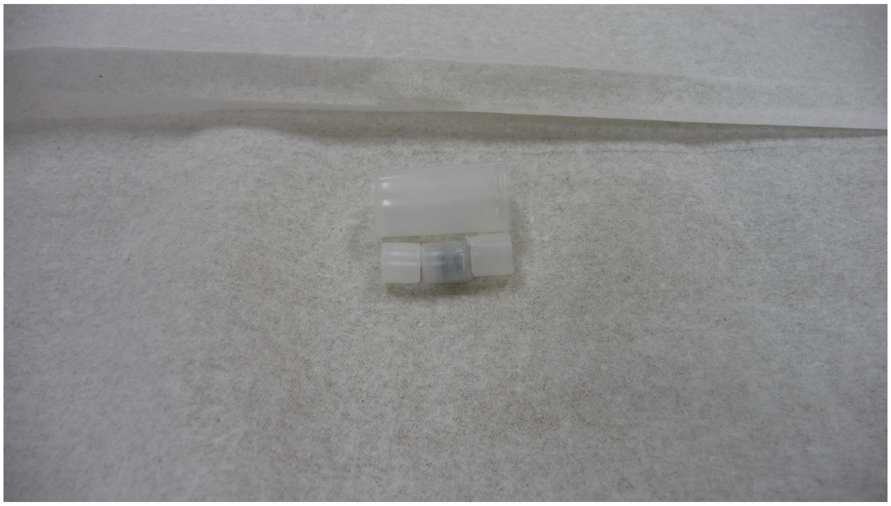

Figure 3.4: Small vial to be placed in the medium vial using halves of another small vial as spacers to center the sample.

(n,α) reaction to produce ^{24}Na with a half life of 14.959 hours [46]. The neutron flux at the point of irradiation can be determined by measuring the activity of to ^{28}Al, ^{60}Co, or ^{24}Na. The wire was measured to be the same length of the small vial containing the sample to be irradiated.

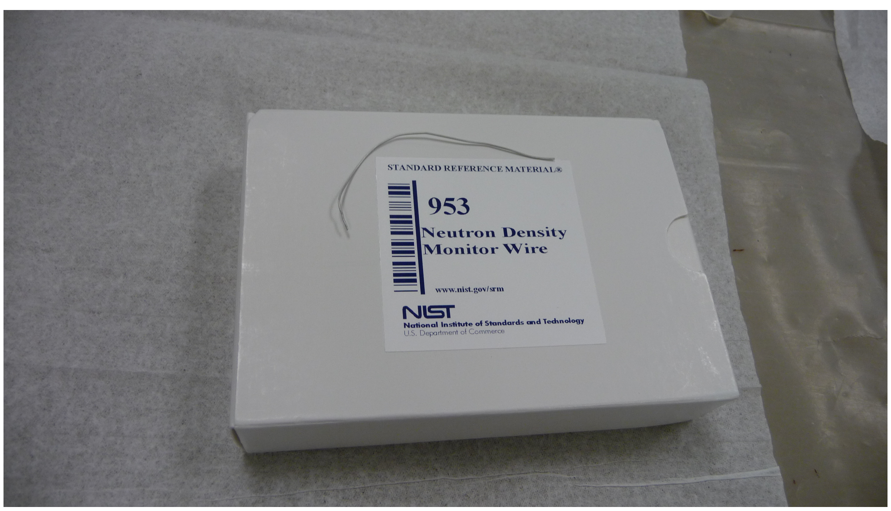

Figure 3.5: The NIST SRM 953 neutron density monitor wire.

The medium vial was then placed in the center of a large vial (8.84 cm^3),

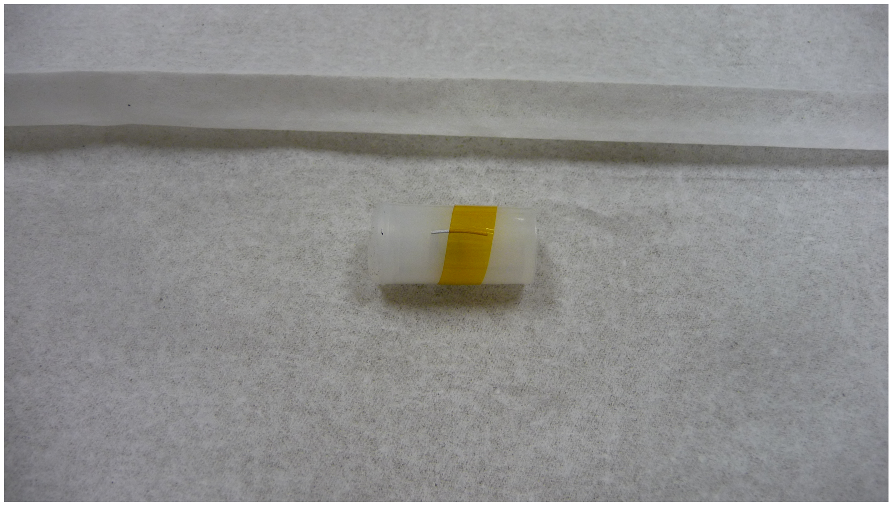

Figure 3.6: SRM 953 taped to the outside of the medium vial.

again using halves of a medium vial as spacers to center the sample and prevent movement inside the vial, shown in Figure 3.7. Table 3.1 gives the specifications for the sample used in this experiment.

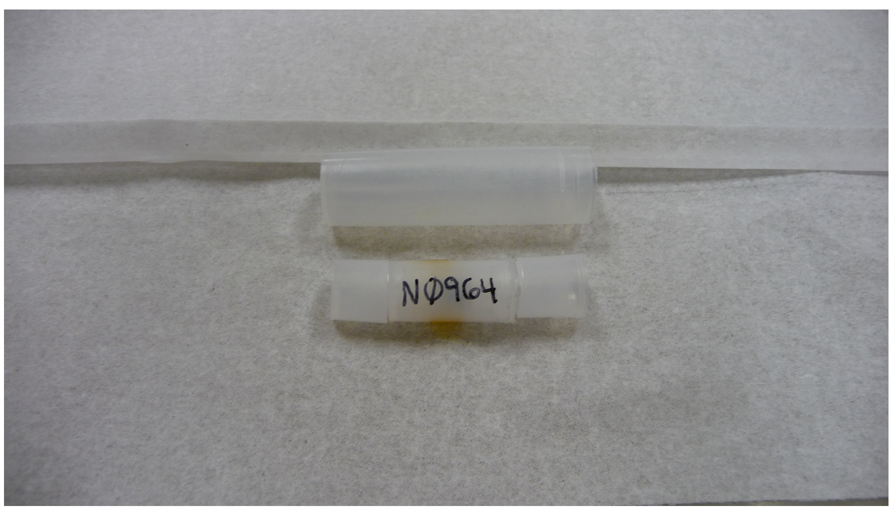

Figure 3.7: Medium vial to be placed in the large vial using halves of another medium vial as spacers to center the sample.

Table 3.1: The mass of CRM 129-A, the mass of ^{235}U, the mass of the SRM 953 flux wire, the mass of ^{27}Al, and the mass of ^{59}Co for the sample [45].

Mass of CRM 129-A (g)	Mass of ^{235}U (g)	Mass of Flux Wire (g)	Mass of ^{27}Al (g)	Mass of ^{59}Co (g)
0.1005 $\pm$ 0.0001	7.245E-04 $\pm$ 8.205E-07	0.00371 $\pm$ 0.00001	0.00371 $\pm$ 9.99E-06	4.30E-06 $\pm$ 7.51E-08

3.2 TRIGA Mark II Research Reactor

The TRIGA Mark II research reactor at The University of Texas at Austin J.J. Pickle Research Campus is a General Atomics-designed research reactor rated to 1 MW. The reactor was designed with in-core irradiation facilities as well as five beam ports [47]. For this experiment, the manual pneumatic transfer system (PNT) was used for in-core irradiation of the sample.

3.3 Counting

Following irradiation, the sample was allowed to decay for about 30 minutes and carried to the detector in a lead container to adhere to the principles of ALARA (As Low As Reasonably Achievable). The sample was then placed on the detector shown in Figure 3.8 at position A (1.0 cm from the face of the detector, Figure 3.9), raised up into the shielding, and then counted in normal mode approximately one, five, and nine days after irradiation. Note that the shielding is present to minimize the background radiation interactions the detector. Table 3.2 shows the acquisition time for each count following irradiation.

The flux wire was counted at position D (9.0 cm from the face of the detector, Figure 3.10) on a separate HPGe detector for five minutes to determine the flux. At Position D, the wire appears as a point source to the detector.

Figure 3.8: The HPGe detector setup.

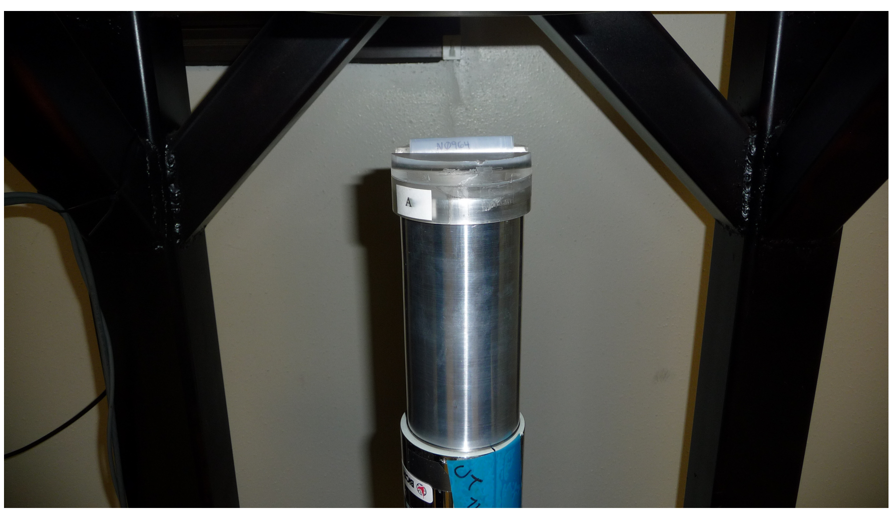

Figure 3.9: Position A on the detector is 1.0 cm from the face of the detector.

Table 3.2: The decay and acquisition times for sample counting.

Decay Time (s)	Acquisition Time (s)
86220	28800
435960	86400
775200	259200

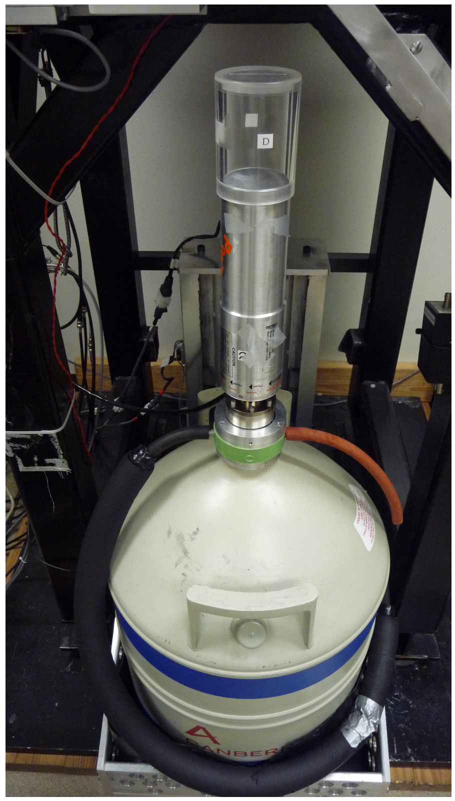

Figure 3.10: Position D on the detector is 9.0 cm from the face of the detector.

The flux was also calculated by normalizing to ^{131}I. The previous method of determining the yield of ^{131}I was used while keeping the flux as an unknown variable, and then back-calculated using the expected FP yield of ^{131}I to determine the flux. The values calculated using the flux wire were inconsistent with the values from normalizing to ^{131}I. Therefore, for the rest of this work, the flux calculated by normalizing to ^{131}I will be used.

3.4 Flux Analysis

To determine the weighted cross-sections of the reactions used in this experiment, a Monte Carlo N-Particle (MCNP) analysis of the PNT was conducted using the MCNP5 code shown in Appendix A. The code simulates the neutron transport in the TRIGA reactor using 1,000,000 neutrons per effective multiplication factor (k_{eff}) cycle for 60 cycles, skipping 10 cycles to let the code converge and initialize the k_{eff} calculation. The output gives the flux per energy bin. The energy bin structure was chosen to match the CINDER'90 63-group cross-sections [48]. Dividing the flux by the width of the energy bin and graphing that against the energy, the flux profile at the point of irradiation in the PNT can be developed, as is demonstrated in Figure 3.11.

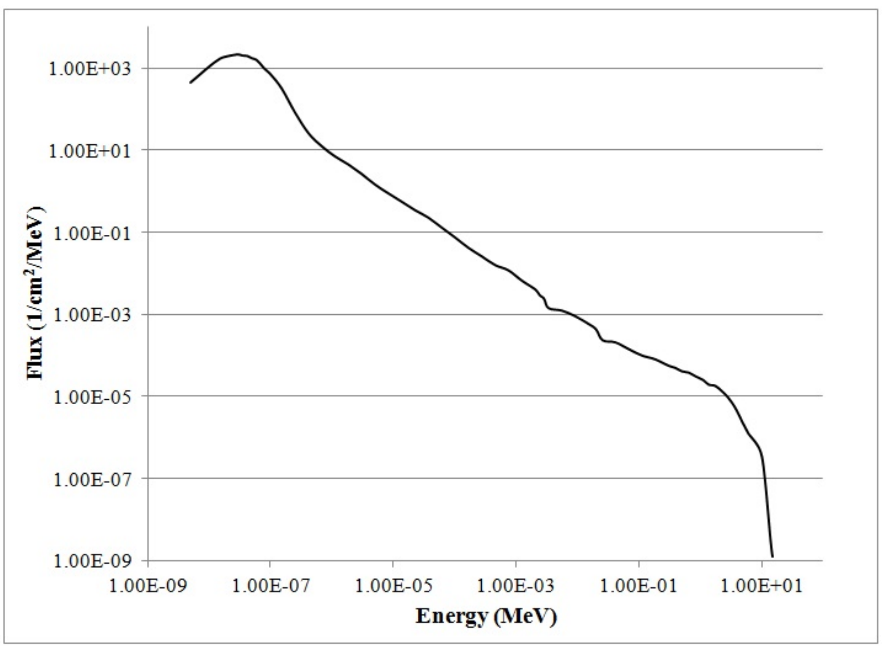

Figure 3.11: Flux profile of the PNT in the TRIGA Mark II reactor.

Once the flux profile has been determined, the weighted cross-section for each reaction can be calculated using Equation 3.1. Table 3.3 gives the weighted cross-sections calculated for each reaction.

$$\bar{\sigma} = \frac{\sum_{i=1}^{63} \phi_i \sigma_i}{\sum_{i=1}^{63} \phi_i} \tag{3.1}$$

where the following apply:

$\bar{\sigma}$ refers to the weighted cross-section for a particular nuclear reaction

ϕ_i is the flux in energy bin i

σ_i is the cross-section in energy bin i

The sums are indexed over the 63 neutron group energy bins given in the CINDER'90 cross-section library [48]

Both total and thermal cross-sections were included for ^{235}U and ^{238}U to prove the first assumption, given in Section 2.4.1, that an overwhelming majority of fissions were from thermal neutron-induced fissions of ^{235}U. The results show that 95.9% of fissions were due to thermal neutron-induced fission of ^{235}U. Note that the total cross-section is the sum of the thermal, epithermal, and fast fission cross-sections.

Table 3.3: The weighted cross-sections for the nuclear reactions used for this work.

Reaction	Weighted Cross-Section (cm^2)
^{27}Al(n,γ)^{28}Al	1.0109E-25
^{59}Co(n,γ)^{60}Co	1.7177E-23
^{235}U(n,f) [Total]	2.7284E-22
^{235}U(n,f) [Thermal]	2.6766E-22
^{238}U(n,f) [Total]	4.75556E-26
^{238}U(n,f) [Thermal]	9.50482E-30

Chapter 4

Results and Discussion

4.1 OrigenArp Analysis

The OrigenArp input, given in Appendix B, was used to analyze the theoretical integrity of this method for multiple nuclides using assumed decay and acquisition times. The analysis was conducted using a simplified mathematical model on the simulated burnup scenario given in Section 2.5 with activation parameters similar to those used in the sample (see Table 2.1). The yield of each nuclide was calculated without considering the effects of their parents and then compared to values given in ENDF-349. Because the model was simplified to only consider the nuclide for which the FP yield was being calculated, the same basic steps given in Section 2.4 were used considering only N_1. Therefore, Equation 4.1 was used to calculate the FP yield of each nuclide. Note that the counts were calculated by inserting Equation 4.2 into Equation 4.3, which simulated counting the sample on a detector. The results of the analysis are given in Appendix C.

$$\chi = \frac{\lambda Counts}{\varepsilon \gamma_1 \phi \sigma_f N_{25} \left(1 - \mathrm{e}^{-\lambda t_i}\right) \left(\mathrm{e}^{\lambda t_d}\right) \left(1 - \mathrm{e}^{-\lambda t_a}\right)} \tag{4.1}$$

where, again, the following apply:

χ is the FP yield

λ is the decay constant

Counts is the number of counts simulated using Equation 4.3

ε is the efficiency of the detector at the decay energy

γ is the gamma ray yield at the decay energy

ϕ is the flux

σ_f is the weighted fission cross-section

N_{25} is the number of ^{235}U atoms

t_i, t_d, and t_a are the irradiation, decay, and acquisition times, respectively

$$Decays = N\left(1 - \mathrm{e}^{-\lambda t_a}\right) \tag{4.2}$$

where N is derived from Equation 2.27.

$$Counts = \varepsilon\gamma Decays \tag{4.3}$$

As can be seen from the results, the validity of the equations given in Chapter 2 hold for many FPs. In fact, since the rest of this work was completed using the more complex model given in Chapter 2, the accuracy of this method is increased for the analysis of the sample. Table 4.1 shows the results of the OrigenArp analysis on the nuclides given in Table 2.2.

There were some limitations in this analysis. When there is a metastable state that is shorter-lived than its ground state, this method of analysis fails for all nuclides further down in the chain. It is uncertain the reasons why other nuclides failed this test.

Table 4.1: Expected cumulative FP yield taken from ENDF library, cumulative yield calculated with OrigenArp results, and ratio of agreement for nuclides calculated in this work.

Nuclide	Expected Cumulative Yield	OrigenArp Cumulative Yield	Ratio Calculated/ Expected
^{95}Zr	0.0650	0.0624	0.9600
^{97}Zr	0.0598	0.0589	0.9849
^{99}Mo	0.0611	0.0605	0.9902
^{103}Ru	0.0303	0.0342	1.1287
^{131}I	0.0289	0.0260	0.8997
^{140}Ba	0.0621	0.0609	0.9807
^{143}Ce	0.0596	0.0574	0.9631
^{145}Pr	0.0393	0.0390	0.9913
^{147}Nd	0.0225	0.0226	1.0044

4.2 Detector Efficiency

To determine the efficiency of the HPGe detectors used to count samples and flux wires, a multi-gamma source was placed on each detector and counted for two hours. The multi-gamma source is composed of 9 nuclides providing 11 distinct gamma ray peaks. The ratio of the count rate as measured by the detector at a given energy with the activity at the time of measurement gives the efficiency of the detector at that particular energy. Tables 4.2 and 4.3 show the gamma rays, their peak energies, their activities at the time of measurement, the number of counts measured, and the detector efficiency at that peak.

Once the efficiencies have been found at multiple energies, an efficiency curve can be created and fitted with a polynomial trendline to develop an equation to estimate the detector efficiency at any energy. Figures 4.1 and 4.3 give the spectra and Figures 4.2 and 4.4 give the efficiency curves for the two detectors used. Equations 4.4 and 4.5 give the efficiency (ε) equations for the detectors used to count the flux wires and FP samples, respectively. Note that $E = LOG(Energy)$.

Table 4.2: Peak energy, activity at time of measurement, counts measured, and detector efficiency for each nuclide in the multi-gamma source on the detector used to count at Position D.

Nuclide	Peak Energy (keV)	Activity at Measurement (Bq)	Counts Under Peak	Detector Efficiency %
^{210}Pb	46.5	441.42 ± 18.10	31605 ± 200	0.99 ± 0.04
^{241}Am	59.5	325.82 ± 11.40	23929 ± 176	1.02 ± 0.04
^{109}Cd	88.0	216.56 ± 10.39	14338 ± 151	0.92 ± 0.05
^{57}Co	122.1	70.97 ± 2.98	4547 ± 105	0.89 ± 0.04
^{139}Ce	165.9	30.39 ± 1.22	1169 ± 62	0.53 ± 0.04
^{113}Sn	391.7	26.56 ± 1.06	774 ± 53	0.41 ± 0.03
^{137}Cs	661.7	285.42 ± 11.70	6039 ± 91	0.29 ± 0.01
^{88}Y	898.0	51.62 ± 2.06	688 ± 41	0.19 ± 0.01
^{60}Co	1173.2	474.44 ± 18.98	6574 ± 91	0.19 ± 0.01
^{60}Co	1332.5	474.52 ± 18.98	6013 ± 84	0.18 ± 0.01
^{88}Y	1836.1	54.69 ± 2.19	503 ± 30	0.13 ± 0.01

Table 4.3: Peak energy, activity at time of measurement, counts measured, and detector efficiency for each nuclide in the multi-gamma source on the detector used to count at Position A.

Nuclide	Peak Energy (keV)	Activity at Measurement (Bq)	Counts Under Peak	Detector Efficiency %
^{210}Pb	46.5	441.09 ± 18.08	310835 ± 610	9.79 ± 0.40
^{241}Am	59.5	325.81 ± 11.40	237228 ± 524	10.11 ± 0.35
^{109}Cd	88.0	213.76 ± 10.26	154747 ± 419	10.05 ± 0.48
^{57}Co	122.1	69.41 ± 2.92	43516 ± 228	8.71 ± 0.37
^{139}Ce	165.9	29.09 ± 1.16	13947 ± 143	6.66 ± 0.27
^{113}Sn	391.7	25.20 ± 1.01	6094 ± 102	3.36 ± 0.15
^{137}Cs	661.7	285.27 ± 11.70	43979 ± 222	2.14 ± 0.09
^{88}Y	898.0	48.79 ± 1.95	5350 ± 103	1.52 ± 0.07
^{60}Co	1173.2	472.95 ± 18.92	42390 ± 215	1.24 ± 0.05
^{60}Co	1332.5	473.04 ± 18.92	38033 ± 199	1.12 ± 0.05
^{88}Y	1836.1	51.68 ± 2.07	3179 ± 60	0.85 ± 0.04

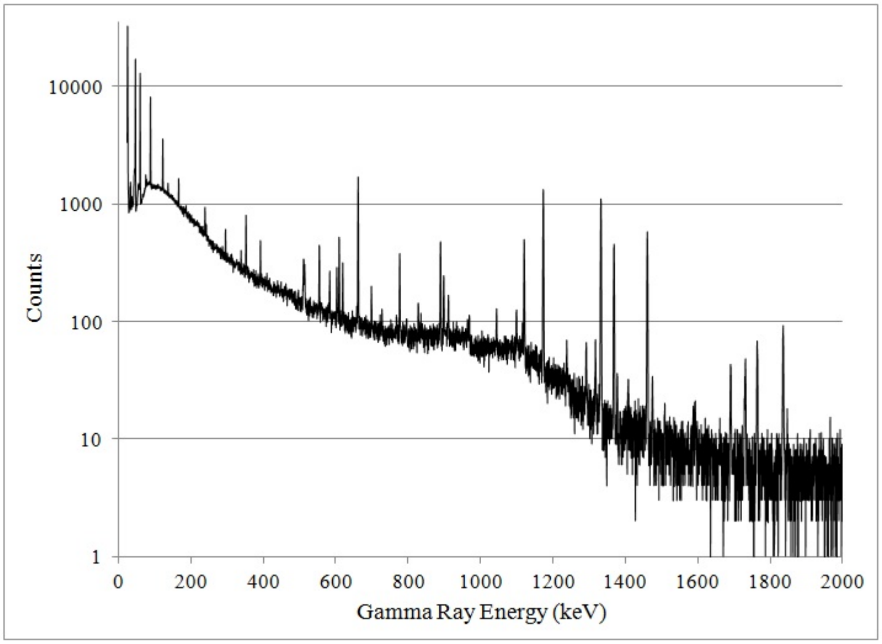

Figure 4.1: Multi-gamma source spectra used to calibrate the efficiency for the detector used to count flux wires at Position D.

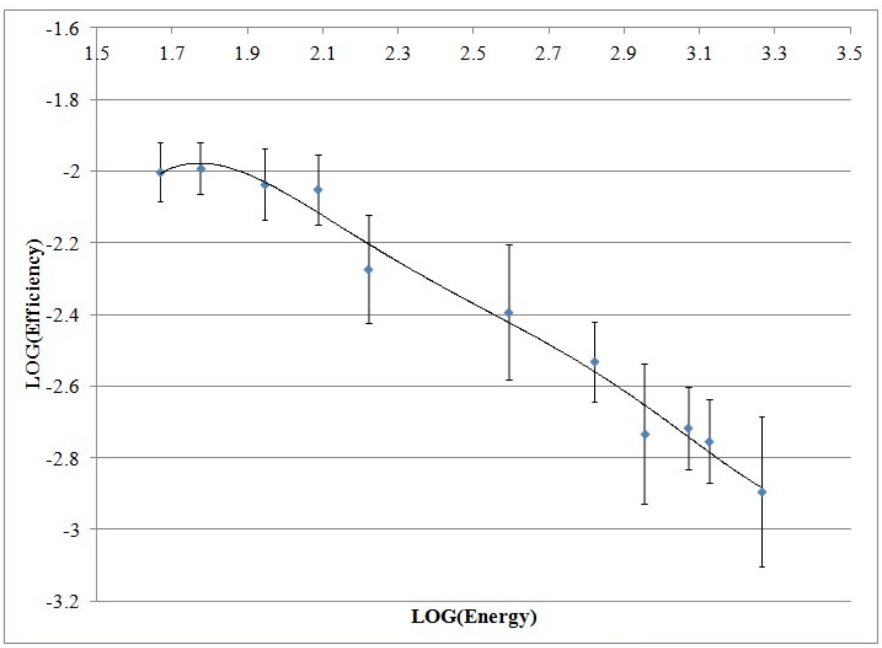

Figure 4.2: Efficiency curve for the detector used to count flux wires at Position D.

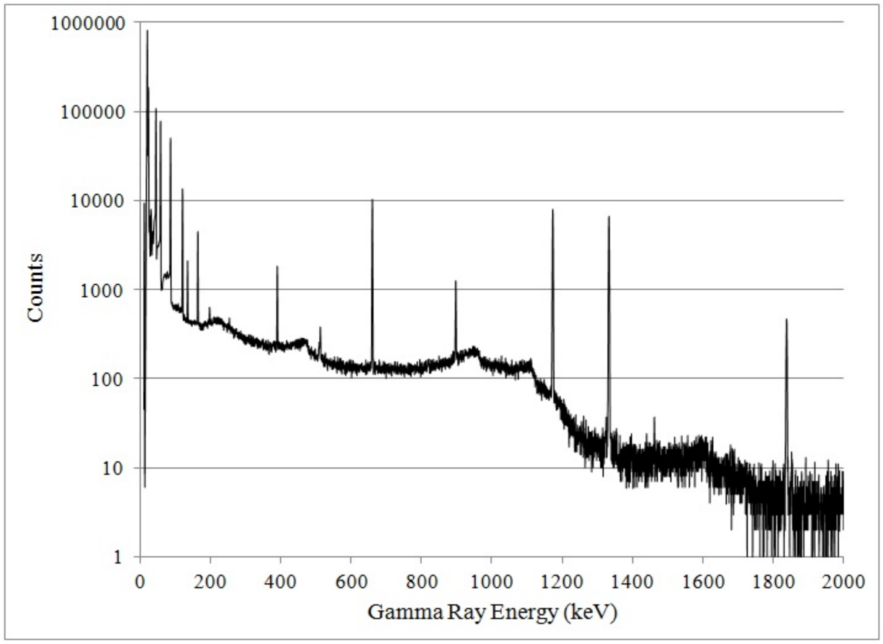

Figure 4.3: Multi-gamma source spectra used to calibrate the efficiency for the detector used to count FP samples at Position A.

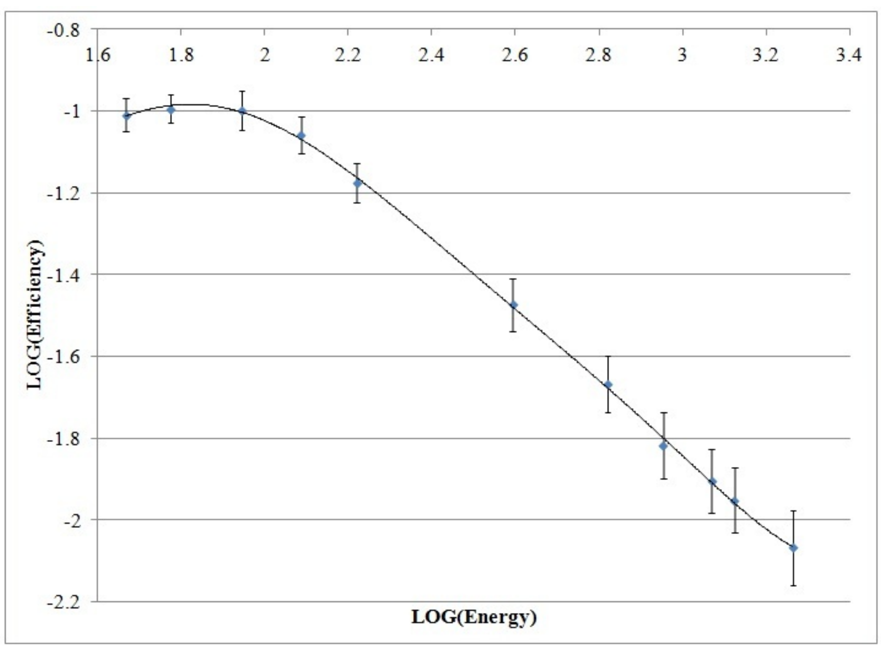

Figure 4.4: Efficiency curve for the detector used to count FP samples at Position A.

$$\varepsilon_{FluxWire} = 10^{1.1331E^5 - 14.219E^4 + 70.506E^3 - 172.73E^2 + 208.62E - 101.16} \tag{4.4}$$

$$\varepsilon_{FP} = 10^{0.5851E^5 - 8.2686E^4 + 46.236E^3 - 128.02E^2 + 174.97E - 96.187} \tag{4.5}$$

4.3 Flux Calculations

As mentioned in the previous chapter, the NIST SRM 953 neutron density monitor wire was used to calculate the neutron flux at the point of irradiation. The weighted cross-section for the radiative capture of ^{27}Al was $\sigma_c = 1.0310 \times 10^{-25}$ cm^2. The gamma ray energy measured was 1778.85 keV, which has a gamma ray yield of $\gamma_{28} = 1.00$. The detector efficiency at this energy was $\varepsilon_{28} = 0.0016674$. Table 4.4 shows the flux calculated for the sample given the spectra in Figure 4.5.

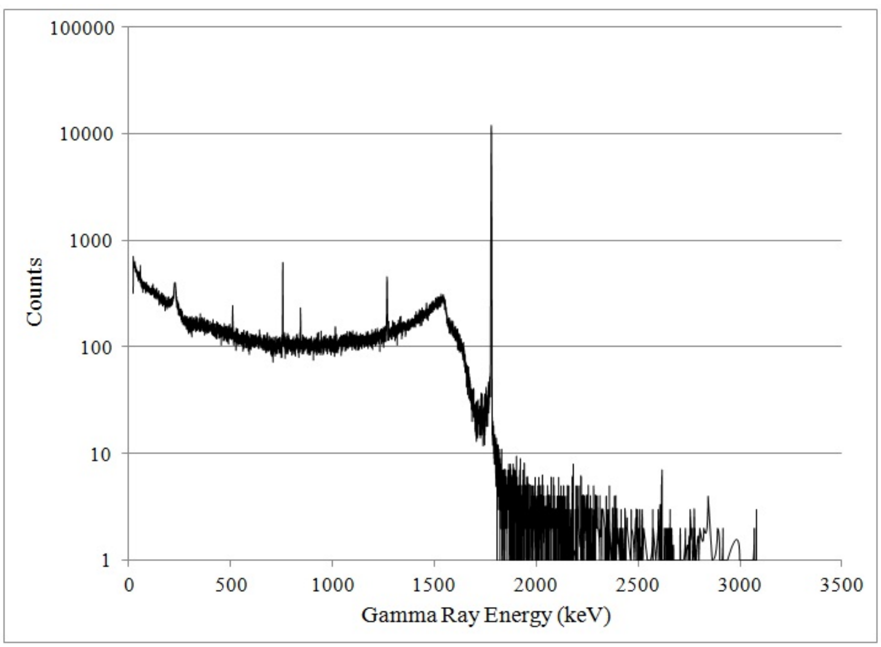

Figure 4.5: ^{28}Al spectra used to calculate the flux at the point of irradiation for the sample.

Table 4.4: Reactor power, irradiation time, decay time, acquisition time, counts measured, and calculated flux for the sample.

Reactor Power (kW)	t_i (s)	t_d (s)	t_a (s)	Counts Under Peak	Flux $\left(\frac{n}{cm^2 s}\right)$
100	10	109	300	78138 ± 285	1.6850E+12 ± 3.0746E+11

The flux to normalize to ^{131}I was calculated to be 3.9070E+11 ± 6.9570E+10 $\frac{n}{cm^2 s}$. This is in line with expected values that were previously calculated for the PNT at the Nuclear Engineering Teaching Laboratory [47]. The Maple™15 worksheet used to perform this calculation can be found in Appendix D. As can be seen from the worksheet, all variables are given, including the FP yield of ^{131}I, while keeping the flux unknown. The calculation was carried out in the same manner as shown in Section 2.4.1; however, rather than calculating the FP yield, the flux was calculated.

It is unclear at this time why the flux wire calculation was approximately four times greater than the normalizing calculation. For the rest of this work, the normalizing flux will be used.

4.4 Fission Product Yield

The normalized flux was inserted into the equations given in the Theory section and FP yields calculated. The spectra given in Figures 4.6, 4.7, and 4.8 were used to determine the counts and their uncertainties for each nuclide in Table 2.2 for decay times of 86220, 435960, and 775200 seconds, respectively. Probabilities of decay to and from a metastable state were taken from the JEFF 3.1.1 nuclear data library [49]. Data used for each FP in the calculations are given in Table 4.5. These data were entered into Maple™15 worksheets to calculate the FP yield of each nuclide using the method prescribed in Chapter 2. These worksheets are given in Appendix D. Table 4.6 gives the calculated cumulative FP yields and their ratio of agreement with expected values from the ENDF library.

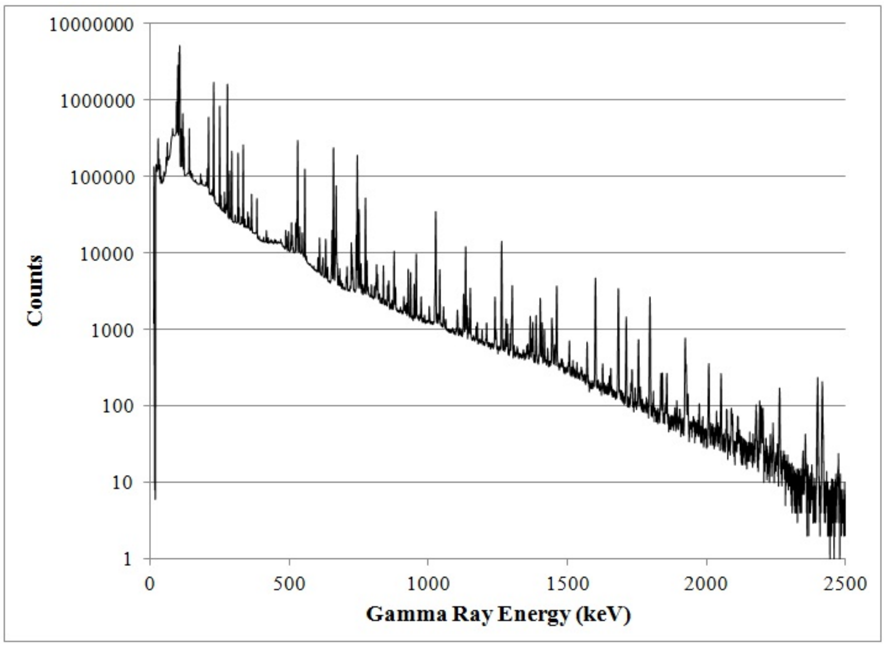

Figure 4.6: The spectra taken from the sample with decay and acquisition times of 86220 and 28800 seconds, respectively.

As can be seen from these data, the FP yields that were calculated align very well with the expected values from the ENDF library. Note that ^{131}I fits the expected value exactly because that is the FP to which the flux was normalized.

4.5 Sources of Error

One of the largest sources of error originated from the MCNP5 analysis. Because of the relatively low number of particles used, errors in the weighted flux per energy bin ranged from 3.12% to 16.77%. The large range of error is due to

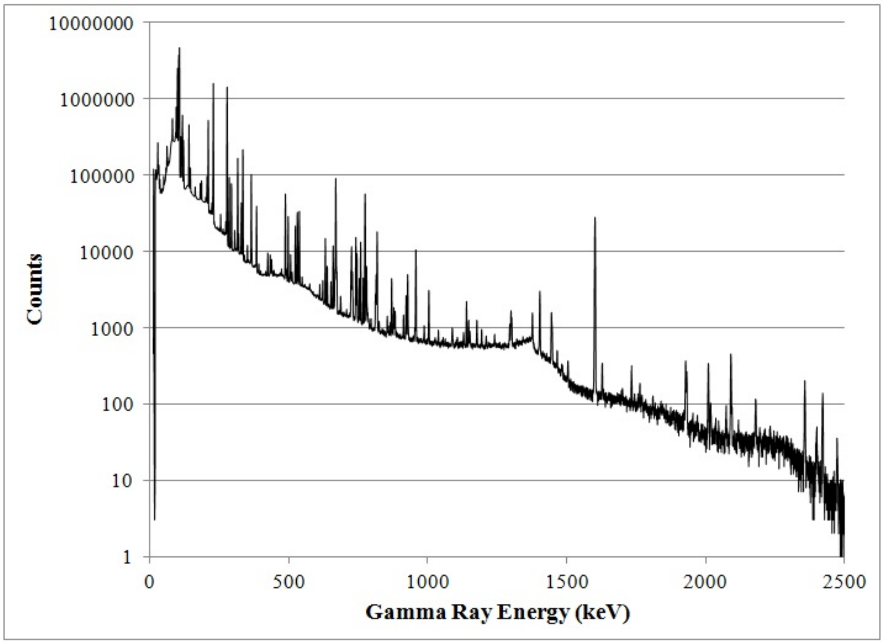

Figure 4.7: The spectra taken from the sample with decay and acquisition times of 435960 and 86400 seconds, respectively.

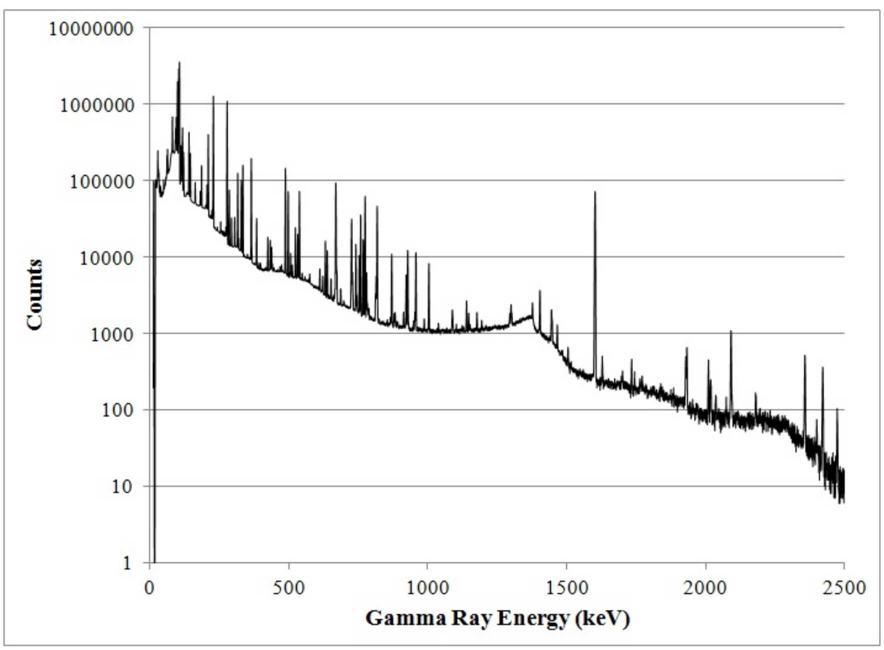

Figure 4.8: The spectra taken from the sample with decay and acquisition times of 775200 and 259200 seconds, respectively.

Table 4.5: Half-life, decay constant, peak energy, efficiency, gamma ray yield, and decay time for FP yield calculations. Note that the acquisition times for each nuclide can be inferred using Table 3.2.

Nuclide	Half-Life (s)	Decay Constant (s^{-1})	Peak Energy (keV)	Efficiency at Peak (%)	Gamma Ray Yield (%)	Decay Time (s)
^{95}Zr	5531328	1.2531E-07	756.7	2.62 ± 0.13	99.81	435960
^{97}Zr	60480	1.1461E-05	743.4	2.68 ± 0.13	98.23	435960
^{99}Mo	237427	2.9194E-06	739.5	2.69 ± 0.13	12.13	775200
^{103}Ru	3392928	2.0429E-07	497.1	3.62 ± 0.17	91.00	435960
^{131}I	694656	9.9783E-07	364.5	4.55 ± 0.22	81.70	86220
^{140}Ba	1101600	6.2922E-07	537.3	3.42 ± 0.16	24.39	86220
^{143}Ce	119232	5.8134E-06	293.3	5.35 ± 0.26	42.80	435960
^{144}Ce	24589440	2.8189E-08	133.5	9.35 ± 0.45	11.09	775200
^{145}Pr	21528	3.2198E-05	121.2	2.67 ± 0.13	52.50	86220
^{147}Nd	948672	7.3065E-07	531.0	3.45 ± 0.17	13.09	775200

Table 4.6: Expected cumulative FP yield taken from ENDF library, calculated cumulative yield, and ratio of agreement for nuclides calculated in this work.

Nuclide	Expected Cumulative Yield	Calculated Cumulative Yield	Ratio Calculated/ Expected
^{95}Zr	0.0650	0.0674 ± 0.0166	1.0364
^{97}Zr	0.0598	0.0637 ± 0.0157	1.0655
^{99}Mo	0.0611	0.0577 ± 0.0142	0.9441
^{103}Ru	0.0303	0.0295 ± 0.0073	0.9750
^{131}I	0.0289	0.0289 ± 0.0071	1.0000
^{140}Ba	0.0621	0.0600 ± 0.0148	0.9654
^{143}Ce	0.0596	0.0574 ± 0.0142	0.9634
^{144}Ce	0.0550	0.0502 ± 0.0127	0.9129
^{145}Pm	0.0393	0.0365 ± 0.0090	0.8996
^{147}Nd	0.0225	0.0365 ± 0.0050	0.9292

the energy bin structure that was chosen. Some energy bins were smaller than others. Therefore, when the MCNP5 code was run, it calculated fewer particles in the smaller energy bins, and, as a result, there is a higher standard error associated with those energy bins. Another source of error came from determining the efficiencies of the detectors used in this work, which can be found in Tables 4.2 and 4.3. This was dependent on both the number of counts for each nuclide in the multi-gamma source and the uncertainty in initial activity given in the calibration of the source, both of which are also given in Tables 4.2 and 4.3. A third source of error stems from the uncertainty in the isotopic composition of the CRM 129-A uranium used in the sample, given in Section 3.1. Finally, there was uncertainty from the calculation of the flux from both the NIST SRM 953 neutron density monitor wire and the normalization to ^{131}I, though it was necessary to produce these errors through propagating other sources of error.

4.5.1 Reducing Error

In order to reduce the error created by the MCNP5 analysis, it would be necessary to increase one or more of the following: the range of the energy bins, the number of particles per cycle, and the number of k_{eff} cycles. This would increase the statistical accuracy of the simulation, thus reducing the error to which the MCNP5 analysis contributed. Increasing the count times for the flux wire and sample would increase the number of counts and reduce the error given by the counting statistics.

Chapter 5

Conclusion

5.1 Summary of Work

During the course of this work, three goals were to be accomplished.

The first goal was to assess the theoretical integrity of determining FP yields via the method given in Chapter 2. This method was validated through analyzing an output given by OrigenArp. A simulated irradiation for 10 seconds of 14x14 PWR fuel with composition similar to that of the physical sample was conducted by OrigenArp. The program output gave the masses of various FPs in grams. From there, the FP yields were calculated through a simplified model using the method provided in Section 4.1. Upon validating the method, the weighted flux of the TRIGA Mark II reactor at the point of irradiation needed to be determined.

Before the flux could be calculated for the point of irradiation, it was necessary to determine the weighted radiative capture cross-sections for ^{27}Al and ^{59}Co, as well as the total and thermal fission cross-sections for ^{235}U and ^{238}U. This was done by developing the neutron flux profile using the MCNP5 code with an input deck that simulated the neutron flux at the PNT in the reactor. After the cross-sections were calculated, the total flux was calculated using a flux wire and also by normalizing to the FP yield of ^{131}I. These values were inconsistent with one another; therefore, the rest of the work was completed using the flux normalized to ^{131}I. This accomplished the second goal. At that time, the FP yields could be calculated.

The normalized flux along with other parameters were used with the method given in Chapter 2, and FP yields were calculated after decay times of approximately 1, 5, and 9 days. Of the FPs used in this work, the yields were all within 10.04% of the expected values from the ENDF library. This completed the third goal of setting up a method of determining FP yields using gamma ray spectroscopy.

5.2 Suggestions for Further Work

It would be necessary to conduct an in-depth study to develop an empirical flux profile of the TRIGA Mark II reactor at the PNT. This would allow calculation of the flux at the point of sample irradiation without normalizing to a FP within the sample itself. With the newly determined flux, more FP yields can be calculated using this method. It is important to note that this work set up the method of determining FP yields using gamma ray spectroscopy and proved its viability. More studies must be done to determine the yields of more FPs, particularly those that are shorter-lived.

Appendices

Appendix A

MCNP5 Input Deck

The following MCNP5 input deck was used to analyze the flux at the point of irradiation in the PNT to provide a means for determining the flux-weighted cross-sections for ^{27}Al, ^{59}Co, ^{235}U, and ^{238}U.

```
-------------- UT-TRIGA - Core Model - 12/16/2011 --------------
c
c    Coordinate origin on core axis at core midplane
c    - Experiment tubes, empty beam ports, empty RSR
c    - Central thimble fixed and flooded with no sample
c    - Core fully fuelled
c  Edited on 10/01/2012 by Christopher Lu to analyze
c  flux at PNT
c
c -------------------------------------------------------------
c             Beginning of Cell Card Specification
c -------------------------------------------------------------
c -----------
c Core region
c -----------
1099  1  -1.0  -202  +206
               -231  +232  -233  +234  -235  +236
               -241  +242  -243  +244  -245  +246
             +5000 +5001 +5002 +5003 +5004 +5005 +5006 +5007 +5008 +5009
             +5010 +5011 +5012 +5013 +5014 +5015 +5016 +5017 +5018 +5019
             +5020 +5021 +5022 +5023 +5024 +5025 +5026 +5027 +5028 +5029
             +5030 +5031 +5032 +5033 +5034 +5035 +5036 +5037 +5038 +5039
             +5040 +5041 +5042 +5043 +5044 +5045 +5046       +5048 +5049
             +5050 +5051 +5052 +5053 +5054 +5055 +5056 +5057 +5058 +5059
             +5060 +5061 +5062 +5063 +5064 +5065 +5066 +5067 +5068 +5069
             +5070 +5071 +5072             +5075 +5076 +5077 +5078 +5079
             +5080 +5081 +5082 +5083 +5084 +5085 +5086 +5087 +5088 +5089
             +5090 +5091 +5092 +5093 +5094 +5095 +5096 +5097 +5098 +5099
             +5100       +5102 +5103 +5104 +5105 +5106 +5107 +5108 +5109
             +5110       +5112 +5113 +5114             +5117       +5119
             +5120
             +1963 +1964 +1965  +1966                   $ Mapping experiment
             +1940                                      $ 3L
             +2000 +2001 +2002 +2003 +2004 +2005 +2006
             +5118                                      $ PNT
c
 520   0   -201 +207 -1963  fill=101 (10) $         Flux mapping water cells
 521   0   -201 +207 -1964  fill=101 (11)
 522   0   -201 +207 -1965  fill=101 (12)
 523   0   -201 +207 -1966  fill=101 (13)
c
 600   0   -110 +120 -5000  fill=82 (100) $ A1 - CT
 601   0   -110 +120 -5001  fill=8  (101) $ B1
 602   0   -110 +120 -5002  fill=8  (102) $ B2
 603   0   -110 +120 -5003  fill=8  (103) $ B3
 604   0   -110 +120 -5004  fill=8  (104) $ B4
 605   0   -110 +120 -5005  fill=8  (105) $ B5
 606   0   -110 +120 -5006  fill=8  (106) $ B6
 607   0   -110 +120 -5007  fill=7  (107) $ C1 - CR(T)
 608   0   -110 +120 -5008  fill=8  (108) $ C2
 609   0   -110 +120 -5009  fill=8  (109) $ C3
 610   0   -110 +120 -5010  fill=8  (110) $ C4
 611   0   -110 +120 -5011  fill=8  (111) $ C5
 612   0   -110 +120 -5012  fill=8  (112) $ C6
 613   0   -110 +120 -5013  fill=9  (113) $ C7 - CR(R)
```

```
 614   0   -110 +120 -5014  fill=8  (114) $ C8
 615   0   -110 +120 -5015  fill=8  (115) $ C9
 616   0   -110 +120 -5016  fill=8  (116) $ C10
 617   0   -110 +120 -5017  fill=8  (117) $ C11
 618   0   -110 +120 -5018  fill=8  (118) $ C12
 619   0   -110 +120 -5019  fill=8  (119) $ D1
 620   0   -110 +120 -5020  fill=8  (120) $ D2
 621   0   -110 +120 -5021  fill=8  (121) $ D3
 622   0   -110 +120 -5022  fill=8  (122) $ D4
 623   0   -110 +120 -5023  fill=8  (123) $ D5
 624   0   -110 +120 -5024  fill=9  (124) $ D6 - CR(S1)
 625   0   -110 +120 -5025  fill=8  (125) $ D7
 626   0   -110 +120 -5026  fill=8  (126) $ D8
 627   0   -110 +120 -5027  fill=8  (127) $ D9
 628   0   -110 +120 -5028  fill=8  (128) $ D10
 629   0   -110 +120 -5029  fill=8  (129) $ D11
 630   0   -110 +120 -5030  fill=8  (130) $ D12
 631   0   -110 +120 -5031  fill=8  (131) $ D13
 632   0   -110 +120 -5032  fill=9  (132) $ D14 - CR(S2)
 633   0   -110 +120 -5033  fill=8  (133) $ D15
 634   0   -110 +120 -5034  fill=8  (134) $ D16
 635   0   -110 +120 -5035  fill=8  (135) $ D17
 636   0   -110 +120 -5036  fill=8  (136) $ D18
 637   0   -110 +120 -5037  fill=8  (137) $ E1
 638   0   -110 +120 -5038  fill=8  (138) $ E2
 639   0   -110 +120 -5039  fill=8  (139) $ E3
 640   0   -110 +120 -5040  fill=8  (140) $ E4
 641   0   -110 +120 -5041  fill=8  (141) $ E5
 642   0   -110 +120 -5042  fill=8  (142) $ E6
 643   0   -110 +120 -5043  fill=8  (143) $ E7
 644   0   -110 +120 -5044  fill=8  (144) $ E8
 645   0   -110 +120 -5045  fill=8  (145) $ E9
 646   0   -110 +120 -5046  fill=8  (146) $ E10
c 647   0   -110 +120 -5047  fill=8  (147) $ E11 - 3L
 648   0   -110 +120 -5048  fill=8  (148) $ E12
 649   0   -110 +120 -5049  fill=8  (149) $ E13
 650   0   -110 +120 -5050  fill=8  (150) $ E14
 651   0   -110 +120 -5051  fill=8  (151) $ E15
 652   0   -110 +120 -5052  fill=8  (152) $ E16
 653   0   -110 +120 -5053  fill=8  (153) $ E17
 654   0   -110 +120 -5054  fill=8  (154) $ E18
 655   0   -110 +120 -5055  fill=8  (155) $ E19
 656   0   -110 +120 -5056  fill=8  (156) $ E20
 657   0   -110 +120 -5057  fill=8  (157) $ E21
 658   0   -110 +120 -5058  fill=8  (158) $ E22
 659   0   -110 +120 -5059  fill=8  (159) $ E23
 660   0   -110 +120 -5060  fill=8  (160) $ E24
 661   0   -110 +120 -5061  fill=8  (161) $ F1
 662   0   -110 +120 -5062  fill=8  (162) $ F2
 663   0   -110 +120 -5063  fill=8  (163) $ F3
 664   0   -110 +120 -5064  fill=8  (164) $ F4
 665   0   -110 +120 -5065  fill=8  (165) $ F5
 666   0   -110 +120 -5066  fill=8  (166) $ F6
 667   0   -110 +120 -5067  fill=8  (167) $ F7
 668   0   -110 +120 -5068  fill=8  (168) $ F8
 669   0   -110 +120 -5069  fill=8  (169) $ F9
 670   0   -110 +120 -5070  fill=8  (170) $ F10
 671   0   -110 +120 -5071  fill=8  (171) $ F11
 672   0   -110 +120 -5072  fill=8  (172) $ F12
c 673   0   -110 +120 -5073  fill=8  (173) $ F13 - 3L
c 674   0   -110 +120 -5074  fill=8  (174) $ F14 - 3L
 675   0   -110 +120 -5075  fill=8  (175) $ F15
 676   0   -110 +120 -5076  fill=8  (176) $ F16
 677   0   -110 +120 -5077  fill=8  (177) $ F17
 678   0   -110 +120 -5078  fill=8  (178) $ F18
 679   0   -110 +120 -5079  fill=8  (179) $ F19
 680   0   -110 +120 -5080  fill=8  (180) $ F20
 681   0   -110 +120 -5081  fill=8  (181) $ F21
 682   0   -110 +120 -5082  fill=8  (182) $ F22
 683   0   -110 +120 -5083  fill=8  (183) $ F23
 684   0   -110 +120 -5084  fill=8  (184) $ F24
 685   0   -110 +120 -5085  fill=8  (185) $ F25
 686   0   -110 +120 -5086  fill=8  (186) $ F26
 687   0   -110 +120 -5087  fill=8  (187) $ F27
 688   0   -110 +120 -5088  fill=8  (188) $ F28
 689   0   -110 +120 -5089  fill=8  (189) $ F29
 690   0   -110 +120 -5090  fill=8  (190) $ F30
 691   0   -110 +120 -5091  fill=6  (191) $ G2 - Graphite
 692   0   -110 +120 -5092  fill=8  (192) $ G3
 693   0   -110 +120 -5093  fill=8  (193) $ G4
 694   0   -110 +120 -5094  fill=8  (194) $ G5
 695   0   -110 +120 -5095  fill=8  (195) $ G6
 696   0   -110 +120 -5096  fill=8  (196) $ G8
 697   0   -110 +120 -5097  fill=8  (197) $ G9
```

```
 698   0   -110 +120 -5098  fill=8  (198) $ G10
 699   0   -110 +120 -5099  fill=8  (199) $ G11
 700   0   -110 +120 -5100  fill=8  (200) $ G12
c 701   0   -110 +120 -5101  fill=6  (201) $ G14
 702   0   -110 +120 -5102  fill=8  (202) $ G15
 703   0   -110 +120 -5103  fill=6  (203) $ G16 - Graphite
 704   0   -110 +120 -5104  fill=8  (204) $ G17
 705   0   -110 +120 -5105  fill=8  (205) $ G18
 706   0   -110 +120 -5106  fill=6  (206) $ G20 - Graphite
 707   0   -110 +120 -5107  fill=8  (207) $ G21
 708   0   -110 +120 -5108  fill=8  (208) $ G22
 709   0   -110 +120 -5109  fill=8  (209) $ G23
 710   0   -110 +120 -5110  fill=6  (210) $ G24 - Graphite
c 711   0   -110 +120 -5111  fill=8  (211) $ G26
 712   0   -110 +120 -5112  fill=8  (212) $ G27
 713   0   -110 +120 -5113  fill=8  (213) $ G28
 714   0   -110 +120 -5114  fill=8  (214) $ G29
c 715   0   -110 +120 -5115  fill=8  (215) $ G30
c 716   0   -110 +120 -5116  fill=8  (216) $ G32 - Source
 717   0   -110 +120 -5117  fill=6  (217) $ G33 - Graphite
c 718   0   -110 +120 -5118  fill=8  (218) $ G34 - PNT
 719   0   -110 +120 -5119  fill=6  (219) $ G35 - Graphite
 720   0   -110 +120 -5120  fill=6  (220) $ G36 - Graphite
c
c 750   0     -110 +120 -1940  fill=96   (50)    $ Sleeve irradiator
c
c 751   0     -110 +120 -961   fill=40   (20)    $ 3L(Mat) irradiator
c
 751   0     -110 +120 -1940   fill=45   (50)    $ 3L(Cd) irradiator
c
 752   0     -110 +120 -5118  fill=30   (218)   $ tPNT irradiator
c
c 752   0     -110 +120 -5118  fill=35   (218)   $ ePNT irradiator
c
c ----------------------
c Lower grid plate region
c ----------------------
  1  2  -2.7   -206  +207
               -211  +212  -213  +214  -215  +216
               -221  +222  -223  +224  -225  +226
             +5000 +5001 +5002 +5003 +5004 +5005 +5006 +5007 +5008 +5009
             +5010 +5011 +5012 +5013 +5014 +5015 +5016 +5017 +5018 +5019
             +5020 +5021 +5022 +5023 +5024 +5025 +5026 +5027 +5028 +5029
             +5030 +5031 +5032 +5033 +5034 +5035 +5036 +5037 +5038 +5039
             +5040 +5041 +5042 +5043 +5044 +5045 +5046       +5048 +5049
             +5050 +5051 +5052 +5053 +5054 +5055 +5056 +5057 +5058 +5059
             +5060 +5061 +5062 +5063 +5064 +5065 +5066 +5067 +5068 +5069
             +5070 +5071 +5072             +5075 +5076 +5077 +5078 +5079
             +5080 +5081 +5082 +5083 +5084 +5085 +5086 +5087 +5088 +5089
             +5090 +5091 +5092 +5093 +5094 +5095 +5096 +5097 +5098 +5099
             +5100       +5102 +5103 +5104 +5105 +5106 +5107 +5108 +5109
             +5110       +5112 +5113 +5114             +5117       +5119
             +5120
             +1963 +1964 +1965  +1966                  $ Mapping experiment
             +1940                                     $ 3L
             +5118                                      $ PNT
c             +5111 +5115
c             +5039 +5040 +5063 +5064 +5065 +5093 +5094  $ Elements in 6L
c             +961                                        $ 3L
c
c ----------------------
c Upper grid plate region
c ----------------------
  2  2  -2.7   -203  -201  +202
             +5000 +5001 +5002 +5003 +5004 +5005 +5006 +5007 +5008 +5009
             +5010 +5011 +5012 +5013 +5014 +5015 +5016 +5017 +5018 +5019
             +5020 +5021 +5022 +5023 +5024 +5025 +5026 +5027 +5028 +5029
             +5030 +5031 +5032 +5033 +5034 +5035 +5036 +5037 +5038 +5039
             +5040 +5041 +5042 +5043 +5044 +5045 +5046       +5048 +5049
             +5050 +5051 +5052 +5053 +5054 +5055 +5056 +5057 +5058 +5059
             +5060 +5061 +5062 +5063 +5064 +5065 +5066 +5067 +5068 +5069
             +5070 +5071 +5072             +5075 +5076 +5077 +5078 +5079
             +5080 +5081 +5082 +5083 +5084 +5085 +5086 +5087 +5088 +5089
             +5090 +5091 +5092 +5093 +5094 +5095 +5096 +5097 +5098 +5099
             +5100       +5102 +5103 +5104 +5105 +5106 +5107 +5108 +5109
             +5110       +5112 +5113 +5114             +5117       +5119
             +5120
             +1963 +1964 +1965  +1966                  $ Mapping experiment
             +1940                                     $ 3L
             +5118                                      $ PNT
c             +5111 +5115
c             +5039 +5040 +5063 +5064 +5065 +5093 +5094  $ Elements in 6L
c             +961                                        $ 3L
c
```

```
c ---------------------
c Reactor core structure
c ---------------------
c Inner core shroud
c -----------------
 10  2  -2.7   -300  +302  -303  +202           $ Alignment ring
 11  2  -2.7   -300  -202  +352                 $ Alignment ring
              (+231: -232: +241: -242:
               +233: -234: +243: -244:
               +235: -236: +245: -246)
 12  2  -2.7   +305  -306  +307                 $ Shroud load ring
              (-311  +312  -321  +322
               -313  +314  -323  +324
               -315  +316  -325  +326)
 13  2  -2.7   -301  -352  +304                 $ Alignment ring
              (+331: -332: +341: -342:
               +333: -334: +343: -344:
               +335: -336: +345: -346)
 14  2  -2.7   +231  -331  -233  +236           $ Reflector plate
               -352  +306
 15  2  -2.7   -232  +332  +234  -235           $ Reflector plate
               -352  +306
 16  2  -2.7   +241  -341  -343  -345           $ Reflector, bp3
               -352  +306  +363
 17  2  -2.7   -242  +342  +344  +346           $ Reflector plate
               -352  +306
 18  2  -2.7   +233  -333  -331  -343           $ Reflector plate
               -352  +306
 19  2  -2.7   -234  +334  +332  +344           $ Reflector plate
               -352  +306
 20  2  -2.7   +235  -335  +332  -345           $ Reflector plate
               -352  +306
 21  2  -2.7   -236  +336  -331  +346           $ Reflector plate
               -352  +306
 22  2  -2.7   +243  -343  -241  -233           $ Reflector plate
               -352  +306
 23  2  -2.7   -244  +344  +242  +234           $ Reflector plate
               -352  +306
 24  2  -2.7   +245  -345  -241  -235           $ Reflector plate
               -352  +306
 25  2  -2.7   -246  +346  +242  +236           $ Reflector plate
               -352  +306
 26  2  -2.7   +241  -363  +364  -360           $ Reflector BP3
 27  2  -2.7   -361  +362  -100                 $ Reflector BP1&5
c
c --------------------------------
c Reflector outer shroud structure
c --------------------------------
 30  2  -2.7   -355  +361                       $ Reflector cylin
               -350  +351  -352  +353
 31  2  -2.7   +355  +363                       $ Reflector cylin
               -350  +351  -352  +353
 32  2  -2.7   -370  +371  -372  +373           $ Cylinder, top
 33  2  -2.7   -374  -375  +376                 $ Cylinder, bot
              (+331: -332: +341: -342:
               +333: -334: +343: -344:
               +335: -336: +345: -346)
 34  2  -2.7   -370  +374  -375  +377           $ Reflector edge ring
 35  2  -2.7   -352  -371  +380  +381           $ Reflector RSR unit
 36  2  -2.7   -380  +300  +381  -382           $ Reflector RSR unit
 37  2  -2.7   -352  +301  -300  +381           $ Reflector RSR unit
 38  1  -1.0   +370  -351  -377  +120           $ Edge ring error
c
c ----------------------------
c Reflector graphite moderator
c ----------------------------
 40  4  -2.25    -400  +401  -402  +403         $ Reflector graphite
 41  4  -2.25    -400  -403  +375  -404  +361
                (+411: -412: +421: -422:
                 +413: -414: +423: -424:
                 +415: -416: +425: -426)
               #(-361  +405)                    $ Graphite, bp1&5
 42  4  -2.25   (-400  -403  +375  +404  +363
                (+411: -412: +421: -422:
                 +413: -414: +423: -424:
                 +415: -416: +425: -426))
               #(-406 +408) #(-407 +409)        $ Graphite, bp3
 43  8 -1.15e-3 (+371 -351 -373 +403)     #40   $ Graphite void?????
 44  8 -1.15e-3 (-351  -403  +375  -404  +361
                (+331: -332: +341: -342:
                 +333: -334: +343: -344:
                 +335: -336: +345: -346)) #41   $ graphite void
 45  8 -1.15e-3 (-351  -403  +375  +404  +363
                (+331: -332: +341: -342:
```

```
                +333: -334: +343: -344:
                +335: -336: +345: -346)) #42    $ graphite void
 46  8 -1.15e-3  -304  +403  -301
               (+331: -332: +341: -342:
                +333: -334: +343: -344:
                +335: -336: +345: -346)         $ graphite void
 47  8 -1.15e-3  +301  -371  +403  -381         $ graphite void
c
c ------------------
c Pool coolant water
c ------------------
 50  1  -1.0   -203  +201  -110                 $ Above upper grid plate
              +5000 +5001 +5002 +5003 +5004 +5005 +5006 +5007 +5008 +5009
              +5010 +5011 +5012 +5013 +5014 +5015 +5016 +5017 +5018 +5019
              +5020 +5021 +5022 +5023 +5024 +5025 +5026 +5027 +5028 +5029
              +5030 +5031 +5032 +5033 +5034 +5035 +5036 +5037 +5038 +5039
              +5040 +5041 +5042 +5043 +5044 +5045 +5046       +5048 +5049
              +5050 +5051 +5052 +5053 +5054 +5055 +5056 +5057 +5058 +5059
              +5060 +5061 +5062 +5063 +5064 +5065 +5066 +5067 +5068 +5069
              +5070 +5071 +5072             +5075 +5076 +5077 +5078 +5079
              +5080 +5081 +5082 +5083 +5084 +5085 +5086 +5087 +5088 +5089
              +5090 +5091 +5092 +5093 +5094 +5095 +5096 +5097 +5098 +5099
              +5100       +5102 +5103 +5104 +5105 +5106 +5107 +5108 +5109
              +5110       +5112 +5113 +5114             +5117       +5119
              +5120
              +1940                                    $ 3L
              +5118                                     $ PNT
c              +5111 +5115
c              +5039 +5040 +5063 +5064 +5065 +5093 +5094  $ Elements in 6L
c              +961                                      $ 3L
c
 51  1  -1.0   +203  -302  +202  -110           $ Upper gridplate
 52  1  -1.0   +302  -300  +303  -110           $ Upper gridplate
 53  1  -1.0   -305  -306  +307                 $ Lower gridplate
              +5000 +5001 +5002 +5003 +5004 +5005 +5006 +5007 +5008 +5009
              +5010 +5011 +5012 +5013 +5014 +5015 +5016 +5017 +5018 +5019
              +5020 +5021 +5022 +5023 +5024 +5025 +5026 +5027 +5028 +5029
              +5030 +5031 +5032 +5033 +5034 +5035 +5036 +5037 +5038 +5039
              +5040 +5041 +5042 +5043 +5044 +5045 +5046       +5048 +5049
              +5050 +5051 +5052 +5053 +5054 +5055 +5056 +5057 +5058 +5059
              +5060 +5061 +5062 +5063 +5064 +5065 +5066 +5067 +5068 +5069
              +5070 +5071 +5072             +5075 +5076 +5077 +5078 +5079
              +5080 +5081 +5082 +5083 +5084 +5085 +5086 +5087 +5088 +5089
              +5090 +5091 +5092 +5093 +5094 +5095 +5096 +5097 +5098 +5099
              +5100       +5102 +5103 +5104 +5105 +5106 +5107 +5108 +5109
              +5110       +5112 +5113 +5114             +5117       +5119
              +5120
              +1940                                    $ 3L
              +5118                                     $ PNT
c              +5111 +5115
c              +5039 +5040 +5063 +5064 +5065 +5093 +5094  $ Elements in 6L
c              +961                                      $ 3L
c
 54  1  -1.0   -307  +120                       $ Lower gridplate
               (-311  +312  -321  +322
                -313  +314  -323  +324
                -315  +316  -325  +326)
              +5000 +5001 +5002 +5003 +5004 +5005 +5006 +5007 +5008 +5009
              +5010 +5011 +5012 +5013 +5014 +5015 +5016 +5017 +5018 +5019
              +5020 +5021 +5022 +5023 +5024 +5025 +5026 +5027 +5028 +5029
              +5030 +5031 +5032 +5033 +5034 +5035 +5036 +5037 +5038 +5039
              +5040 +5041 +5042 +5043 +5044 +5045 +5046       +5048 +5049
              +5050 +5051 +5052 +5053 +5054 +5055 +5056 +5057 +5058 +5059
              +5060 +5061 +5062 +5063 +5064 +5065 +5066 +5067 +5068 +5069
              +5070 +5071 +5072             +5075 +5076 +5077 +5078 +5079
              +5080 +5081 +5082 +5083 +5084 +5085 +5086 +5087 +5088 +5089
              +5090 +5091 +5092 +5093 +5094 +5095 +5096 +5097 +5098 +5099
              +5100       +5102 +5103 +5104 +5105 +5106 +5107 +5108 +5109
              +5110       +5112 +5113 +5114             +5117       +5119
              +5120
              +1940                                    $ 3L
              +5118                                    $ PNT
c              +5111 +5115
c              +5039 +5040 +5063 +5064 +5065 +5093 +5094  $ Elements in 6L
c              +961                                     $ 3L
c
 55  1  -1.0   -207  +306                       $ Lower gridplate
               (-231  +232  -241  +242
                -233  +234  -243  +244
                -235  +236  -245  +246)
              +5000 +5001 +5002 +5003 +5004 +5005 +5006 +5007 +5008 +5009
              +5010 +5011 +5012 +5013 +5014 +5015 +5016 +5017 +5018 +5019
              +5020 +5021 +5022 +5023 +5024 +5025 +5026 +5027 +5028 +5029
              +5030 +5031 +5032 +5033 +5034 +5035 +5036 +5037 +5038 +5039
```

```
            +5040 +5041 +5042 +5043 +5044 +5045 +5046       +5048 +5049
            +5050 +5051 +5052 +5053 +5054 +5055 +5056 +5057 +5058 +5059
            +5060 +5061 +5062 +5063 +5064 +5065 +5066 +5067 +5068 +5069
            +5070 +5071 +5072             +5075 +5076 +5077 +5078 +5079
            +5080 +5081 +5082 +5083 +5084 +5085 +5086 +5087 +5088 +5089
            +5090 +5091 +5092 +5093 +5094 +5095 +5096 +5097 +5098 +5099
            +5100       +5102 +5103 +5104 +5105 +5106 +5107 +5108 +5109
            +5110       +5112 +5113 +5114             +5117       +5119
            +5120
            +1940                                      $ 3L
            +5118                                       $ PNT
c            +5111 +5115
c            +5039 +5040 +5063 +5064 +5065 +5093 +5094  $ Elements in 6L
c            +961                                        $ 3L
c
 56  1  -1.0   -206  +207                        $ Lower gridplate
            (+211: -212: +221: -222:
             +213: -214: +223: -224:
             +215: -216: +225: -226)
            (-231  +232  -241  +242
             -233  +234  -243  +244
             -235  +236  -245  +246)
 57  1  -1.0   -351  +371  +372  -110           $ Upper reflector
 58  1  -1.0   -374  -376  +120                 $ Lower reflector
            (+311: -312: +321: -322:
             +313: -314: +323: -324:
             +315: -316: +325: -326)
 59  1  -1.0   +306  -376                        $ Lower reflector
            (+331: -332: +341: -342:
             +333: -334: +343: -344:
             +335: -336: +345: -346)
            (-311  +312  -321  +322
             -313  +314  -323  +324
             -315  +316  -325  +326)
c
c ------------------
c Pool coolant water
c ------------------
 950  8 -1.15e-3 -150 +160 -165
      *TRCL (-60.00    00.00   00.00   00  90  90   90  00  90) $NP
 951  8 -1.15e-3 -150 +160 -165
      *TRCL ( 57.96   -15.53   00.00   00  90  90   90  00  90) $NPP
 952  8 -1.15e-3 -150 +160 -165
      *TRCL ( 42.43    42.43   00.00   00  90  90   90  00  90) $FC
 60  1  -1.0   +350  -355  +361
            (-100  -110  +120) #950 #951       $ Beam ports 1&5
 61  1  -1.0   +350  +355  +363
            (-100  -110  +120) #950 #952
           #(-406 +408) #(-407 +409)           $ Beam ports 2&4
 62  1  -1.0   -363  +364  +360  -100           $ Reflector BP3
 63  1  -1.0   -350  +351  +352  -110           $ Reflector cylinder
 64  1  -1.0   -350  +351  -353  +120           $ Reflector cylinder
 65  1  -1.0   -370  +374  -377  +120           $ Reflector edgering
 66  1  -1.0   +300  -371  +303  -110           $ RSR removal
 67  2  -2.7   +370  -351  -375  +377           $ edge ring error
 68  2  -2.7   -351  +370  -372  +373           $ edge ring error
c ---------------------
c BP2, BP4 structure
c ---------------------
 71  2  -2.7    (-406  +430) +350  +355  -100    $ Reflector BP2
 72  2  -2.7    (-407  +440) +350  +355  -100    $ Reflector BP4
c
c -------------
c BP3 structure
c -------------
 73  2  -2.7     +461  -462  -464               $ Reflector BP3
 74  2  -2.7     -463  +464  +461  -100         $ Reflector BP3
 75  1  -1.0     +241  -364  -461               $ Reflector BP3
 76  1  -1.0     +463  -364  +461  -100         $ Reflector BP3
c
c --------------------
c BP1, BP3, BP5 cavity
c --------------------
 77  8 -1.15e-3  +450  -362  -451                 $ Reflector BP1
 78  8 -1.15e-3  +462  -464  -453                 $ Reflector BP3
 79  8 -1.15e-3  -450  -362  +455
c
c ------------------------------
c BP1, BP2, BP3, BP4, BP5 cavity
c ------------------------------
 81  8 -1.15e-3  +451  -362  -100       #95  VOL=1   $ Reflector BP1
 82  8 -1.15e-3 (-430  +408) +350  -100 #96  VOL=1   $ Reflector BP2
 83  8 -1.15e-3  +453  -464  -100       #97  VOL=1   $ Reflector BP3
 84  8 -1.15e-3 (-440  +409) +350  -100 #98  VOL=1   $ Reflector BP4
```

```
 85  8 -1.15e-3  -455  -362  -100       #99  VOL=1   $ Reflector BP5
c
 95  8 -1.15e-3  -171
 96  8 -1.15e-3  -172
 97  8 -1.15e-3  -173
 98  8 -1.15e-3  -174
 99  8 -1.15e-3  -175
c
c ------------------------------
c Rotary specimen rack (RSR) unit
c ------------------------------
 90  8 -1.15e-3  +300  -303  +352  -371          $ RSR unit
 91  8 -1.15e-3  +300  +304  -352  -380          $ RSR unit
 92  8 -1.15e-3  +300  -304  -380  +382          $ RSR unit
       vol=1
c
c ----------------------------------
c Fill universe for reactor core grid
c ----------------------------------
c Graphite reflector elements, U=6
c -------------------------------
 100  1 -1.0     #101  #102  #103
                 #104  #105  #106       u=6
 101  2 -2.7     -623  -609  +206       u=6      $ lower fitting
 102  2 -2.7     -605  -620  +621       u=6      $ end closure
 103  4 -2.25    -605  -621  +622       u=6      $ graphite
 104  2 -2.7     -605  -622  +623       u=6      $ end closure
 105  2 -2.7     +620  -609  -201       u=6      $ upper fitting
 106  2 -2.7     +605  -607  -620  +623  u=6      $ element clad
c
c -------------------------
c Transient control rod, U=7
c -------------------------
 110  1 -1.0     #111  #112  #113  #114
                 #115  #116  #117       u=7
 111  2 -2.7     -500  -510  +511       u=7      $ end plug
 112  2 -2.7     -500  -511  +512       u=7      $ spacer plug
 113  6 -2.52    -500  -512  +513       u=7      $ absorber
 114  2 -2.7     -500  -513  +514       u=7      $ spacer plug
 115  8 -1.15e-3 -500  -514  +515       u=7      $ air follower
 116  3 -7.8     -500  -515  +516       u=7      $ end plug
 117  3 -7.8     +500  -502  -510  +516  u=7      $ element clad
c
c -------------------------------
c Standard triga fuel element, U=8
c -------------------------------
c Temperature in fuel rod assumed 600 K at full power
 120  1 -1.0     #121  #122  #123
                 #124  #125  #126
                 #127  #128  #129       u=8      $ element clad
 121  3 -7.8     -615  -603  +206       u=8      $ lower fitting
 122  3 -7.8     -600  -610  +611       u=8      $ end closure
 123  4 -2.25    -600  -611  +612       u=8      $ graphite
 124  5 -6.05    -600  -612  +613  +650  u=8    TMP1=5.1702E-8  $ fuel at 600K
 125  7 -6.49    -650  -612  +613       u=8      $ Zr rod
 126  4 -2.25    -600  -613  +614       u=8      $ graphite
 127  3 -7.8     -600  -614  +615       u=8      $ end closure
 128  3 -7.8     +610  -603  -201       u=8      $ upper fitting
 129  3 -7.8     +600  -602  -610  +615  u=8      $ element clad
c
c --------------------------------------------------
c Fuel follower control rods (reg, shim1, shim2), U=9
c --------------------------------------------------
c Temperature assumed 300 C at full power
 130  1  -1.0     #131  #132  #133  #134  #135
                  #136  #137  #138  #139  #140
                  #141  #142  #143        u=9
 131  3  -7.8     -505  -520  +521        u=9      $ end plug
 132  8  -1.15e-3 -505  -521  +522        u=9      $ top space
 133  2  -2.7     -505  -522  +523        u=9      $ spacer plug
 134  8  -1.15e-3 -505  -523  +524        u=9      $ void gap
 135  6  -2.52    -505  -524  +525        u=9      $ absorber
 136  2  -2.7     -505  -525  +526        u=9      $ spacer plug
 137  8  -1.15e-3 -505  -526  +527        u=9      $ void gap
 138  5  -6.05    -505  -527  +528  +550   u=9  TMP1=5.1702E-8 $ fuel follower
 139  7  -6.49    -550  -527  +528        u=9      $ Zr rod
 140  2  -2.7     -505  -528  +529        u=9      $ spacer plug
 141  8  -1.15e-3 -505  -529  +530        u=9      $ bot space
 142  3  -7.8     -505  -530  +531        u=9      $ end plug
 143  3  -7.8     +505  -507  -520  +531   u=9      $ element clad
c
c --------------------------------------
c Modifications and experiment components
c --------------------------------------
```

```
c Pneumatic transfer system (PTS) without Cd, U=30 - JDB - 4/13/2007
c -------------------------------------------------
 300   1  -1.0     #301 #302 #303
                   #304 #305 #306
                   #307 #308             U=30    $ Water surrounding PTS
 301   2  -2.7     -910 +911 +933        U=30    $ Al transport tube
 302   8  -1.15e-3 -911 +912 +933        U=30    $ Air gap
 303   2  -2.7     -912 +913 +915        U=30    $ Al sample tube
 304   8  -1.15e-3 -913      +915 #308   U=30    $ Sample location
 305   2  -2.7     -910 +934 -933        U=30    $ Al transport tube bottom
 306   2  -2.7     -912 +931 -915        U=30    $ Al sample tube bottom
 307   8  -1.15e-3 +933 -931 -912        U=30    $ Air gap beneath sample tube
 308   8  -1.15e-3 -908 +909 -907        U=30    $ Sample location for tally
c
c ---------------------------------------------
c Pneumatic transfer system (PTS) with Cd, U=35 - JDB - 4/13/2007
c ---------------------------------------------
c 350   1  -1.0     #351 #352 #353
c                   #354 #355 #356
c                   #357 #358 #359 #360    U=35    $ Water surrounding PTS
c 351   2  -2.7     -910 +911 +933         U=35    $ Al transport tube
c 352   8  -1.15e-3 -911 +914 +933         U=35    $ Air gap
c 353  10  -8.65    -914 +912 +931         U=35    $ Cd liner
c 354   2  -2.7     -912 +913 +915         U=35    $ Al sample tube
c 355   8  -1.15e-3 -913      +915 #360    U=35    $ Sample location
c 356   2  -2.7     -910 +934 -933         U=35    $ Al transport tube bottom
c 357   2  -2.7     -912 +931 -915         U=35    $ Al sample tube bottom
c 358  10  -8.65    -914 -931 +932         U=35    $ Cd liner beneath sample
c 359   8  -1.15e-3 +933 -932 -914         U=35    $ Air gap beneath sample tube
c 360   8  -1.15e-3 -908 +909 -907         U=35    $ Sample location for tally
c
c ----------------------------------
c 3-element irradiator with Cd, U=40
c ----------------------------------
 400   1  -1.0    #401  #402  #403  #404
                  #405  #406  #407  #408
                  #409  #410              u=40    $ Water
 401   2  -2.7    -920  +921  -958  +959  u=40    $ Al outer
 402   8 -1.15e-3 -921  +924  -958  +959  u=40    $ Air gap
 403  10 -8.65    -924  +922  -958  +959  u=40    $ Pb liner
 404   2  -2.7    -922  +923  -958  +959  u=40    $ Al liner
 405   8 -1.15e-3 -923        -963  +965  u=40    $ Air in sample location
 406   8 -1.15e-3 -923        -958  +963  u=40    $ Air above sample location
 407   2  -2.7    -962        -957  +958  u=40    $ Upper end cap
 408   2  -2.7    -920        -959  +960  u=40    $ Lower end cap
 409   2  -2.7    -923        -965  +966  u=40
 410  10 -8.65    -923        -966  +959  u=40
c
c ----------------------------------
c 3-element irradiator with Cd, U=45
c ----------------------------------
c 450  1  -1.0   #451  #452  #453  #454          $ #461 #462 #463 #465
c                #455  #456  #457  #458
c                #459  #460              U=45     $ Water
c 451  1  -1.0   -920  +921  -958  +959  U=45     $ Al outer
c 452  1  -1.0   -922  +923  -958  +959  U=45     $ Al liner
c 453  1  -1.0   +922  -924  -958  +959  U=45     $ Cd liner
c 454  1  -1.0   -921  +924  -958  +959  U=45     $ Air gap
c 455  1  -1.0   -923        -963  +965  U=45     $ Air in sample location
c 456  1  -1.0   -923        -958  +963  u=45     $ Air above sample location
c 457  1  -1.0   -962        -957  +958  u=45     $ Upper end cap
c 458  1  -1.0   -920        -959  +960  u=45     $ Lower end cap
c 459  1  -1.0   -923        -965  +966  u=45
c 460  1  -1.0   -923        -966  +959  u=45
c
 450  1  -1.0    #451  #452  #453  #454          $ #461 #462 #463 #465
                 #455  #456  #457  #458
                 #459  #460              U=45     $ Water
 451  2  -2.7    -920  +921  -958  +959  U=45     $ Al outer
 452  2  -2.7    -922  +923  -958  +959  U=45     $ Al liner
 453 11  -11.34   +922  -924  -958  +959  U=45     $ Pb liner
 454  8 -1.15e-3 -921  +924  -958  +959  U=45     $ Air gap
 455  8 -1.15e-3 -923        -958  +959  U=45     $ Air in sample location
            vol=1452
 456  8 -1.15e-3 -923        -958  +963  u=45     $ Air above sample location
 457  2  -2.7    -962        -957  +958  u=45     $ Upper end cap
 458  2  -2.7    -920        -959  +960  u=45     $ Lower end cap
 459  2  -2.7    -923        -965  +966  u=45
 460 11  -8.65   -923        -966  +959  u=45     $ Changed to Pb
c
c 461  2  -2.7       +1956  -957 -1941 +1942 U=45     $ Al outer
c 462 11 -11.4       +1955  -958 -1942 +1943 U=45     $ Pb in sleeve
c 463  2  -2.7       +1956  -957 -1943 +1944 u=45     $ Al inner
c 464  2  -2.7        +958  -957 -1942 +1943 u=45     $ Al donut top (lid)
```

```
c 465  2  -2.7       +1956 -1955 -1942 +1943 u=45     $ Al donut bottom
c
c ------------------------------------
c 3-element irradiator (unlined), U=50
c ------------------------------------
 490  8 -1.15e-3 #491  #492  #493  #494  U=50     $
 491  2  -2.7    -922  +923  -950  +955  U=50     $ T3 can cylinder
 492  2  -2.7    +922  -924  -950  +955  U=50     $ T3 can liner
 493  2  -2.7    -923  +950  -951        U=50     $ T3 can upper
 494  2  -2.7    -923  -955  +956        U=50     $ T3 can lower
c
c -----------------------------------------
c Water cells for mapping experiment, u=101
c -----------------------------------------
 515   1    -1.0  #516                u=101
 516   1    -1.0  -754 +782 -750       u=101
c
c ------------------------------------------
c Large irradiator with cadmium sleeve, u=96
c ------------------------------------------
 811   1  -1.0       #812  #813  #814  #815
                     #816  #817  #818  #819
                     #820  #821              u=96    $ Water outside of 7L
 812   2  -2.7      -1941 +1942 -1951 +1955   u=96    $ Al clad outer, sleeve
 813   8  -1.15e-3  -1942 +1947 -1951 +1955   u=96    $ Air, sleeve
 821  10  -8.65     -1947 +1943 -1951 +1955   u=96    $ Cadmium, sleeve
 814   2  -2.7      -1943 +1944 -1951 +1955   u=96    $ Al clad inner, sleeve
 815   2  -2.7      -1945 +1946 -1951 +1955   u=96    $ Al clad, can
 816   8  -1.15e-3  -1946       -1951 +1955   u=96    $ Air inside can
 817   2  -2.7      -1950 +1951 -1941 +1944   u=96    $ Al lid, sleeve, upper
 818   2  -2.7      -1955 +1956 -1941 +1944   u=96    $ Al lid, sleeve, lower
 819   2  -2.7      -1950 +1951 -1945         u=96    $ Al lid, can, upper
 820   2  -2.7      -1955 +1956 -1945         u=96    $ Al lid, can, lower
c
c ---------------
c 1-inch detector
c ---------------
 1740  1  -1.0     #1741  #1742            U=81     $ element clad
 1741  8  -1.15e-3 -638 -639 +640 #1742     U=81
 1742  8  -1.15e-3 -638 -641 +642           U=81     $ flux tally for 1" dia FC
c
c ---------------------
c Central thimble (CT), u=82 - JDB
c ---------------------
 1750  1  -1.0  #1751 #1752           u=82
 1751  2  -2.7  -442  +443  +207      u=82
 1752  1  -1.0  -446  +447  -445      u=82
c
c
c ---------------------------
c Photon Radial Profile Holes
c ---------------------------
 1800  1  -1.0  -2000
 1801  1  -1.0  -2001
 1802  1  -1.0  -2002
 1803  1  -1.0  -2003
 1804  1  -1.0  -2004
 1805  1  -1.0  -2005
 1806  1  -1.0  -2006
c
c -------------
c Outside world
c -------------
 2999  0          +100: +110: -120
c
c ---------------------------------------------------------------
c                 End of Cell Card Specification
c ---------------------------------------------------------------

c ---------------------------------------------------------------
c           Beginning of Surface Card Specification
c ---------------------------------------------------------------
c Hexagonal cell lattice surfaces
c -------------------------------
 101     PX      +2.17678              $ Fuel lattice hex-prism
 102     PX      -2.17678              $ Fuel lattice hex-prism
 103     P   +1   1.73205  0  +4.35356  $ Fuel lattice hex-prism
 104     P   +1   1.73205  0  -4.35356  $ Fuel lattice hex-prism
 105     P   -1   1.73205  0  +4.35356  $ Fuel lattice hex-prism
 106     P   -1   1.73205  0  -4.35356  $ Fuel lattice hex-prism
 107     CZ      +2.51353              $ Maximum lattice diagonal radius
c
 108     py       5.65531
 109     py      -5.65531
```

```
c
c ----------------------
c Axial and radial domain
c ----------------------
 100     CZ     +75
 110     PZ     +100                   $ Upper bound
 120     PZ     -75                    $ Lower bound
 150     CZ     +5.08                  $ Detector Cylinder
 160     PZ     +10                    $ Detector Lower
 165     PZ     +30                    $ Detector Upper
c
 171     s      60.000 -36.000  -6.985  2.5     $ BP1
 172     s      60.000  36.000  -6.985  2.5     $ BP2
 173     s       0.000  70.000  -6.985  2.5     $ BP3
 174     s     -60.000  36.000  -6.985  2.5     $ BP4
 175     s     -60.000 -36.000  -6.985  2.5     $ BP5
c
c -------------------------------
c Reactor core grid plate surfaces
c -------------------------------
 200     CZ       1.91135              $ Grid plate element holes
 201     PZ     +32.3850               $ Upper grid plate region
 202     PZ     +30.7975               $ Upper grid plate region
 203     CZ      27.6225               $ Upper grid plate diameter - effective core diameter
 205     CZ       1.5875               $ Grid plate coolant holes
 206     PZ     -33.17875              $ Lower grid plate region
 207     PZ     -36.35375              $ Lower grid plate region
 211     PX     +26.1216               $ Lower grid plate edge
 212     PX     -26.1216               $ Lower grid plate edge
 213     P   +1   0.57735  0  +29.0240 $ Lower grid plate edge
 214     P   +1   0.57735  0  -29.0240 $ Lower grid plate edge
 215     P   -1   0.57735  0  +29.0240 $ Lower grid plate edge
 216     P   -1   0.57735  0  -29.0240 $ Lower grid plate edge
 221     PY     +25.1360               $ Lower grid plate edge
 222     PY     -25.1360               $ Lower grid plate edge
 223     P   +1   1.73205  0  +52.2432 $ Lower grid plate edge
 224     P   +1   1.73205  0  -52.2432 $ Lower grid plate edge
 225     P   -1   1.73205  0  +52.2432 $ Lower grid plate edge
 226     P   -1   1.73205  0  -52.2432 $ Lower grid plate edge
 231     PX     +26.6700               $ Core shroud inside surface
 232     PX     -26.6700               $ Core shroud inside surface
 233     P   +1   0.57735  0  +29.2100 $ Core shroud inside surface
 234     P   +1   0.57735  0  -29.2100 $ Core shroud inside surface
 235     P   -1   0.57735  0  +29.2100 $ Core shroud inside surface
 236     P   -1   0.57735  0  -29.2100 $ Core shroud inside surface
 241     PY     +25.4000               $ Core shroud inside surface
 242     PY     -25.4000               $ Core shroud inside surface
 243     P   +1   1.73205  0  +54.9275 $ Core shroud inside surface
 244     P   +1   1.73205  0  -54.9275 $ Core shroud inside surface
 245     P   -1   1.73205  0  +54.9275 $ Core shroud inside surface
 246     P   -1   1.73205  0  -54.9275 $ Core shroud inside surface
c
c ----------------------
c Core structure surfaces
c ----------------------
c Reflector inner shroud
c ---------------------
 300     CZ      30.083125             $ Grid plate alignment ring
 301     CZ      29.765625             $ Grid plate alignment ring
 302     CZ      27.9400               $ Grid plate alignment ring
 303     PZ     +33.9725               $ Grid plate alignment ring
 304     PZ     +26.3525               $ Grid plate alignment ring
c
c ---------------
c Shroud load ring
c ---------------
 305     CZ      27.9400               $ Reflector shroud load ring   $ 24.7650
 306     PZ     -37.30625              $ Reflector shroud load ring
 307     PZ     -39.52875              $ Reflector shroud load ring
c
 311     PX     +29.2100               $ Reflector shroud support
 312     PX     -29.2100               $ Reflector shroud support
 313     P   +1   0.57735  0  +32.385  $ Reflector shroud support
 314     P   +1   0.57735  0  -32.385  $ Reflector shroud support
 315     P   -1   0.57735  0  +32.385  $ Reflector shroud support
 316     P   -1   0.57735  0  -32.385  $ Reflector shroud support
 321     PY     +27.9400               $ Reflector shroud support
 322     PY  -27.9400                  $ Reflector shroud support
 323     P   +1   1.73205  0  +59.3725 $ Reflector shroud support
 324     P   +1   1.73205  0  -59.3725 $ Reflector shroud support
 325     P   -1   1.73205  0  +59.3725 $ Reflector shroud support
 326     P   -1   1.73205  0  -59.3725 $ Reflector shroud support
c
 331     PX     +27.3050               $ Core shroud plate exterior
```

```
 332     PX     -27.3050               $ Core shroud plate exterior
 333     P   +1   0.57735  0  +29.8450 $ Core shroud plate exterior
 334     P   +1   0.57735  0  -29.8450 $ Core shroud plate exterior
 335     P   -1   0.57735  0  +29.8450 $ Core shroud plate exterior
 336     P   -1   0.57735  0  -29.8450 $ Core shroud plate exterior
 341     PY     +26.0350               $ Core shroud plate exterior
 342     PY     -26.0350               $ Core shroud plate exterior
 343     P   +1   1.73205  0  +56.5150 $ Core shroud plate exterior
 344     P   +1   1.73205  0  -56.5150 $ Core shroud plate exterior
 345     P   -1   1.73205  0  +56.5150 $ Core shroud plate exterior
 346     P   -1   1.73205  0  -56.5150 $ Core shroud plate exterior
c
c ---------------------
c Reflector outer shroud
c ---------------------
 350     CZ     +54.76875    $ Reflector outer shroud
 351     CZ     +53.49875    $ Reflector outer shroud
 352     PZ     +28.8925     $ Outer shroud upper edge
 353     PZ     -32.0675     $ Outer shroud lower edge
 355     PY       0.0        $ Core shroud section plane
c
c --------------------
c Reflector beam ports
c --------------------
 360     PY     +55.5625                  $ Radial penetrating beam port
 361     C/X    -35.2552  -6.985   7.62   $ Tangential thru beam port
 362     C/X    -35.2552  -6.985   6.9088 $ Tangential thru beam port
 363     C/Y      0.0     -6.985  10.160  $ Radial penetrating beam port
 364     C/Y      0.0     -6.985   9.525  $ Radial penetrating beam port
c
 370     CZ      53.3400     $ Reflector top shroud
 371     CZ      37.4650     $ Reflector top shroud
 372     PZ     +29.5275     $ Reflector top shroud
 373     PZ     +28.2575     $ Reflector top shroud
 374     CZ      52.0700     $ Reflector inner shroud base
 375     PZ     -27.9400     $ Reflector inner shroud base
 376     PZ     -29.5275     $ Reflector inner shroud base
 377     PZ     -36.8300     $ Reflector shroud edge ring
c
c ---------------------
c RSR experiment system
c ---------------------
 380     CZ     +37.1475     $ RSR cavity outer ring
 381     PZ      +6.9850     $ RSR cavity base
 382     PZ      +7.3025     $ RSR cavity base
c
c ---------------------------
c Graphite reflector surfaces
c ---------------------------
 400     CZ      53.0225     $ Graphite reflector outer radius
 401     CZ      37.7825     $ Graphite reflector inner radius
 402     PZ      27.6225     $ Graphite reflector upper section
 403     PZ       6.3500     $ Graphite reflector section plane
 404     PY     -20.32       $ Graphite reflector section plane
 405     PY     -35.2552     $ Beam port penetration
c        C/Y      0.0     -6.985  10.160         $ Radial penetrating beam port, bp3
c        C/X    -35.2552  -6.985   7.62          $ Tangential thru beam port,  bp1&5
 406  2  CY      7.62        $ Tangential beam port, bp2
 407  4  CY      7.62        $ Radial beam port, bp4
 408  2  PY      0.0         $ Tangential beam port, bp2
 409  4  PY      0.0         $ Radial beam port, bp4
 411     PX    +27.78125                $ Graphite inner surface
 412     PX    -27.78125                $ Graphite inner surface
 413     P   +1  0.57735  0  +31.00875  $ Graphite inner surface +1
 414     P   +1  0.57735  0  -31.00875  $ Graphite inner surface +1
 415     P   -1  0.57735  0  +31.00875  $ Graphite inner surface +1
 416     P   -1  0.57735  0  -31.00875  $ Graphite inner surface +1
 421     PY    +26.431875               $ Graphite inner surface
 422     PY    -26.431875               $ Graphite inner surface
 423     P   +1  1.73205  0  +57.30875  $ Graphite inner surface +1
 424     P   +1  1.73205  0  -57.30875  $ Graphite inner surface +1
 425     P   -1  1.73205  0  +57.30875  $ Graphite inner surface +1
 426     P   -1  1.73205  0  -57.30875  $ Graphite inner surface +1
c
 430  2  CY      6.9088      $ Tangential beam port, bp2
 440  4  CY      6.9088      $ Radial beam port, bp4
 450     PX      0.0         $ BP1&5 origin
c
c --------------
c Central thimble - JLP
c --------------
 442     CZ      1.50        $ Central thimble guide rod OD
 443     CZ      1.415       $ Central thimble guid rod ID
 444     CZ      1.25        $ Central thimble sample holder OD
```

```
 445     CZ      1.185       $ Central thimble sample holder ID
 446     PZ      2.5         $ Central thimble upper sample hodler
 447     PZ     -2.5         $ Central thibmle lower sample holder
c    beam port tally surfaces bp1&5 and bp3
 451     PX     +10.16       $ BP1
 453     PY     +40.90       $ BP3
 455     PX     -10.16       $ BP5
c    pool structure pipe, bp3
 461     PY     +25.600                $ Radial penetrating beam port, bp3
 462     PY     +26.235                $ Radial penetrating beam port, bp3
 463     C/Y      0.0  -6.985  7.62    $ Radial penetrating beam port, bp3
 464     C/Y      0.0  -6.985  6.9088  $ Radial penetrating beam port, bp3
c
c -----------------------
c Control element surfaces
c -----------------------
 500     CZ       1.5113     $ Control element - absorber surface, radius
 502     CZ       1.5875     $ Control element - clad outer surface
 505     CZ       1.6637     $ Control element - absorber surface, radius
 507     CZ       1.7145     $ Control element - clad outer surface
c
 510  7   PZ     +24.765      $ Control element - element plug, end
 511  7   PZ     +24.13       $ Control element - magneform plug, upper
 512  7   PZ     +19.05       $ Control element - absorber surface,length/2
 513  7   PZ     -19.05       $ Control element - absorber surface,length/2
 514  7   PZ     -21.59       $ Control element - magneform plug, lower
 515  7   PZ     -70.8025     $ Control element - air follower section
 516  7   PZ     -72.7075     $ Control element - element plug, end
c
 517      pz     +75
 518      pz     -75
 519      cz     1.5875
 532      cz     1.7145
c
 520  7   PZ     +34.925      $ Control element - element plug, end
 521  7   PZ     +31.115      $ Control element - void gap
 522  7   PZ     +20.6375     $ Control element - magneform plug, upper
 523  7   PZ     +19.3675     $ Control element - void gap
 524  7   PZ     +19.05       $ Control element - absorber surface,length/2
 525  7   PZ     -19.05       $ Control element - absorber surface,length/2
 526  7   PZ     -20.32       $ Control element - magneform plug, lower
 527  7   PZ     -20.955      $ Control element - void gap
 528  7   PZ     -59.055      $ Control element - fuel follower section
 529  7   PZ     -61.595      $ Control element - void gap
 530  7   PZ     -74.93       $ Control element - magneform plug, bottom
 531  7   PZ     -74.99       $ Control element - element plug, end
c
 550     CZ       0.28575    $ Zirconium rod
c
c ----------------------------------
c Fuel and moderator element surfaces
c ----------------------------------
 600     CZ       1.816      $ Fuel element - fuel region surface, radius
 602     CZ       1.867      $ Fuel element - clad outer surface
 603     CZ       1.5306     $ Fuel - adapter effective radius, lower
 604     CZ       1.9426     $ Fuel - adapter effective radius, upper
 605     CZ       1.816      $ Graphite element - element surface, radius
 606     CZ       1.867      $ Graphite element - clad outer surface
 607     CZ       1.867      $ Graphite element - clad outer surface
 608     CZ       1.9426     $ Graphite - adapter effective radius, upper
 609     CZ       1.5306     $ Graphite - adapter effective radius, lower
c
 610     PZ     +28.5877     $ Fuel element - element end region, upper
 611     PZ     +27.7368     $ Fuel element - graphite end region, upper
 612     PZ     +19.05       $ Fuel element - fuel surface, length/2
 613     PZ     -19.05       $ Fuel element - fuel surface, length/2
 614     PZ     -27.7368     $ Fuel element - graphite end region, lower
 615     PZ     -28.5877     $ Fuel element - element end region, lower
c
 620     PZ     +28.5877     $ Graphite element - element end, upper
 621     PZ     +27.7368     $ Graphite element - graphite end, upper
 622     PZ     -27.7368     $ Graphite element - graphite end, lower
 623     PZ     -28.5877     $ Graphite element - element end, lower
c
 635     PZ      15.24               $ Flux Tally
 636     PZ     -15.24               $ Flux Tally
 637     CZ      0.4                 $ Flux Tally hole for the KSU detector
 638     CZ      1.27
 639     PZ      7.7851
 640     PZ     -7.7851
 641     PZ      6.35
 642     PZ     -6.35
c
 650     CZ       0.28575          $ Zirconium rod
```

```
c
 660     CZ       1.5306           $ Element adapter effective radius
 661     CZ       1.867            $ Element clad outer surface
 662     PZ     +32.3850           $ Upper grid plate, top
 663     PZ     +28.5877           $ Element end region, upper
 664     PZ     -28.5877           $ Element end region, lower
 665     PZ     -33.17875          $ Lower grid plate, top
 666     cz       1.91135          $ Upper grid plate holes
c
c -------------------------------
c Boundaries for large irradiator
c -------------------------------
 701     PX     +8.70712
 703     PX    +10.8839
 708     PX    +19.59102
 710     PX     21.7678
 712     PX     19.59102
 717     PX     10.8839
 702      P     -1   1.73205   0  -26.12136
 704      P     -1   1.73205   0  -21.7678
 705      P      1   1.73205   0    4.35356
 706      P     -1   1.73205   0  -26.12136
 707      P      1   1.73205   0    8.70712
 709      P      1   1.73205   0    4.35356
 711      P     -1   1.73205   0  -43.5356
 713      P     -1   1.73205   0  -47.88916
 714      P      1   1.73205   0  -13.06068
 715      P     -1   1.73205   0  -43.5356
 716      P      1   1.73205   0  -17.41424
 718      P      1   1.73205   0  -13.06068
c
c --------------------------
c Reactor core modifications
c --------------------------
c Center tube irradiations
c ------------------------
 900     CZ       1.905                $ Center tube outer radius
 901     CZ       1.69418              $ Center tube inner radius
 905     CZ       1.5                  $ Sample radius
 907     PZ      +0.5                  $ Sample length
 908     CZ       0.5                  $ Sample radius (PTS)
 909     PZ      -0.5                  $ Sample length
c
c -------------------
c PNT tube dimensions
c -------------------
 910     CZ      +1.74625              $ Al transport tube outer radius
 911     CZ      +1.53543              $ Al transport tube inner radius
 912     CZ      +1.11125              $ Al sample tube outer radius
 913     CZ      +0.86995              $ Al sample tube inner radius
 914     CZ      +1.16205              $ Cd two layer liner
 915     PZ      -2.07645              $ PTS sample stop
 916     PZ     -18.89125              $ Cd absorber end
 917     PZ     -21.1264591            $ Cd absorber disk, upper edge
 918     PZ     -21.17725              $ Cd absorber disk, lower edge
 919     PZ     -30.32125              $ PTS bottom section
 931     PZ      -2.94775              $ Al sample tube bottom
 932     PZ      -2.99855              $ Bottom of Cd liner
 933     PZ      -3.37193              $ Top of Al transport tube
 934     PZ      -3.58275              $ Bottom of Al transport tube
c
c ----------------------------------
c 3-element irradiator with Cd or Pb
c ----------------------------------
c Reference to lower grid plate -33.17875
 920     c/z      0 0 +2.38125              $ Al can outer radius
 921     c/z      0 0 +2.23393              $ Al can inner radius
 922     c/z      0 0 +2.06375              $ Al sleeve outer radius
 923     c/z      0 0 +1.93929              $ Al sleeve inner radius
 924     c/z     0 0 +2.16535              $ Cd liner outer radius
c 930     c/z     0 -0 +0.47625              $ Al structure rod
c 940     PZ     -30.xxxx              $ Al bearing section
 950     PZ      +2.54                 $ Al upper end cap
 951     PZ      +2.5908               $ Al upper end cap
 955     PZ      -2.54                 $ Al lower end cap
 956     PZ      -2.5908               $ Al lower end cap
c
 957     pz     +99.82125              $ Al upper end cap, top
 958     pz     +96.82125              $ Al upper end cap, bottom
 963     pz     +30.7975               $ Bottom of upper grid plate
 959     pz     -26.19375              $ Al lower end cap, top
 960     pz     -31.27385              $ Al lower end cap, bottom
 962     c/z    -15.23746 -8.79856 +3.00000
c
```

```
 961    c/z     -15.23746 -8.79856 +3.0099
c
 965     pz     -25.55875             $ Top of Al in Al sleeve
 966     pz     -26.09215             $ Top of Cd liner in sleeve
 967     pz     -26.19375             $ Top of lower end cap
c
c --------------------------------------------
c Large irradiator surfaces with cadmium sleeve
c --------------------------------------------
c 1940     c/z     15.23746  -11.31062  5.27939   $ Center of irradiator
c 1940     c/z     +10.8839  +8.79856  2.4        $ Center of 3L irradiator
 1940     c/z     -15.24 -8.80 +2.4               $ Center of 3L irradiator
c
  1941     cz      5.08
  1942     cz      4.7625
  1943     cz      3.81
  1944     cz      3.4925
  1945     cz      3.175
  1946     cz      2.8575
  1947     cz      2.0000
 c
 1950      pz      +32.3850             $ Al upper end cap
 1951      pz      +32.22625            $ Al upper end cap
 1955      pz      -33.02               $ Al lower end cap
 1956      pz      -33.17875            $ Al lower end cap
c
c -------------------------------------
c Surfaces for flux mapping with Ni wire - JDB
c -------------------------------------
 1963    c/z    2.17678  -1.2573   +0.16   $ A
 1964    c/z   15.23746  -1.2573   +0.16   $ K
 1965    c/z   19.59102  -1.2573   +0.16   $ L
 1966    c/z   23.94458  -1.2573   +0.16   $ M
c
 750  cz     0.15875
 751  cz     0.16
 754  pz    32.385
 782  pz    -36.35375
c
c --------------------------
c Photon Radial Profile Holes
c --------------------------
 2000  s    +0.0  +2.51353      +0.0  0.3175
 2001  s    +0.0  +5.020706     +0.0  0.3175
 2002  s    +0.0  +10.05412     +0.0  0.3175
 2003  s    +0.0  +12.56765     +0.0  0.3175
 2004  s    +0.0  +17.59470     +0.0  0.3175
 2005  s    +0.0  +20.10823     +0.0  0.3175
 2006  s    +0.0  +25.0         +0.0  0.3175
c
c
c ---------------------
c Upper grid plate holes
c ---------------------
 5000  c/z  +0.00000  +0.00000  +1.91135  $ Upper grid plate hole, A1
 5001  c/z  +4.35356  +0.00000  +1.91135  $ Upper grid plate hole, B1
 5002  c/z  +2.17678  -3.76936  +1.91135  $ Upper grid plate hole, B2
 5003  c/z  -2.17678  -3.76936  +1.91135  $ Upper grid plate hole, B3
 5004  c/z  -4.35356  +0.00000  +1.91135  $ Upper grid plate hole, B4
 5005  c/z  -2.17678  +3.76936  +1.91135  $ Upper grid plate hole, B5
 5006  c/z  +2.17678  +3.76936  +1.91135  $ Upper grid plate hole, B6
 5007  c/z  +8.70712  +0.00000  +1.91135  $ Upper grid plate hole, C1
 5008  c/z  +6.53034  -3.76936  +1.91135  $ Upper grid plate hole, C2
 5009  c/z  +4.35356  -7.54126  +1.91135  $ Upper grid plate hole, C3
 5010  c/z  -0.00000  -7.54126  +1.91135  $ Upper grid plate hole, C4
 5011  c/z  -4.35356  -7.54126  +1.91135  $ Upper grid plate hole, C5
 5012  c/z  -6.53034  -3.76936  +1.91135  $ Upper grid plate hole, C6
 5013  c/z  -8.70712  +0.00000  +1.91135  $ Upper grid plate hole, C7
 5014  c/z  -6.53034  +3.76936  +1.91135  $ Upper grid plate hole, C8
 5015  c/z  -4.35356  +7.54126  +1.91135  $ Upper grid plate hole, C9
 5016  c/z  -0.00000  +7.54126  +1.91135  $ Upper grid plate hole, C10
 5017  c/z  +4.35356  +7.54126  +1.91135  $ Upper grid plate hole, C11
 5018  c/z  +6.53034  +3.76936  +1.91135  $ Upper grid plate hole, C12
 5019  c/z +13.06068  +0.00000  +1.91135  $ Upper grid plate hole, D1
 5020  c/z +10.88390  -3.76936  +1.91135  $ Upper grid plate hole, D2
 5021  c/z  +8.70712  -7.54126  +1.91135  $ Upper grid plate hole, D3
 5022  c/z  +6.53034 -11.31062  +1.91135  $ Upper grid plate hole, D4
 5023  c/z  +2.17678 -11.31062  +1.91135  $ Upper grid plate hole, D5
 5024  c/z  -2.17678 -11.31062  +1.91135  $ Upper grid plate hole, D6
 5025  c/z  -6.53034 -11.31062  +1.91135  $ Upper grid plate hole, D7
 5026  c/z  -8.70712  -7.54126  +1.91135  $ Upper grid plate hole, D8
 5027  c/z -10.88390  -3.76936  +1.91135  $ Upper grid plate hole, D9
 5028  c/z -13.06068  +0.00000  +1.91135  $ Upper grid plate hole, D10
 5029  c/z -10.88390  +3.76936  +1.91135  $ Upper grid plate hole, D11
```

```
5030  c/z  -8.70712  +7.54126  +1.91135  $ Upper grid plate hole, D12
5031  c/z  -6.53034 +11.31062  +1.91135  $ Upper grid plate hole, D13
5032  c/z  -2.17678 +11.31062  +1.91135  $ Upper grid plate hole, D14
5033  c/z  +2.17678 +11.31062  +1.91135  $ Upper grid plate hole, D15
5034  c/z  +6.53034 +11.31062  +1.91135  $ Upper grid plate hole, D16
5035  c/z  +8.70712  +7.54126  +1.91135  $ Upper grid plate hole, D17
5036  c/z +10.88390  +3.76936  +1.91135  $ Upper grid plate hole, D18
5037  c/z +17.41424  +0.00000  +1.91135  $ Upper grid plate hole, E1
5038  c/z +15.23746  -3.76936  +1.91135  $ Upper grid plate hole, E2
5039  c/z +13.06068  -7.54126  +1.91135  $ Upper grid plate hole, E3
5040  c/z +10.88390 -11.31062  +1.91135  $ Upper grid plate hole, E4
5041  c/z  +8.70712 -15.08252  +1.91135  $ Upper grid plate hole, E5
5042  c/z  +4.35356 -15.08252  +1.91135  $ Upper grid plate hole, E6
5043  c/z  -0.00000 -15.08252  +1.91135  $ Upper grid plate hole, E7
5044  c/z  -4.35356 -15.08252  +1.91135  $ Upper grid plate hole, E8
5045  c/z  -8.70712 -15.08252  +1.91135  $ Upper grid plate hole, E9
5046  c/z -10.88390 -11.31062  +1.91135  $ Upper grid plate hole, E10
5047  c/z -13.06068  -7.54126  +1.91135  $ Upper grid plate hole, E11
5048  c/z -15.23746  -3.76936  +1.91135  $ Upper grid plate hole, E12
5049  c/z -17.41424  +0.00000  +1.91135  $ Upper grid plate hole, E13
5050  c/z -15.23746  +3.76936  +1.91135  $ Upper grid plate hole, E14
5051  c/z -13.06068  +7.54126  +1.91135  $ Upper grid plate hole, E15
5052  c/z -10.88390 +11.31062  +1.91135  $ Upper grid plate hole, E16
5053  c/z  -8.70712 +15.08252  +1.91135  $ Upper grid plate hole, E17
5054  c/z  -4.35356 +15.08252  +1.91135  $ Upper grid plate hole, E18
5055  c/z  -0.00000 +15.08252  +1.91135  $ Upper grid plate hole, E19
5056  c/z  +4.35356 +15.08252  +1.91135  $ Upper grid plate hole, E20
5057  c/z  +8.70712 +15.08252  +1.91135  $ Upper grid plate hole, E21
5058  c/z +10.88390 +11.31062  +1.91135  $ Upper grid plate hole, E22
5059  c/z +13.06068  +7.54126  +1.91135  $ Upper grid plate hole, E23
5060  c/z +15.23746  +3.76936  +1.91135  $ Upper grid plate hole, E24
5061  c/z +21.76780  +0.00000  +1.91135  $ Upper grid plate hole, F1
5062  c/z +19.59102  -3.76936  +1.91135  $ Upper grid plate hole, F2
5063  c/z +17.41424  -7.54126  +1.91135  $ Upper grid plate hole, F3
5064  c/z +15.23746 -11.31062  +1.91135  $ Upper grid plate hole, F4
5065  c/z +13.06068 -15.08252  +1.91135  $ Upper grid plate hole, F5
5066  c/z +10.88390 -18.85188  +1.91135  $ Upper grid plate hole, F6
5067  c/z  +6.53034 -18.85188  +1.91135  $ Upper grid plate hole, F7
5068  c/z  +2.17678 -18.85188  +1.91135  $ Upper grid plate hole, F8
5069  c/z  -2.17678 -18.85188  +1.91135  $ Upper grid plate hole, F9
5070  c/z  -6.53034 -18.85188  +1.91135  $ Upper grid plate hole, F10
5071  c/z -10.88390 -18.85188  +1.91135  $ Upper grid plate hole, F11
5072  c/z -13.06068 -15.08252  +1.91135  $ Upper grid plate hole, F12
5073  c/z -15.23746 -11.31062  +1.91135  $ Upper grid plate hole, F13
5074  c/z -17.41424  -7.54126  +1.91135  $ Upper grid plate hole, F14
5075  c/z -19.59102  -3.76936  +1.91135  $ Upper grid plate hole, F15
5076  c/z -21.76780  +0.00000  +1.91135  $ Upper grid plate hole, F16
5077  c/z -19.59102  +3.76936  +1.91135  $ Upper grid plate hole, F17
5078  c/z -17.41424  +7.54126  +1.91135  $ Upper grid plate hole, F18
5079  c/z -15.23746 +11.31062  +1.91135  $ Upper grid plate hole, F19
5080  c/z -13.06068 +15.08252  +1.91135  $ Upper grid plate hole, F20
5081  c/z -10.88390 +18.85188  +1.91135  $ Upper grid plate hole, F21
5082  c/z  -6.53034 +18.85188  +1.91135  $ Upper grid plate hole, F22
5083  c/z  -2.17678 +18.85188  +1.91135  $ Upper grid plate hole, F23
5084  c/z  +2.17678 +18.85188  +1.91135  $ Upper grid plate hole, F24
5085  c/z  +6.53034 +18.85188  +1.91135  $ Upper grid plate hole, F25
5086  c/z +10.88390 +18.85188  +1.91135  $ Upper grid plate hole, F26
5087  c/z +13.06068 +15.08252  +1.91135  $ Upper grid plate hole, F27
5088  c/z +15.23746 +11.31062  +1.91135  $ Upper grid plate hole, F28
5089  c/z +17.41424  +7.54126  +1.91135  $ Upper grid plate hole, F29
5090  c/z +19.59102  +3.76936  +1.91135  $ Upper grid plate hole, F30
5091  c/z +23.94458  -3.76936  +1.91135  $ Upper grid plate hole, G2
5092  c/z +21.76780  -7.54126  +1.91135  $ Upper grid plate hole, G3
5093  c/z +19.59102 -11.31062  +1.91135  $ Upper grid plate hole, G4
5094  c/z +17.41424 -15.08252  +1.91135  $ Upper grid plate hole, G5
5095  c/z +15.23746 -18.85188  +1.91135  $ Upper grid plate hole, G6
5096  c/z  +8.70712 -22.62124  +1.91135  $ Upper grid plate hole, G8
5097  c/z  +4.35356 -22.62124  +1.91135  $ Upper grid plate hole, G9
5098  c/z  -0.00000 -22.62124  +1.91135  $ Upper grid plate hole, G10
5099  c/z  -4.35356 -22.62124  +1.91135  $ Upper grid plate hole, G11
5100  c/z  -8.70712 -22.62124  +1.91135  $ Upper grid plate hole, G12
5101  c/z -15.23746 -18.85188  +1.91135  $ Upper grid plate hole, G14
5102  c/z -17.41424 -15.08252  +1.91135  $ Upper grid plate hole, G15
5103  c/z -19.59102 -11.31062  +1.91135  $ Upper grid plate hole, G16
5104  c/z -21.76780  -7.54126  +1.91135  $ Upper grid plate hole, G17
5105  c/z -23.94458  -3.76936  +1.91135  $ Upper grid plate hole, G18
5106  c/z -23.94458  +3.76936  +1.91135  $ Upper grid plate hole, G20
5107  c/z -21.76780  +7.54126  +1.91135  $ Upper grid plate hole, G21
5108  c/z -19.59102 +11.31062  +1.91135  $ Upper grid plate hole, G22
5109  c/z -17.41424 +15.08252  +1.91135  $ Upper grid plate hole, G23
5110  c/z -15.23746 +18.85188  +1.91135  $ Upper grid plate hole, G24
5111  c/z  -8.70712 +22.62124  +1.91135  $ Upper grid plate hole, G26
5112  c/z  -4.35356 +22.62124  +1.91135  $ Upper grid plate hole, G27
5113  c/z  +4.35356 +22.62124  +1.91135  $ Upper grid plate hole, G29
```

```
 5114  c/z  -0.00000 +22.62124  +1.91135  $ Upper grid plate hole, G28
 5115  c/z  +8.70712 +22.62124  +1.91135  $ Upper grid plate hole, G30
 5116  c/z +15.23746 +18.85188  +1.91135  $ Upper grid plate hole, G32
 5117  c/z +17.41424 +15.08252  +1.91135  $ Upper grid plate hole, G33
 5118  c/z +19.59102 +11.31062  +1.91135  $ Upper grid plate hole, G34
 5119  c/z +21.76780  +7.54126  +1.91135  $ Upper grid plate hole, G35
 5120  c/z +23.94458  +3.76936  +1.91135  $ Upper grid plate hole, G36
c
c ----------------------
c Cut planes for tallies
c ----------------------
 6000  pz   +32
 6001  pz   +31
 6002  pz   +30
 6003  pz   +29
 6004  pz   +28
 6005  pz   +27
 6006  pz   +26
 6007  pz   +25
 6008  pz   +24
 6009  pz   +23
 6010  pz   +22
 6011  pz   +21
 6012  pz   +20
 6013  pz   +19
 6014  pz   +18
 6015  pz   +17
 6016  pz   +16
 6017  pz   +15
 6018  pz   +14
 6019  pz   +13
 6020  pz   +12
 6021  pz   +11
 6022  pz   +10
 6023  pz    +9
 6024  pz    +8
 6025  pz    +7
 6026  pz    +6
 6027  pz    +5
 6028  pz    +4
 6029  pz    +3
 6030  pz    +2
 6031  pz    +1
 6032  pz    +0
 6033  pz    -1
 6034  pz    -2
 6035  pz    -3
 6036  pz    -4
 6037  pz    -5
 6038  pz    -6
 6039  pz    -7
 6040  pz    -8
 6041  pz    -9
 6042  pz   -10
 6043  pz   -11
 6044  pz   -12
 6045  pz   -13
 6046  pz   -14
 6047  pz   -15
 6048  pz   -16
 6049  pz   -17
 6050  pz   -18
 6051  pz   -19
 6052  pz   -20
 6053  pz   -21
 6054  pz   -22
 6055  pz   -23
 6056  pz   -24
 6057  pz   -25
 6058  pz   -26
 6059  pz   -27
 6060  pz   -28
 6061  pz   -29
 6062  pz   -30
 6063  pz   -31
 6064  pz   -32
 6065  pz   -33
 6066  pz   -34
 6067  pz   -35
 6068  pz   -36
c
 7000  pz   +30.861
 7001  pz   +27.305
 7002  pz   +25.781
```

```
 7003  pz   +22.225
 7004  pz   +20.701
 7005  pz   +17.145
 7006  pz   +15.621
 7007  pz   +12.065
 7008  pz   +10.541
 7009  pz    +6.985
 7010  pz    +5.461
 7011  pz    +1.905
 7012  pz    +0.381
 7013  pz    -3.175
 7014  pz    -4.699
 7015  pz    -8.255
 7016  pz    -9.779
 7017  pz   -13.335
 7018  pz   -14.859
 7019  pz   -18.415
 7020  pz   -19.939
 7021  pz   -23.495
 7022  pz   -25.019
 7023  pz   -28.575
 7024  pz   -30.099
 7025  pz   -33.655
 7026  pz   -35.179
c
 8000  pz     +30.7975              $ Bottom of upper grid plate region
 8001  pz     +27.7368              $ Top of graphite region
 8002  pz     +19.05                $ Top of fuel region
 8003  pz     -19.05                $ Bottom of fuel region
 8004  pz     -27.7368              $ Bottom of graphite region
 8005  pz     -33.17875             $ Top of lower grid plate region
c
c -----------------------------------------------------------------
c              End of Surface Card Specification
c -----------------------------------------------------------------

c -----------------------------------------------------------------
c           Beginning of Material Card Specification
c -----------------------------------------------------------------
c -------------------------
c Beam tube transformations
c -------------------------
c tr1: Through port, small, BP1
c tr2: Tangential port, small, BP2
c tr3: Radial port, large, BP3
c tr4: Radial port, small, BP4
c tr5: Through port, large, BP5
c
 *tr1  0.0      -35.255  -6.985   00  90  90    90  00  90
 *tr2  +35.255  -06.222  -6.985   30 120  90    60  30  90
 *tr3  0.0      +25.600  -6.985   00  90  90    90  00  90
 *tr4  -22.871  +13.216  -6.985   60  30  90   150  60  90
 *tr5  0.0      -35.255  -6.985   00  90  90    90  00  90
c
c the '*' just makes the transformation in degrees
c
c ---------------------------
c Control rod transformations
c ---------------------------
c Shutdown condition - 000 units
c Low power critical - 525 units
c Design high power - 700 units
c Full out condition - 960 units
c
 tr6  0  0  00.00     1 0 0  0 1 0
 tr7  0  0  15.00     1 0 0  0 1 0                $ Formerly 19.05, 8.33, 12.37
 tr8  0  0  27.78     1 0 0  0 1 0
 tr9  0  0  38.10     1 0 0  0 1 0
c
c -----------------------------------
c Mapping experiment transformations
c -----------------------------------
 tr10    +2.17678  -1.2573  0.0
 tr11   +15.23746  -1.2573  0.0
 tr12   +19.59102  -1.2573  0.0
 tr13   +23.94458  -1.2573  0.0
c
c -------------------------------------
c Irradiation facility transformations
c -------------------------------------
 tr20   -15.23746 -8.79856  0.0       $ Center of 3L irradiator
c tr50  +15.23746 -11.31062 0.0       $ Center of 6L irradiator
c tr50  +10.8839  +8.79856  0.0       $ Center of 3L irradiator
 tr50   -15.24    -8.80     0.0       $ Center of 3L irradiator
```

```
c
c -------------------------------
c Grid plate hole transformations
c -------------------------------
 tr100   -0.00000  +0.00000  0.0    $  A1
 tr101   +4.35356  +0.00000  0.0    $  B1
 tr102   +2.17678  -3.76936  0.0    $  B2
 tr103   -2.17678  -3.76936  0.0    $  B3
 tr104   -4.35356  +0.00000  0.0    $  B4
 tr105   -2.17678  +3.76936  0.0    $  B5
 tr106   +2.17678  +3.76936  0.0    $  B6
 tr107   +8.70712  +0.00000  0.0    $  C1
 tr108   +6.53034  -3.76936  0.0    $  C2
 tr109   +4.35356  -7.54126  0.0    $  C3
 tr110   -0.00000  -7.54126  0.0    $  C4
 tr111   -4.35356  -7.54126  0.0    $  C5
 tr112   -6.53034  -3.76936  0.0    $  C6
 tr113   -8.70712  +0.00000  0.0    $  C7
 tr114   -6.53034  +3.76936  0.0    $  C8
 tr115   -4.35356  +7.54126  0.0    $  C9
 tr116   -0.00000  +7.54126  0.0    $  C10
 tr117   +4.35356  +7.54126  0.0    $  C11
 tr118   +6.53034  +3.76936  0.0    $  C12
 tr119  +13.06068  +0.00000  0.0    $  D1
 tr120  +10.88390  -3.76936  0.0    $  D2
 tr121   +8.70712  -7.54126  0.0    $  D3
 tr122   +6.53034 -11.31062  0.0    $  D4
 tr123   +2.17678 -11.31062  0.0    $  D5
 tr124   -2.17678 -11.31062  0.0    $  D6
 tr125   -6.53034 -11.31062  0.0    $  D7
 tr126   -8.70712  -7.54126  0.0    $  D8
 tr127  -10.88390  -3.76936  0.0    $  D9
 tr128  -13.06068  +0.00000  0.0    $  D10
 tr129  -10.88390  +3.76936  0.0    $  D11
 tr130   -8.70712  +7.54126  0.0    $  D12
 tr131   -6.53034 +11.31062  0.0    $  D13
 tr132   -2.17678 +11.31062  0.0    $  D14
 tr133   +2.17678 +11.31062  0.0    $  D15
 tr134   +6.53034 +11.31062  0.0    $  D16
 tr135   +8.70712  +7.54126  0.0    $  D17
 tr136  +10.88390  +3.76936  0.0    $  D18
 tr137  +17.41424  +0.00000  0.0    $  E1
 tr138  +15.23746  -3.76936  0.0    $  E2
 tr139  +13.06068  -7.54126  0.0    $  E3
 tr140  +10.88390 -11.31062  0.0    $  E4
 tr141   +8.70712 -15.08252  0.0    $  E5
 tr142   +4.35356 -15.08252  0.0    $  E6
 tr143   -0.00000 -15.08252  0.0    $  E7
 tr144   -4.35356 -15.08252  0.0    $  E8
 tr145   -8.70712 -15.08252  0.0    $  E9
 tr146  -10.88390 -11.31062  0.0    $  E10
 tr147  -13.06068  -7.54126  0.0    $  E11
 tr148  -15.23746  -3.76936  0.0    $  E12
 tr149  -17.41424  +0.00000  0.0    $  E13
 tr150  -15.23746  +3.76936  0.0    $  E14
 tr151  -13.06068  +7.54126  0.0    $  E15
 tr152  -10.88390 +11.31062  0.0    $  E16
 tr153   -8.70712 +15.08252  0.0    $  E17
 tr154   -4.35356 +15.08252  0.0    $  E18
 tr155   -0.00000 +15.08252  0.0    $  E19
 tr156   +4.35356 +15.08252  0.0    $  E20
 tr157   +8.70712 +15.08252  0.0    $  E21
 tr158  +10.88390 +11.31062  0.0    $  E22
 tr159  +13.06068  +7.54126  0.0    $  E23
 tr160  +15.23746  +3.76936  0.0    $  E24
 tr161  +21.76780  +0.00000  0.0    $  F1
 tr162  +19.59102  -3.76936  0.0    $  F2
 tr163  +17.41424  -7.54126  0.0    $  F3
 tr164  +15.23746 -11.31062  0.0    $  F4
 tr165  +13.06068 -15.08252  0.0    $  F5
 tr166  +10.88390 -18.85188  0.0    $  F6
 tr167   +6.53034 -18.85188  0.0    $  F7
 tr168   +2.17678 -18.85188  0.0    $  F8
 tr169   -2.17678 -18.85188  0.0    $  F9
 tr170   -6.53034 -18.85188  0.0    $  F10
 tr171  -10.88390 -18.85188  0.0    $  F11
 tr172  -13.06068 -15.08252  0.0    $  F12
 tr173  -15.23746 -11.31062  0.0    $  F13
 tr174  -17.41424  -7.54126  0.0    $  F14
 tr175  -19.59102  -3.76936  0.0    $  F15
 tr176  -21.76780  +0.00000  0.0    $  F16
 tr177  -19.59102  +3.76936  0.0    $  F17
 tr178  -17.41424  +7.54126  0.0    $  F18
 tr179  -15.23746 +11.31062  0.0    $  F19
```

```
 tr180  -13.06068 +15.08252  0.0    $  F20
 tr181  -10.88390 +18.85188  0.0    $  F21
 tr182   -6.53034 +18.85188  0.0    $  F22
 tr183   -2.17678 +18.85188  0.0    $  F23
 tr184   +2.17678 +18.85188  0.0    $  F24
 tr185   +6.53034 +18.85188  0.0    $  F25
 tr186  +10.88390 +18.85188  0.0    $  F26
 tr187  +13.06068 +15.08252  0.0    $  F27
 tr188  +15.23746 +11.31062  0.0    $  F28
 tr189  +17.41424  +7.54126  0.0    $  F29
 tr190  +19.59102  +3.76936  0.0    $  F30
 tr191  +23.94458  -3.76936  0.0    $  G2
 tr192  +21.76780  -7.54126  0.0    $  G3
 tr193  +19.59102 -11.31062  0.0    $  G4
 tr194  +17.41424 -15.08252  0.0    $  G5
 tr195  +15.23746 -18.85188  0.0    $  G6
 tr196   +8.70712 -22.62124  0.0    $  G8
 tr197   +4.35356 -22.62124  0.0    $  G9
 tr198   -0.00000 -22.62124  0.0    $  G10
 tr199   -4.35356 -22.62124  0.0    $  G11
 tr200   -8.70712 -22.62124  0.0    $  G12
 tr201  -15.23746 -18.85188  0.0    $  G14
 tr202  -17.41424 -15.08252  0.0    $  G15
 tr203  -19.59102 -11.31062  0.0    $  G16
 tr204  -21.76780  -7.54126  0.0    $  G17
 tr205  -23.94458  -3.76936  0.0    $  G18
 tr206  -23.94458  +3.76936  0.0    $  G20
 tr207  -21.76780  +7.54126  0.0    $  G21
 tr208  -19.59102 +11.31062  0.0    $  G22
 tr209  -17.41424 +15.08252  0.0    $  G23
 tr210  -15.23746 +18.85188  0.0    $  G24
 tr211   -8.70712 +22.62124  0.0    $  G26
 tr212   -4.35356 +22.62124  0.0    $  G27
 tr213   +4.35356 +22.62124  0.0    $  G29
 tr214   -0.00000 +22.62124  0.0    $  G28
 tr215   +8.70712 +22.62124  0.0    $  G30
 tr216  +15.23746 +18.85188  0.0    $  G32
 tr217  +17.41424 +15.08252  0.0    $  G33
 tr218  +19.59102 +11.31062  0.0    $  G34
 tr219  +21.76780  +7.54126  0.0    $  G35
 tr220  +23.94458  +3.76936  0.0    $  G36
c
c ---------------------------
c Reactor component materials
c ---------------------------
c m1 - water
c m2 - aluminum (structural) type 6061
c m3 - stainless steel (structural) type 304
c m4 - graphite (carbon)
c m5 - fresh U-ZrH fuel
c m6 - B4C (boron carbide)
c m7 - zirconium (rod)
c m8 - air
c m10 - cadmium (neutron absorber liner)
c m11 - lead (neutron absorber liner)
c m54 - ar cme
 m1   1001         0.66667
      8016         0.33333
mt1  lwtr.60t                  $294K cme
c mpn1  0 0
 m2  13027        -0.9685
     26000.50c    -0.0070
     29000.50c    -0.0025
     14000.60c    -0.0060
     12000.66c    -0.0110
     24000.50c    -0.0035
     25055        -0.0015
c mpn2 0 0 0 0 0 0 0
 m3  26000.50c    -0.6785
      6000        -0.0080
     14000.60c    -0.0100
     24000.50c    -0.1800
     28000.50c    -0.0980
     25055        -0.0180
     15031        -0.0045
     16000.66c    -0.0030
c mpn3  0 0 0 0 0 0 0 0
 m4    6000         1.0
mt4  grph.60t                    $ 294K cme
c mpn4  0
 m5  40090.71c        -0.462589265
     40091.71c        -0.100879525
     40092.71c        -0.154196422
     40094.71c        -0.156264362
```

```
     40096.71c        -0.025174926
      1001.71c        -0.0158955
     92238.71c        -0.068170
     92235.71c        -0.016830
c mpn5 0 0 82208 82208
mt5  zr/h.62t                $600K cme
     h/zr.62t                $600K cme
 m6    5010        0.1584
       5011        0.6416
       6000        0.2
c mpn6  0 0 0
 m7   40090       51.45
      40091       11.22
      40092       17.15
      40094       17.38
      40096       2.8
c mpn7  0
 m8    8016       -0.23
       7014       -0.77
c mpn8  0 0
 m10  48000.42c    1.0
c mpn10 0
 m11  82000.42c   -1.0
c mpn11 0
 m12  28058        1             $  nickel     (n,p)  a/o  68.0
 m13  28064        1             $  nickel     (n,g)  a/o   0.9
 m14  79197        1             $  gold       (n,g)  a/o 100.0
 m15  29063        1             $  copper     (n,g)  a/o  69.1
 m16  26058        1             $  iron       (n,g)  a/o   0.2
 m17  26054        1             $  iron       (n,p)  a/o   5.8
 m18  42098        1             $  molybdenum (n,g)  a/o  24.1
 m19  27059        1             $  cobalt     (n,g)  a/o 100.0
 m20  13027        1             $  aluminum   (n,g)  a/o 100.0
c m54     18036  0.003365          $cme
c       18038  0.000632
c       18040  0.996003
c       18037  1e-36
c       18039  1e-36
c       18041  1e-36
c       18042  1e-36
c       18043  1e-36
c       17037  1e-36
c       19039  1e-36
c      19041  1e-36
c
c -------
c Tallies
c -------
c
c f14:n    (1752<u=82)
c fc14     Flux tally for CT
c e14      0.50e-6 1.00e-2 1.50e+1  T
c
 f24:n    (1752<u=82)
 fc24     Flux tally for CT spectrum
 e24     1.000E-11 5.000E-09 1.000E-08 1.500E-08 2.000E-08 2.500E-08
          3.000E-08 3.500E-08 4.200E-08 5.000E-08 5.800E-08 6.700E-08
          8.000E-08 1.000E-07 1.520E-07 2.510E-07 4.140E-07 6.830E-07
          1.125E-06 1.855E-06 3.059E-06 5.040E-06 8.315E-06 1.371E-05
          2.260E-05 3.727E-05 6.144E-05 1.013E-04 1.670E-04 2.754E-04
          4.540E-04 7.485E-04 1.234E-03 2.035E-03 2.404E-03 2.840E-03
          3.355E-03 5.531E-03 9.119E-03 1.503E-02 1.989E-02 2.554E-02
          4.087E-02 6.738E-02 1.111E-01 1.832E-01 3.020E-01 3.887E-01
          4.979E-01 6.392E-01 8.208E-01 1.108 1.353 1.737
          2.231 2.865 3.678 4.965 6.065 10.0
          14.91 16.90 20.00 25.00 T
c
c  f74:n    455                                                  $(455<u=45) this is old input
c fc74     Flux tally for 3L(Pb) profile
c fs74     6002 6007 6012 6017 6022 6027 6032 6037 6042 6047 6052 6057
c fq74     s f
c
 f84:n    (308<u=30)                                                   $PNT tally
 fc84     Flux tally for PNT(Pb) spectrum
c fs84     6002 6007 6012 6017 6022 6027 6032 6037 6042 6047 6052 6057
 e84      1.000E-11 5.000E-09 1.000E-08 1.500E-08 2.000E-08 2.500E-08
          3.000E-08 3.500E-08 4.200E-08 5.000E-08 5.800E-08 6.700E-08
          8.000E-08 1.000E-07 1.520E-07 2.510E-07 4.140E-07 6.830E-07
          1.125E-06 1.855E-06 3.059E-06 5.040E-06 8.315E-06 1.371E-05
          2.260E-05 3.727E-05 6.144E-05 1.013E-04 1.670E-04 2.754E-04
          4.540E-04 7.485E-04 1.234E-03 2.035E-03 2.404E-03 2.840E-03
          3.355E-03 5.531E-03 9.119E-03 1.503E-02 1.989E-02 2.554E-02
          4.087E-02 6.738E-02 1.111E-01 1.832E-01 3.020E-01 3.887E-01
          4.979E-01 6.392E-01 8.208E-01 1.108 1.353 1.737
```

```
         2.231 2.865 3.678 4.965 6.065 10.0
         14.91 16.90 20.00 25.00 T
c
 f15:n  -15.24 -8.8 -22.0 0                                          $Point detector at Flux Wire
 fc15   Point detector at middle of 3L
  e15      1.000E-11 5.000E-09 1.000E-08 1.500E-08 2.000E-08 2.500E-08
         3.000E-08 3.500E-08 4.200E-08 5.000E-08 5.800E-08 6.700E-08
         8.000E-08 1.000E-07 1.520E-07 2.510E-07 4.140E-07 6.830E-07
         1.125E-06 1.855E-06 3.059E-06 5.040E-06 8.315E-06 1.371E-05
         2.260E-05 3.727E-05 6.144E-05 1.013E-04 1.670E-04 2.754E-04
         4.540E-04 7.485E-04 1.234E-03 2.035E-03 2.404E-03 2.840E-03
         3.355E-03 5.531E-03 9.119E-03 1.503E-02 1.989E-02 2.554E-02
         4.087E-02 6.738E-02 1.111E-01 1.832E-01 3.020E-01 3.887E-01
         4.979E-01 6.392E-01 8.208E-01 1.108 1.353 1.737
         2.231 2.865 3.678 4.965 6.065 10.0
         14.91 16.90 20.00 25.00 T
c
c f25:n  -15.24 -8.8 0 2.4                                          $Ring detector at middle of 3L
c fc25   Ring detector at middle of 3L
c  e25      1.000E-11 5.000E-09 1.000E-08 1.500E-08 2.000E-08 2.500E-08
c          3.000E-08 3.500E-08 4.200E-08 5.000E-08 5.800E-08 6.700E-08
c          8.000E-08 1.000E-07 1.520E-07 2.510E-07 4.140E-07 6.830E-07
c          1.125E-06 1.855E-06 3.059E-06 5.040E-06 8.315E-06 1.371E-05
c          2.260E-05 3.727E-05 6.144E-05 1.013E-04 1.670E-04 2.754E-04
c          4.540E-04 7.485E-04 1.234E-03 2.035E-03 2.404E-03 2.840E-03
c          3.355E-03 5.531E-03 9.119E-03 1.503E-02 1.989E-02 2.554E-02
c          4.087E-02 6.738E-02 1.111E-01 1.832E-01 3.020E-01 3.887E-01
c          4.979E-01 6.392E-01 8.208E-01 1.108 1.353 1.737
c          2.231 2.865 3.678 4.965 6.065 10.0
c          14.91 16.90 20.00 25.00 T
c
c f35:n  -15.24 -8.8 -26.19375 0
c fc35   Point Detector at bottom of 3L
c
c f45:n  -15.24 -8.8 -19 0
c fc45   Point detector at bottom of fuel in 3L
c
c f55:n  -15.24 -8.8 +19 0
c fc55   Point detector at top of fuel in 3L
c
c f65:n  -15.24 -8.8 +30.7975 0
c fc65  Point detector at top of 3L
c f114:n   92
c fc114    Flux tally for RSR
c fs114    6022
c e114     0.50e-6 1.00e-2 1.50e+1  T
c
 f124:n   92
 fc124    Flux tally for RSR spectrum
 fs124             6022          $ 2nd segment is approx. sample location
 e124    1.000E-11 5.000E-09 1.000E-08 1.500E-08 2.000E-08 2.500E-08
         3.000E-08 3.500E-08 4.200E-08 5.000E-08 5.800E-08 6.700E-08
         8.000E-08 1.000E-07 1.520E-07 2.510E-07 4.140E-07 6.830E-07
         1.125E-06 1.855E-06 3.059E-06 5.040E-06 8.315E-06 1.371E-05
         2.260E-05 3.727E-05 6.144E-05 1.013E-04 1.670E-04 2.754E-04
         4.540E-04 7.485E-04 1.234E-03 2.035E-03 2.404E-03 2.840E-03
         3.355E-03 5.531E-03 9.119E-03 1.503E-02 1.989E-02 2.554E-02
         4.087E-02 6.738E-02 1.111E-01 1.832E-01 3.020E-01 3.887E-01
         4.979E-01 6.392E-01 8.208E-01 1.108 1.353 1.737
         2.231 2.865 3.678 4.965 6.065 10.0
         14.91 16.90 20.00 25.00 T
c
 f184:n    (124<u=8)                                                 $TRIGA Fuel
 fc184     Flux tally for TRIGA Fuel spectrum
 e184      1.000E-11 5.000E-09 1.000E-08 1.500E-08 2.000E-08 2.500E-08
         3.000E-08 3.500E-08 4.200E-08 5.000E-08 5.800E-08 6.700E-08
         8.000E-08 1.000E-07 1.520E-07 2.510E-07 4.140E-07 6.830E-07
         1.125E-06 1.855E-06 3.059E-06 5.040E-06 8.315E-06 1.371E-05
         2.260E-05 3.727E-05 6.144E-05 1.013E-04 1.670E-04 2.754E-04
         4.540E-04 7.485E-04 1.234E-03 2.035E-03 2.404E-03 2.840E-03
         3.355E-03 5.531E-03 9.119E-03 1.503E-02 1.989E-02 2.554E-02
         4.087E-02 6.738E-02 1.111E-01 1.832E-01 3.020E-01 3.887E-01
         4.979E-01 6.392E-01 8.208E-01 1.108 1.353 1.737
         2.231 2.865 3.678 4.965 6.065 10.0
         14.91 16.90 20.00 25.00 T
c f134:n   (516<u=101)
c fc134    Flux tally for mapping experiment profile
c fs134    7001 7003 7005 7007 7009 7011 7013 7015 7017 7019 7021 7023 7025
c fq134    s f
c
c f204:n   (124<u=8) T
c fc204    Total fission power tally for fuel elements
c fm204    -3.84962E+02 5 -6
c fq204    f s
```

```
c
c f214:n   (138<u=9) T
c fc214    Total fission power tally for fuel followers
c fm214    -3.21529E+02 5 -6
c fq214    f s
c
c f224:n   (124<u=8)   T
c fc224    Total flux for fuel elements
c fq224    f s
c
c f234:n   (138<u=9) T
c fc234    Total flux for fuel followers
c fq234    f s
c
c f244:n   (124<u=8) (138<u=9)  T
c fc244    Total flux for fuel
c fq244    f s
c
c f314:n   (1752<u=82)
c fc314    Reaction rate tally for CT
c fm314    (1  14  102)
c
c f394:n   (455<u=45)
c fc394    Reaction rate tally for 3L(Cd) profile
c fs394    6002 6007 6012 6017 6022 6027 6032 6037 6042 6047 6052 6057
c fm394    (1  12  103)
c          (1  13  102)
c          (1  14  102)
c          (1  15  102)
c          (1  16  102)
c          (1  17  103)
c          (1  18  102)
c          (1  19  102)
c          (1  20  102)
c fq394    s f
c
c f414:n   92
c fc414    Reaction rate tally for RSR
c fs414    6022
c fm414    (1  12  103)
c          (1  14  102)
c          (1  19  102)
c fq414    s f
c
c f434:n   (516<u=101)
c fc434    Reaction rate tally for mapping experiment
c fm434    (1   12  103)
c fs434    7001 7003 7005 7007 7009 7011 7013 7015 7017 7019 7021 7023 7025
c fq434    s f
c
c f504:n   95  96 97 98 99
c fc504    BP Neutron Flux Tally by Three Energy Groups
c e504     0.50e-6 1.00e-2 1.50e+1  T
c
c f624:p   (455<u=45)
c fc624    Photon tally for 3L(Cd) profile
c fs624    6002 6007 6012 6017 6022 6027 6032 6037 6042 6047 6052 6057
c fq624    s f
c
c f644:n   (455<u=45)
c fc644    Flux tally for 3L(Cd) profile
c fs644    6002 6007 6012 6017 6022 6027 6032 6037 6042 6047 6052 6057
c e644     0.50e-6 1.00e-2 1.50e+1  T
c
c f654:n   (455<u=45)
c fc654    3L Neutron Tally for Calculation of Neutron Dose (Kerma)
c de654    2.50E-08 1.00E-07 1.00E-06 1.00E-05 1.00E-04 1.00E-03
c          1.00E-02 1.00E-01 5.00E-01 1 2 2.5 5 7 10 14 20
c df654    3.67E-06 3.67E-06 4.46E-06 4.54E-06 4.18E-06 3.76E-06
c          3.56E-06 2.17E-05 9.26E-05 1.32E-04 1.43E-04 1.25E-04
c          1.56E-04 1.47E-04 1.47E-04 2.08E-04 2.27E-04
c fs654    6002 6007 6012 6017 6022 6027 6032 6037 6042 6047 6052 6057
c fq654    s f
c
c f664:p   (455<u=45)
c fc664    3L Photon Tally for Calculation of Photon Dose (Kerma)
c de664    1.00E-02 3.00E-02 5.00E-02 7.00E-02 1.00E-01 1.50E-01
c          2.00E-01 2.50E-01 3.00E-01 0.35 0.4 0.45 0.5 0.55 0.6
c          0.65 0.7 0.8 1.0 1.4 1.8 2.2 2.6 2.8 3.25 3.75 4.25 4.75
c          5.0 5.25 5.75 6.25 6.75 7.5 9.0 11.0 13.0 15.0
c df664    3.96E-06 5.82E-07 2.90E-07 2.58E-07 2.83E-07 3.79E-07
c          5.01E-07 6.31E-07 7.59E-07 8.78E-07 9.85E-07 1.08E-06
c          1.17E-06 1.27E-06 1.36E-06 1.44E-06 1.52E-06 1.68E-06
c          1.98E-06 2.51E-06 2.99E-06 3.42E-06 3.82E-06 4.01E-06
```

```
c          4.41E-06 4.83E-06 5.23E-06 5.60E-06 5.80E-06 6.01E-06
c          6.37E-06 6.74E-06 7.11E-06 7.66E-06 8.77E-06 1.03E-05
c          1.18E-05 1.33E-05
c fs664    6002 6007 6012 6017 6022 6027 6032 6037 6042 6047 6052 6057
c fq664    s f
c
c f674:n   (455<u=45)
c fc674    3L Neutron Tally for Calculation of Hardness Factor
c de674    1.03E-10 1.08E-10 1.13E-10 1.18E-10 1.24E-10 1.31E-10 1.39E-10
c          1.46E-10 1.55E-10 1.65E-10 1.75E-10 1.85E-10 1.95E-10 2.05E-10
c          2.15E-10 2.25E-10 2.35E-10 2.48E-10 2.63E-10 2.75E-10 2.90E-10
c          3.10E-10 3.30E-10 3.50E-10 3.70E-10 3.90E-10 4.13E-10 4.38E-10
c          4.63E-10 4.88E-10 5.13E-10 5.38E-10 5.63E-10 5.88E-10 6.15E-10
c          6.45E-10 6.75E-10 7.05E-10 7.40E-10 7.80E-10 8.20E-10 8.60E-10
c          9.00E-10 9.40E-10 9.80E-10 1.03E-09 1.08E-09 1.13E-09 1.18E-09
c          1.24E-09 1.31E-09 1.39E-09 1.46E-09 1.55E-09 1.65E-09 1.75E-09
c          1.85E-09 1.95E-09 2.05E-09 2.15E-09 2.25E-09 2.35E-09 2.48E-09
c          2.63E-09 2.75E-09 2.90E-09 3.10E-09 3.30E-09 3.50E-09 3.70E-09
c          3.90E-09 4.13E-09 4.38E-09 4.63E-09 4.88E-09 5.13E-09 5.38E-09
c          5.63E-09 5.88E-09 6.15E-09 6.45E-09 6.75E-09 7.05E-09 7.40E-09
c          7.80E-09 8.20E-09 8.60E-09 9.00E-09 9.40E-09 9.80E-09 1.03E-08
c          1.08E-08 1.13E-08 1.18E-08 1.24E-08 1.31E-08 1.39E-08 1.46E-08
c          1.55E-08 1.65E-08 1.75E-08 1.85E-08 1.95E-08 2.05E-08 2.15E-08
c          2.25E-08 2.35E-08 2.48E-08 2.63E-08 2.75E-08 2.90E-08 3.10E-08
c          3.30E-08 3.50E-08 3.70E-08 3.90E-08 4.13E-08 4.38E-08 4.63E-08
c          4.88E-08 5.13E-08 5.38E-08 5.63E-08 5.88E-08 6.15E-08 6.45E-08
c          6.75E-08 7.05E-08 7.40E-08 7.80E-08 8.20E-08 8.60E-08 9.00E-08
c          9.40E-08 9.80E-08 1.03E-07 1.08E-07 1.13E-07 1.18E-07 1.24E-07
c          1.31E-07 1.39E-07 1.46E-07 1.55E-07 1.65E-07 1.75E-07 1.85E-07
c          1.95E-07 2.05E-07 2.15E-07 2.25E-07 2.35E-07 2.48E-07 2.63E-07
c          2.75E-07 2.90E-07 3.10E-07 3.30E-07 3.50E-07 3.70E-07 3.90E-07
c          4.13E-07 4.38E-07 4.63E-07 4.88E-07 5.13E-07 5.38E-07 5.63E-07
c          5.88E-07 6.15E-07 6.45E-07 6.75E-07 7.05E-07 7.40E-07 7.80E-07
c          8.20E-07 8.60E-07 9.00E-07 9.40E-07 9.80E-07 1.03E-06 1.08E-06
c          1.13E-06 1.18E-06 1.24E-06 1.31E-06 1.39E-06 1.46E-06 1.55E-06
c          1.65E-06 1.75E-06 1.85E-06 1.95E-06 2.05E-06 2.15E-06 2.25E-06
c          2.35E-06 2.48E-06 2.63E-06 2.75E-06 2.90E-06 3.10E-06 3.30E-06
c          3.50E-06 3.70E-06 3.90E-06 4.13E-06 4.38E-06 4.63E-06 4.88E-06
c          5.13E-06 5.38E-06 5.63E-06 5.88E-06 6.15E-06 6.45E-06 6.75E-06
c          7.05E-06 7.40E-06 7.80E-06 8.20E-06 8.60E-06 9.00E-06 9.40E-06
c          9.80E-06 1.03E-05 1.08E-05 1.13E-05 1.18E-05 1.24E-05 1.31E-05
c          1.39E-05 1.46E-05 1.55E-05 1.65E-05 1.75E-05 1.85E-05 1.95E-05
c          2.05E-05 2.15E-05 2.25E-05 2.35E-05 2.48E-05 2.63E-05 2.75E-05
c          2.90E-05 3.10E-05 3.30E-05 3.50E-05 3.70E-05 3.90E-05 4.13E-05
c          4.38E-05 4.63E-05 4.88E-05 5.13E-05 5.38E-05 5.63E-05 5.88E-05
c          6.15E-05 6.45E-05 6.75E-05 7.05E-05 7.40E-05 7.80E-05 8.20E-05
c          8.60E-05 9.00E-05 9.40E-05 9.80E-05 1.03E-04 1.08E-04 1.13E-04
c          1.18E-04 1.24E-04 1.31E-04 1.39E-04 1.46E-04 1.55E-04 1.65E-04
c          1.75E-04 1.85E-04 1.95E-04 2.05E-04 2.15E-04 2.25E-04 2.35E-04
c          2.48E-04 2.63E-04 2.75E-04 2.90E-04 3.10E-04 3.30E-04 3.50E-04
c          3.70E-04 3.90E-04 4.13E-04 4.38E-04 4.63E-04 4.88E-04 5.13E-04
c          5.38E-04 5.63E-04 5.88E-04 6.15E-04 6.45E-04 6.75E-04 7.05E-04
c          7.40E-04 7.80E-04 8.20E-04 8.60E-04 9.00E-04 9.40E-04 9.80E-04
c          1.03E-03 1.08E-03 1.13E-03 1.18E-03 1.24E-03 1.31E-03 1.39E-03
c          1.46E-03 1.55E-03 1.65E-03 1.75E-03 1.85E-03 1.95E-03 2.05E-03
c          2.15E-03 2.25E-03 2.35E-03 2.48E-03 2.63E-03 2.75E-03 2.90E-03
c          3.10E-03 3.30E-03 3.50E-03 3.70E-03 3.90E-03 4.13E-03 4.38E-03
c          4.63E-03 4.88E-03 5.13E-03 5.37E-03 5.63E-03 5.88E-03 6.15E-03
c          6.45E-03 6.75E-03 7.05E-03 7.40E-03 7.80E-03 8.20E-03 8.60E-03
c          9.00E-03 9.40E-03 9.80E-03 1.03E-02 1.08E-02 1.13E-02 1.18E-02
c          1.24E-02 1.31E-02 1.39E-02 1.46E-02 1.55E-02 1.65E-02 1.75E-02
c          1.85E-02 1.95E-02 2.05E-02 2.15E-02 2.25E-02 2.35E-02 2.48E-02
c          2.63E-02 2.75E-02 2.90E-02 3.10E-02 3.30E-02 3.50E-02 3.70E-02
c          3.90E-02 4.13E-02 4.38E-02 4.63E-02 4.88E-02 5.13E-02 5.38E-02
c          5.63E-02 5.88E-02 6.15E-02 6.45E-02 6.75E-02 7.05E-02 7.40E-02
c          7.80E-02 8.20E-02 8.60E-02 9.00E-02 9.40E-02 9.80E-02 0.1025
c          0.1075   0.1125   0.1175   0.12375  0.13125  0.13875  0.14625
c          0.155    0.165    0.175    0.185    0.195    0.205    0.215
c          0.225    0.235    0.2475   0.2625   0.275    0.29     0.31
c          0.33     0.35     0.37     0.39     0.4125   0.4375   0.4625
c          0.4875   0.5125   0.5375   0.5625   0.5875   0.615    0.645
c          0.675    0.705    0.74     0.78     0.82     0.86     0.9
c          0.94     0.98     1.05     1.15     1.25     1.35     1.45
c          1.55     1.65     1.75     1.85     1.95     2.05     2.15
c          2.25     2.35     2.45     2.55     2.65     2.75     2.85
c          2.95     3.05     3.15     3.25     3.35     3.45     3.55
c          3.65     3.75     3.85     3.95     4.05     4.15     4.25
c          4.35     4.45     4.55     4.65     4.75     4.85     4.95
c          5.05     5.15     5.25     5.35     5.45     5.55     5.65
c          5.75     5.85     5.95     6.05     6.15     6.25     6.35
c          6.45     6.55     6.65     6.75     6.85     6.95     7.05
c          7.15     7.25     7.35     7.45     7.55     7.65     7.75
c          7.85     7.95     8.05     8.15     8.25     8.35     8.45
c          8.55     8.65     8.75     8.85     8.95     9.05     9.15
```

```
c       9.25    9.35    9.45    9.55    9.65    9.75    9.85
c       9.95    10.05   10.15   10.25   10.35   10.45   10.55
c       10.65   10.75   10.85   10.95   11.05   11.15   11.25
c       11.35   11.45   11.55   11.65   11.75   11.85   11.95
c       12.05   12.15   12.25   12.35   12.45   12.55   12.65
c       12.75   12.85   12.95   13.05   13.15   13.25   13.35
c       13.45   13.55   13.65   13.75   13.85   13.95   14.05
c       14.15   14.25   14.35   14.45   14.55   14.65   14.75
c       14.85   14.95   15.05   15.15   15.25   15.35   15.45
c       15.55   15.65   15.75   15.85   15.95   16.05   16.15
c       16.25   16.35   16.45   16.55   16.65   16.75   16.85
c       16.95   17.05   17.15   17.25   17.35   17.45   17.55
c       17.65   17.75   17.85   17.95   18.05   18.15   18.25
c       18.35   18.45   18.55   18.65   18.75   18.85   18.95
c       19.05   19.15   19.25   19.35   19.45   19.55   19.65
c       19.75   19.85   19.95
c df674  1.5471  1.5117  1.4764  1.445   1.4081  1.3668  1.3294
c       1.2948  1.2575  1.2189  1.1834  1.1511  1.1225  1.0945
c       1.0678  1.0447  1.0217  0.99545 0.96654 0.94426 0.91947
c       0.88938 0.86182 0.83681 0.81396 0.79319 0.77183 0.7487
c       0.72869 0.70929 0.69201 0.67559 0.66034 0.64626 0.63144
c       0.61669 0.60274 0.58979 0.57569 0.56079 0.54754 0.53445
c       0.52212 0.51126 0.50044 0.48942 0.47822 0.46705 0.45713
c       0.44546 0.43241 0.42057 0.40964 0.39784 0.38565 0.37444
c       0.36422 0.35519 0.34632 0.33791 0.3306  0.32333 0.31504
c       0.30591 0.29887 0.29105 0.28154 0.27283 0.26492 0.2577
c       0.25113 0.24438 0.23706 0.23072 0.22458 0.21911 0.21391
c       0.20908 0.20461 0.19992 0.19525 0.19082 0.18672 0.18225
c       0.17753 0.17332 0.16917 0.16525 0.1618  0.15837 0.15485
c       0.15125 0.14773 0.14461 0.14084 0.13677 0.13295 0.1295
c       0.12577 0.12187 0.11834 0.11522 0.11215 0.10936 0.10684
c       0.10435 0.10215 9.95E-02 9.66E-02 9.43E-02 9.19E-02 8.89E-02
c       8.61E-02 8.36E-02 8.13E-02 7.92E-02 7.70E-02 7.47E-02 7.27E-02
c       7.08E-02 6.90E-02 6.74E-02 6.59E-02 6.45E-02 6.31E-02 6.16E-02
c       6.03E-02 5.90E-02 5.77E-02 5.62E-02 5.48E-02 5.35E-02 5.23E-02
c       5.12E-02 5.02E-02 4.91E-02 4.80E-02 4.69E-02 4.59E-02 4.47E-02
c       4.35E-02 4.23E-02 4.12E-02 4.00E-02 3.88E-02 3.76E-02 3.65E-02
c       3.56E-02 3.47E-02 3.39E-02 3.31E-02 3.24E-02 3.16E-02 3.07E-02
c       3.00E-02 2.92E-02 2.82E-02 2.74E-02 2.65E-02 2.57E-02 2.51E-02
c       2.44E-02 2.37E-02 2.31E-02 2.25E-02 2.19E-02 2.14E-02 2.09E-02
c       2.05E-02 2.00E-02 1.96E-02 1.91E-02 1.87E-02 1.83E-02 1.78E-02
c       1.74E-02 1.70E-02 1.66E-02 1.62E-02 1.59E-02 1.55E-02 1.52E-02
c       1.48E-02 1.45E-02 1.41E-02 1.37E-02 1.33E-02 1.29E-02 1.26E-02
c       1.22E-02 1.18E-02 1.15E-02 1.12E-02 1.10E-02 1.07E-02 1.05E-02
c       1.03E-02 9.99E-03 9.71E-03 9.50E-03 9.24E-03 8.92E-03 8.64E-03
c       8.36E-03 8.12E-03 7.90E-03 7.68E-03 7.48E-03 7.27E-03 7.07E-03
c       6.89E-03 6.74E-03 6.59E-03 6.44E-03 6.30E-03 6.16E-03 6.03E-03
c       5.89E-03 5.76E-03 5.61E-03 5.48E-03 5.36E-03 5.24E-03 5.12E-03
c       5.00E-03 4.89E-03 4.79E-03 4.69E-03 4.59E-03 4.47E-03 4.35E-03
c       4.24E-03 4.13E-03 4.01E-03 3.88E-03 3.76E-03 3.65E-03 3.55E-03
c       3.46E-03 3.38E-03 3.31E-03 3.24E-03 3.16E-03 3.06E-03 3.00E-03
c       2.92E-03 2.82E-03 2.73E-03 2.65E-03 2.57E-03 2.50E-03 2.44E-03
c       2.37E-03 2.31E-03 2.25E-03 2.19E-03 2.14E-03 2.10E-03 2.05E-03
c       2.00E-03 1.96E-03 1.91E-03 1.87E-03 1.82E-03 1.78E-03 1.73E-03
c       1.69E-03 1.65E-03 1.62E-03 1.58E-03 1.55E-03 1.52E-03 1.48E-03
c       1.45E-03 1.41E-03 1.37E-03 1.33E-03 1.29E-03 1.25E-03 1.22E-03
c       1.32E-03 2.30E-03 3.42E-03 5.14E-03 7.47E-03 9.81E-03 1.21E-02
c       1.50E-02 1.72E-02 1.88E-02 2.07E-02 2.41E-02 2.85E-02 3.25E-02
c       3.45E-02 3.63E-02 3.92E-02 4.34E-02 4.75E-02 5.17E-02 5.54E-02
c       5.88E-02 6.22E-02 6.56E-02 6.89E-02 7.21E-02 7.53E-02 7.87E-02
c       8.35E-02 8.90E-02 9.40E-02 9.84E-02 0.1028  0.10719 0.11159
c       0.1168  0.12285 0.1289  0.13495 0.14249 0.15156 0.16064
c       0.16972 0.17996 0.19106 0.20215 0.21324 0.22433 0.2355
c       0.24679 0.25808 0.26937 0.28343 0.3002  0.31377 0.32985
c       0.35143 0.37279 0.39399 0.41513 0.43618 0.45989 0.48723
c       0.52114 0.60851 0.58219 0.60668 0.63186 0.65704 0.6847
c       0.71492 0.74514 0.77536 0.80966 0.84755 0.88541 0.92327
c       0.96113 0.99898 1.036   1.0762  1.121   1.1658  1.2108
c       1.2701  1.3422  1.4141  1.4853  1.5655  1.6551  1.7385
c       1.8209  1.9007  1.9792  2.0501  2.1161  2.1808  2.2613
c       2.3631  2.4527  2.5568  2.6896  2.8231  2.9491  2.9958
c       3.6977  3.2342  3.0268  2.8203  2.4702  1.847   1.4987
c       47.95   11.453  7.992   6.9729  7.1782  6.8319  6.5956
c       6.3106  6.1853  6.0401  5.8443  5.6119  5.4173  5.1978
c       4.876   4.4319  3.9828  3.3528  2.5526  1.8707  1.3509
c       4.3232  19.048  64.493  114.1   111.28  91.836  78.667
c       69.75   64.073  58.46   54.959  52.558  51.326  50.237
c       49.28   50.095  49.722  52.107  51.897  52.654  53.508
c       55.405  57.416  77.958  124.55  58.334  52.618  55.29
c       56.767  59.302  64.575  87.944  136.8   78.336  87.781
c       111.49  111.79  75.692  62.673  88.994  88.76   98.979
c       105.98  163.02  78.342  129.21  129.4   95.218  106.92
c       105.49  102.82  118.92  131.19  115.67  106.91  135.04
c       98.845  120.2   131.5   118.02  113.87  119.06  111.27
```

```
c          69.524   115.13   108.84   134.34   131.64   108.71   164.41
c          134.86   140.92   138.38   158.64   185.61   160.67   145.5
c          149.16   170.31   145.7    120.15   116.98   145.6    152.07
c          180.05   164.7    137.1    153      127.71   175.38   150.09
c          139.27   119.27   150.92   162.25   146.89   141.77   161.1
c          139.16   169.27   168.43   167.05   162.91   170.31   174.8
c          175.34   186.4    165      154.43   158.42   162.02   166.61
c          165.83   163.86   146.75   160.22   177.57   174.58   153.88
c          150.69   166.21   169.82   164.41   156.1    161.96   164.06
c          164.49   166.21   168.63   163.36   164.67   154.76   154.6
c          155.51   159      162.91   160.05   158.75   155.61   159.52
c          166.03   165.38   168.62   165.79   166.62   165.46   165.66
c          168.17   167.95   167.71   167.47   167.22   167.27   167.6
c          167.94   168.28   168.62   168.66   168.39   168.11   167.83
c          167.53   167.16   166.73   166.29   165.86   165.4    165.54
c          166.34   167.14   167.94   168.73   169.21   169.37   169.52
c          169.66   169.79   169.93   170.09   170.25   170.4    170.56
c          170.72   170.86   171.32   173.63   176.3    177.74   177.89
c          178.03   178.18   178.32   178.27   178.01   177.76   177.5
c          177.24   177.49   178.28   179.08   179.88   180.67   181.24
c          181.58   181.91   182.24   182.59   182.94   183.28   183.62
c          183.97   184.31   184.45   184.37   184.28   184.2    184.11
c          184      183.88   183.75   183.63   183.51   183.38   183.25
c          183.12   183      182.87
c fs674    6002 6007 6012 6017 6022 6027 6032 6037 6042 6047 6052 6057
c fq674    s f
c
c *f694:n  (455<u=45)
c fc694    3L Neutron Tally for Calculation of Average Neutron Energy
c fs694    6002 6007 6012 6017 6022 6027 6032 6037 6042 6047 6052 6057
c fq694    s f
c
c *f704:p  (455<u=45)
c fc704    3L Photon Tally for Calculation of Average Photon Energy
c fs704    6002 6007 6012 6017 6022 6027 6032 6037 6042 6047 6052 6057
c fq704    s f
c
c f714:p   (1752<u=82)
c fc714    CT Photon Tally
c
c f724:p   (1752<u=82)
c fc724    CT Photon Tally for Calculation of Photon Dose (Kerma)
c de724    1.00E-02 3.00E-02 5.00E-02 7.00E-02 1.00E-01 1.50E-01
c          2.00E-01 2.50E-01 3.00E-01 0.35 0.4 0.45 0.5 0.55 0.6
c          0.65 0.7 0.8 1.0 1.4 1.8 2.2 2.6 2.8 3.25 3.75 4.25 4.75
c          5.0 5.25 5.75 6.25 6.75 7.5 9.0 11.0 13.0 15.0
c df724    3.96E-06 5.82E-07 2.90E-07 2.58E-07 2.83E-07 3.79E-07
c          5.01E-07 6.31E-07 7.59E-07 8.78E-07 9.85E-07 1.08E-06
c          1.17E-06 1.27E-06 1.36E-06 1.44E-06 1.52E-06 1.68E-06
c          1.98E-06 2.51E-06 2.99E-06 3.42E-06 3.82E-06 4.01E-06
c          4.41E-06 4.83E-06 5.23E-06 5.60E-06 5.80E-06 6.01E-06
c          6.37E-06 6.74E-06 7.11E-06 7.66E-06 8.77E-06 1.03E-05
c          1.18E-05 1.33E-05
c
c *f734:p  (1752<u=82)
c fc734    CT Photon Tally for Calculation of Average Photon Energy
c
c f804:p   1800 1801 1802 1803 1804 1805 1806
c fc804    Photon Tally for Radial Profile
c
c f824:n   (124<u=8)
c fc824    Neutron flux tally for peaking factors in fuel pins
c fs824    6015 6017 6019 6021 6023 6025 6027 6029 6031 6033 6035 6037
c          6039 6041 6043 6045 6047 6049 T
c fq824    s f
c
c f17:n    (124<u=8)
c fc17     Fission energy deposition averaged over a cell [MeV/g]
c fs17     6015 6017 6019 6021 6023 6025 6027 6029 6031 6033 6035 6037
c          6039 6041 6043 6045 6047 6049 T
c fq17     s f
c
c -----------------------
c Criticality calculation
c -----------------------
c 100000 n/cycle, 1.000 as initial guess, skip 10, total of 60 keff cycles,
c automatic plotting of three combined keff tally
c
 kcode   1000000 1.000 10 60 4500 0 6500 1
 mplot freq 10 kcode 16 scales 2
 ksrc     -4.5  21.8  13   0    21.8  13   4.5  21.8  13  -11    18    13
          -6.5  18.0  13  -2    18.0  13   2.0  18    13    6.5  18    13
          11    18    13 -17.5  14.3  13 -13    14.3  13   -9    14.3  13
          -4.5  14.3  13   0    14.3  13   4.5  14.3  13    9    14.3  13
```

```
          13    14.3  13 -19.5  10.5  13 -15.5  10.5  13  -11    10.5  13
          -6.5  10.5  13   2    10.5  13   6.5  10.5  13   11    10.5  13
          15.5  10.5  13  19.5  10.5  13 -22     6.8  13  -17.5   6.8  13
         -13     6.8  13  -9     6.8  13  -4.5   6.8  13    0     6.8  13
           4.5   6.8  13   9     6.8  13  13     6.8  13   17.5   6.8  13
         -19.5   2.8  13 -15.5   2.8  13 -11     2.8  13   -6.5   2.8  13
          -2     2.8  13   2     2.8  13   6.5   2.8  13   11     2.8  13
          15.5   2.8  13  19.5   2.8  13 -22    -0.8  13  -17.5  -0.8  13
         -13    -0.8  13  -4.5  -0.8  13   4.5  -0.8  13   13    -0.8  13
          17.5  -0.8  13  22    -0.8  13 -24    -4.6  13  -19.5  -4.6  13
         -15.5  -4.6  13 -11    -4.6  13  -6.5  -4.6  13   -2    -4.6  13
           2    -4.6  13   6.5  -4.6  13  11    -4.6  13   15.5  -4.6  13
          19.5  -4.6  13 -22    -8.3  13  -9    -8.3  13   -4.5  -8.3  13
           0    -8.3  13   4.5  -8.3  13   9    -8.3  13   13    -8.3  13
          17.5  -8.3  13  22    -8.3  13 -11   -12    13   -6.5 -12    13
           2   -12    13   6.5 -12    13  11   -12    13   15.5 -12    13
          19.5 -12    13 -17.5 -15.9  13 -13   -15.9  13   -9   -15.9  13
          -4.5 -15.9  13   0   -15.9  13   4.5 -15.9  13    9   -15.9  13
          13   -15.9  13  17.5 -15.9  13 -15.5 -19.7  13  -11   -19.7  13
          -6.5 -19.7  13  -2   -19.7  13   2   -19.7  13    6.5 -19.7  13
          11   -19.7  13  -4.5 -23.5  13   0   -23.5  13    4.5 -23.5  13
c
c KCODE nsrck rkk ikz kct msrk knrm mrkp kc8
c  nsrck - number of source histories per cycle (def=1000)
c  rkk   - initial guess for keff (def=1.0)
c  ikz   - number of cycles to be skipped before beginning tally accumulation
c  kct   - number of cycles to be done (def=ikz+100)
c  msrk  - number of source points for which to allocate storage (def=4500)
c  knrm  - controls normalization of tallies
c           knrm=0, normalization by weight (def)
c           knrm=1, normalization by number of histories
c  mrkp  - maximum number of cycle values on MCTAL or RUNTPE (def=6500)
c  kc8   - controls the number of cycles over which summary and tally info
c         are averaged
c           kc8=0, averaged over all cycles
c           kc8=1, averaged over all active cycles (def)
c
c PIKMT    1001  0   5010  0   5011  0   6000  0   7014  0   8016  0
c        12000  0  13027  0  14000  0  15031  0  16000  0  24000  0
c        25055  0  26000  0  26054  0  26058  0  27059  0  28000  0
c        28058  0  28064  0  29000  0  29063  0  30000  0  40090  0
c        40091  0  40092  0  40094  0  40096  0  42098  0  48000 -1
c        79197  0  82000  0  92235  0  92238  0
 thtme 0     $ time in shakes (1e-8 sec) at which thermal temperatures...
 mode n p
 phys:p  100 0 0 0 1 -102     $ -102, Analog sampling, models only, multigroup + line emission
 imp:n   1 301r 0
 imp:p   1 301r 0
 print
c
c BURN
c  TIME=T1,T2,T3...  - duration of burn step i (days)
c  PFRAC=F1,F2,F3... - power fraction of each time step
c  POWER=P           - power level (MW)
c  MAT=M1,M2,M3...   - list of material numbers to include in the burn
c  OMIT=J1,N1,I11,I12... J2,N2,I21,I22...
c  AFMIN=A           - atom frac. min. below which the atom frac. is set to zero
c  BOPT=B1,B2,B3...  - B1 - Q value multiplier
c                      B2 - burn table output frequency, ordering, content flag
c
c tmesh
c  cmesh1:n
c  cora1 0 44i 45
c  corb1 -45 59i 45
c  corc1 1 358i 360
c endmd
```

Appendix B

OrigenArp Input File

Below is the input file entered into OrigenArp to conduct the validity test. The example simulated 0.09988 grams of naturally-enriched actce14x14 fuel irradiated at a thermal flux of 1.5266E+09 $\frac{n}{cm^2 s}$ and allowed to decay, providing output FP masses (in grams), at the following time steps (in seconds): 0, 0.001, 0.003, 0.01, 0.03, 0.1, 0.3, 1, 3, 10, 30, 100, 150, 300, 750, 1000, 1250, 1500, 3000, 7500, 10000, 12500, 15000, 30000, 75000, 100000, 125000, 150000, 300000, 750000, 1000000, 1250000, 1500000, 3000000.

```
'This SCALE input file was generated by
'OrigenArp Version  6.1 Compiled on Thu Oct  7 11:31:00 2010
=arp
actce14x14
1.0
1
0.0001157407
1.5266e+09
1
1.0
ft33f001
end
#origens
0$$ a4 33 a11 71 e t
actce14x14
3$$ 33 a3 1 0 a16 2 a33 0 e t
35$$ 0 t
56$$ 10 10 1 a6 1 a10 0 a13 3 a14 1 a15 3 a18 1 e
57** 0 a3 1e-05 1 e
95$$ 1 t
Case 1
0.09988 grams
59** 1.5266e+09 1.5266e+09 1.5266e+09 1.5266e+09 1.5266e+09 1.5266e+09
 1.5266e+09 1.5266e+09 1.5266e+09 1.5266e+09
60** 1 2 3 4 5 6 7 8 9 10
66$$ a1 2 a5 2 a9 2 e
73$$ 922350 922380 922340
74** 0.000719136 0.09915537 5.4934e-06
75$$ 2 2 2
t
56$$ 0 0 a10  1 e t
56$$ 0 0 a10  2 e t
56$$ 0 0 a10  3 e t
56$$ 0 0 a10  4 e t
56$$ 0 0 a10  5 e t
56$$ 0 0 a10  6 e t
56$$ 0 0 a10  7 e t
56$$ 0 0 a10  8 e t
56$$ 0 0 a10  9 e t
56$$ 0 0 a10  10 e t
54$$ a8 1 a11 0  e
56$$ a2 10 a6 1 a10 10 a14 1 a15 3 a17 4 e
57** 0 a3 1e-05 e
95$$ 1 t
Case 2
0.09988 grams
60** 0 0.001 0.003 0.01 0.03 0.1 0.3 1 3 10
61** f5e-06
65$$
'Gram-Atoms   Grams   Curies   Watts-All   Watts-Gamma
 3z   1   0   0   3z   3z   3z   6z
 3z   1   0   0   3z   3z   3z   6z
 3z   1   0   0   3z   3z   3z   6z
t
```

```
56$$ 0 0 a10  1 e t
56$$ 0 0 a10  2 e t
56$$ 0 0 a10  3 e t
56$$ 0 0 a10  4 e t
56$$ 0 0 a10  5 e t
56$$ 0 0 a10  6 e t
56$$ 0 0 a10  7 e t
56$$ 0 0 a10  8 e t
56$$ 0 0 a10  9 e t
56$$ 0 0 a10  10 e t
54$$ a8 1 a11 0  e
56$$ a2 10 a6 1 a10 10 a14 1 a15 3 a17 4 e
57** 10 a3 1e-05 e
95$$ 1 t
Case 3
0.09988 grams
60** 30 100 150 300 750 1000 1250 1500 3000 7500
61** f0.05
65$$
'Gram-Atoms   Grams   Curies   Watts-All   Watts-Gamma
 3z   1   0   0   3z   3z   3z   6z
 3z   1   0   0   3z   3z   3z   6z
 3z   1   0   0   3z   3z   3z   6z
t
56$$ 0 0 a10  1 e t
56$$ 0 0 a10  2 e t
56$$ 0 0 a10  3 e t
56$$ 0 0 a10  4 e t
56$$ 0 0 a10  5 e t
56$$ 0 0 a10  6 e t
56$$ 0 0 a10  7 e t
56$$ 0 0 a10  8 e t
56$$ 0 0 a10  9 e t
56$$ 0 0 a10  10 e t
54$$ a8 1 a11 0  e
56$$ a2 10 a6 1 a10 10 a14 1 a15 3 a17 4 e
57** 7500 a3 1e-05 e
95$$ 1 t
Case 4
0.09988 grams
60** 10000 12500 15000 30000 75000 100000 125000 150000 300000 750000
61** f0.05
65$$
'Gram-Atoms   Grams   Curies   Watts-All   Watts-Gamma
 3z   1   0   0   3z   3z   3z   6z
 3z   1   0   0   3z   3z   3z   6z
 3z   1   0   0   3z   3z   3z   6z
t
56$$ 0 0 a10  1 e t
56$$ 0 0 a10  2 e t
56$$ 0 0 a10  3 e t
56$$ 0 0 a10  4 e t
56$$ 0 0 a10  5 e t
56$$ 0 0 a10  6 e t
56$$ 0 0 a10  7 e t
56$$ 0 0 a10  8 e t
56$$ 0 0 a10  9 e t
56$$ 0 0 a10  10 e t
54$$ a8 1 a11 0  e
56$$ a2 4 a6 1 a10 10 a14 1 a15 3 a17 4 e
57** 750000 a3 1e-05 e
95$$ 1 t
Case 5
0.09988 grams
60** 1000000 1250000 1500000 3000000
61** f0.05
65$$
'Gram-Atoms   Grams   Curies   Watts-All   Watts-Gamma
 3z   1   0   0   3z   3z   3z   6z
 3z   1   0   0   3z   3z   3z   6z
 3z   1   0   0   3z   3z   3z   6z
t
56$$ 0 0 a10  1 e t
56$$ 0 0 a10  2 e t
56$$ 0 0 a10  3 e t
56$$ 0 0 a10  4 e t
56$$ f0 t
end
=opus
LIBUNIT=33
TYPARAMS=NUCLIDES
UNITS=GRAMS
SYMNUC=Ag-106 Ag-107 Ag-108 Ag-108M Ag-109 Ag-109M Ag-110 Ag-110M Ag-111
 Ag-111M Ag-112 Ag-113 Ag-113M Ag-114 Ag-115 Ag-115M Ag-116 Ag-116M
```

```
 Ag-117 Ag-117M Ag-118 Ag-118M Ag-119 Ag-120 Ag-121 Ag-122 Ag-123 Ag-124
 Ag-125 Ag-126 Ag-127 Ag-128 As-75 As-76 As-77 As-78 As-79 As-80 As-81
 As-82 As-82M As-83 As-84 As-85 As-86 As-87 As-88 As-89 As-90 Ba-132
 Ba-133 Ba-134 Ba-135 Ba-135M Ba-136 Ba-136M Ba-137 Ba-137M Ba-138
 Ba-139 Ba-140 Ba-141 Ba-142 Ba-143 Ba-144 Ba-145 Ba-146 Ba-147 Ba-148
 Ba-149 Ba-150 Ba-151 Ba-152 Be-10 Be-9 Br-79 Br-79M Br-80 Br-80M Br-81
 Br-82 Br-82M Br-83 Br-84 Br-84M Br-85 Br-86 Br-86M Br-87 Br-88 Br-89
 Br-90 Br-91 Br-92 Br-93 Br-94 Br-95 Br-96 C-14 Cd-108 Cd-109 Cd-110
 Cd-111 Cd-111M Cd-112 Cd-113 Cd-113M Cd-114 Cd-115 Cd-115M Cd-116
 Cd-117 Cd-117M Cd-118 Cd-119 Cd-119M Cd-120 Cd-121 Cd-122 Cd-123 Cd-124
 Cd-125 Cd-126 Cd-127 Cd-128 Cd-129 Cd-130 Cd-131 Cd-132 Ce-139 Ce-140
 Ce-141 Ce-142 Ce-143 Ce-144 Ce-145 Ce-146 Ce-147 Ce-148 Ce-149 Ce-150
 Ce-151 Ce-152 Ce-153 Ce-154 Ce-155 Ce-156 Ce-157 Co-72 Co-73 Co-74
 Co-75 Cs-132 Cs-133 Cs-134 Cs-134M Cs-135 Cs-135M Cs-136 Cs-137 Cs-138
 Cs-138M Cs-139 Cs-140 Cs-141 Cs-142 Cs-143 Cs-144 Cs-145 Cs-146 Cs-147
 Cs-148 Cs-149 Cs-150 Cu-66 Cu-67 Cu-72 Cu-73 Cu-74 Cu-75 Cu-76 Cu-77
 Cu-78 Cu-79 Cu-80 Cu-81 Dy-160 Dy-161 Dy-162 Dy-163 Dy-164 Dy-165
 Dy-165M Dy-166 Er-166 Er-167 Er-167M Er-168 Er-169 Er-170 end
NRANK=200
LIBTYPE=FISS
TIME=SEC
NPOSITION=11 12 13 14 15 16 17 18 19 20 21 22 23 24 25 26 27 28 29 30 31
 32 33 34 35 36 37 38 39 40 41 42 43 44 end
end
=opus
LIBUNIT=33
TYPARAMS=NUCLIDES
UNITS=GRAMS
SYMNUC=Er-171 Er-172 Eu-149 Eu-150 Eu-151 Eu-152 Eu-152M Eu-153 Eu-154
 Eu-155 Eu-156 Eu-157 Eu-158 Eu-159 Eu-160 Eu-161 Eu-162 Eu-163 Eu-164
 Eu-165 Ga-69 Ga-70 Ga-71 Ga-72 Ga-73 Ga-74 Ga-75 Ga-76 Ga-77 Ga-78
 Ga-79 Ga-80 Ga-81 Ga-82 Ga-83 Ga-84 Ga-85 Gd-152 Gd-153 Gd-154 Gd-155
 Gd-155M Gd-156 Gd-157 Gd-158 Gd-159 Gd-160 Gd-161 Gd-162 Gd-163 Gd-164
 Gd-165 Ge-70 Ge-71 Ge-71M Ge-72 Ge-73 Ge-73M Ge-74 Ge-75 Ge-75M Ge-76
 Ge-77 Ge-77M Ge-78 Ge-79 Ge-80 Ge-81 Ge-82 Ge-83 Ge-84 Ge-85 Ge-86
 Ge-87 Ge-88 H-3 Ho-165 Ho-166 Ho-166M I-127 I-128 I-129 I-130 I-130M
 I-131 I-132 I-133 I-133M I-134 I-134M I-135 I-136 I-136M I-137 I-138
 I-139 I-140 I-141 I-142 I-143 I-144 I-145 In-113 In-113M In-114 In-114M
 In-115 In-115M In-116 In-116M In-117 In-117M In-118 In-118M In-119
 In-119M In-120 In-120M In-121 In-121M In-122 In-122M In-123 In-123M
 In-124 In-125 In-125M In-126 In-127 In-127M In-128 In-129 In-130 In-131
 In-132 In-133 In-134 Kr-79 Kr-80 Kr-81 Kr-81M Kr-82 Kr-83 Kr-83M Kr-84
 Kr-85 Kr-85M Kr-86 Kr-87 Kr-88 Kr-89 Kr-90 Kr-91 Kr-92 Kr-93 Kr-94
 Kr-95 Kr-96 Kr-97 Kr-98 La-138 La-139 La-140 La-141 La-142 La-143
 La-144 La-145 La-146 La-147 La-148 La-149 La-150 La-151 La-152 La-153
 La-154 La-155 Li-6 Li-7 Mo-100 Mo-101 Mo-102 Mo-103 Mo-104 Mo-105
 Mo-106 Mo-107 Mo-108 Mo-109 Mo-110 Mo-111 Mo-112 Mo-113 Mo-114 Mo-115
 Mo-95 Mo-96 Mo-97 Mo-98 end
NRANK=200
LIBTYPE=FISS
TIME=SEC
NPOSITION=11 12 13 14 15 16 17 18 19 20 21 22 23 24 25 26 27 28 29 30 31
 32 33 34 35 36 37 38 39 40 41 42 43 44 end
end
=opus
LIBUNIT=33
TYPARAMS=NUCLIDES
UNITS=GRAMS
SYMNUC=Mo-99 Nb-100 Nb-100M Nb-101 Nb-102 Nb-103 Nb-104 Nb-105 Nb-106
 Nb-107 Nb-108 Nb-109 Nb-110 Nb-111 Nb-112 Nb-91 Nb-92 Nb-93 Nb-93M
 Nb-94 Nb-94M Nb-95 Nb-95M Nb-96 Nb-97 Nb-97M Nb-98 Nb-98M Nb-99 Nb-99M
 Nd-141 Nd-142 Nd-143 Nd-144 Nd-145 Nd-146 Nd-147 Nd-148 Nd-149 Nd-150
 Nd-151 Nd-152 Nd-153 Nd-154 Nd-155 Nd-156 Nd-157 Nd-158 Nd-159 Nd-160
 Nd-161 Ni-66 Ni-72 Ni-73 Ni-74 Ni-75 Ni-76 Ni-77 Ni-78 Pd-102 Pd-104
 Pd-105 Pd-106 Pd-107 Pd-107M Pd-108 Pd-109 Pd-109M Pd-110 Pd-111
 Pd-111M Pd-112 Pd-113 Pd-114 Pd-115 Pd-116 Pd-117 Pd-118 Pd-119 Pd-120
 Pd-121 Pd-122 Pd-123 Pd-124 Pd-125 Pd-126 Pm-145 Pm-146 Pm-147 Pm-148
 Pm-148M Pm-149 Pm-150 Pm-151 Pm-152 Pm-152M Pm-153 Pm-154 Pm-154M
 Pm-155 Pm-156 Pm-157 Pm-158 Pm-159 Pm-160 Pm-161 Pm-162 Pr-139 Pr-140
 Pr-141 Pr-142 Pr-142M Pr-143 Pr-144 Pr-144M Pr-145 Pr-146 Pr-147 Pr-148
 Pr-149 Pr-150 Pr-151 Pr-152 Pr-153 Pr-154 Pr-155 Pr-156 Pr-157 Pr-158
 Pr-159 Rb-100 Rb-101 Rb-85 Rb-86 Rb-86M Rb-87 Rb-88 Rb-89 Rb-90 Rb-90M
 Rb-91 Rb-92 Rb-93 Rb-94 Rb-95 Rb-96 Rb-97 Rb-98 Rb-99 Rh-102 Rh-103
 Rh-103M Rh-104 Rh-104M Rh-105 Rh-105M Rh-106 Rh-106M Rh-107 Rh-108
 Rh-108M Rh-109 Rh-109M Rh-110 Rh-110M Rh-111 Rh-112 Rh-113 Rh-114
 Rh-115 Rh-116 Rh-117 Rh-118 Rh-119 Rh-120 Rh-121 Rh-122 Rh-123 Ru-100
 Ru-101 Ru-102 Ru-103 Ru-104 Ru-105 Ru-106 Ru-107 Ru-108 Ru-109 Ru-110
 Ru-111 Ru-112 Ru-113 Ru-114 Ru-115 Ru-116 Ru-117 Ru-118 Ru-119 Ru-120
 Ru-99 end
NRANK=200
LIBTYPE=FISS
TIME=SEC
NPOSITION=11 12 13 14 15 16 17 18 19 20 21 22 23 24 25 26 27 28 29 30 31
 32 33 34 35 36 37 38 39 40 41 42 43 44 end
```

```
end
=opus
LIBUNIT=33
TYPARAMS=NUCLIDES
UNITS=GRAMS
SYMNUC=Sb-121 Sb-122 Sb-122M Sb-123 Sb-124 Sb-124M Sb-125 Sb-126 Sb-126M
 Sb-127 Sb-128 Sb-128M Sb-129 Sb-130 Sb-130M Sb-131 Sb-132 Sb-132M
 Sb-133 Sb-134 Sb-134M Sb-135 Sb-136 Sb-137 Sb-138 Sb-139 Se-76 Se-77
 Se-77M Se-78 Se-79 Se-79M Se-80 Se-81 Se-81M Se-82 Se-83 Se-83M Se-84
 Se-85 Se-85M Se-86 Se-87 Se-88 Se-89 Se-90 Se-91 Se-92 Se-93 Sm-145
 Sm-146 Sm-147 Sm-148 Sm-149 Sm-150 Sm-151 Sm-152 Sm-153 Sm-154 Sm-155
 Sm-156 Sm-157 Sm-158 Sm-159 Sm-160 Sm-161 Sm-162 Sm-163 Sm-164 Sm-165
 Sn-114 Sn-115 Sn-116 Sn-117 Sn-117M Sn-118 Sn-119 Sn-119M Sn-120 Sn-121
 Sn-121M Sn-122 Sn-123 Sn-123M Sn-124 Sn-125 Sn-125M Sn-126 Sn-127
 Sn-127M Sn-128 Sn-129 Sn-129M Sn-130 Sn-131 Sn-132 Sn-133 Sn-134 Sn-135
 Sn-136 Sr-100 Sr-101 Sr-102 Sr-103 Sr-104 Sr-86 Sr-87 Sr-87M Sr-88
 Sr-89 Sr-90 Sr-91 Sr-92 Sr-93 Sr-94 Sr-95 Sr-96 Sr-97 Sr-98 Sr-99
 Tb-159 Tb-160 Tb-161 Tb-162 Tb-162M Tb-163 Tb-163M Tb-164 Tb-165 Tc-100
 Tc-101 Tc-102 Tc-102M Tc-103 Tc-104 Tc-105 Tc-106 Tc-107 Tc-108 Tc-109
 Tc-110 Tc-111 Tc-112 Tc-113 Tc-114 Tc-115 Tc-116 Tc-117 Tc-118 Tc-98
 Tc-99 Tc-99M Te-122 Te-123 Te-123M Te-124 Te-125 Te-125M Te-126 Te-127
 Te-127M Te-128 Te-129 Te-129M Te-130 Te-131 Te-131M Te-132 Te-133
 Te-133M Te-134 Te-135 Te-136 Te-137 Te-138 Te-139 Te-140 Te-141 Te-142
 Tm-169 Tm-170 Tm-170M Tm-171 Tm-172 Xe-126 Xe-127 Xe-128 Xe-129 Xe-129M
 Xe-130 Xe-131 Xe-131M Xe-132 Xe-133 Xe-133M Xe-134 Xe-134M Xe-135
 Xe-135M Xe-136 end
NRANK=200
LIBTYPE=FISS
TIME=SEC
NPOSITION=11 12 13 14 15 16 17 18 19 20 21 22 23 24 25 26 27 28 29 30 31
 32 33 34 35 36 37 38 39 40 41 42 43 44 end
end
=opus
LIBUNIT=33
TYPARAMS=NUCLIDES
UNITS=GRAMS
SYMNUC=Xe-137 Xe-138 Xe-139 Xe-140 Xe-141 Xe-142 Xe-143 Xe-144 Xe-145
 Xe-146 Xe-147 Y-100 Y-101 Y-102 Y-103 Y-104 Y-105 Y-106 Y-107 Y-89
 Y-89M Y-90 Y-90M Y-91 Y-91M Y-92 Y-93 Y-94 Y-95 Y-96 Y-97 Y-98 Y-99
 Yb-168 Yb-169 Yb-170 Yb-171 Yb-172 Zn-66 Zn-67 Zn-68 Zn-69 Zn-69M Zn-70
 Zn-71 Zn-71M Zn-72 Zn-73 Zn-74 Zn-75 Zn-76 Zn-77 Zn-78 Zn-79 Zn-80
 Zn-81 Zn-82 Zn-83 Zr-100 Zr-101 Zr-102 Zr-103 Zr-104 Zr-105 Zr-106
 Zr-107 Zr-108 Zr-109 Zr-90 Zr-90M Zr-91 Zr-92 Zr-93 Zr-94 Zr-95 Zr-96
 Zr-97 Zr-98 Zr-99 end
NRANK=79
LIBTYPE=FISS
TIME=SEC
NPOSITION=11 12 13 14 15 16 17 18 19 20 21 22 23 24 25 26 27 28 29 30 31
 32 33 34 35 36 37 38 39 40 41 42 43 44 end
end
=opus
LIBUNIT=33
TYPARAMS=NUCLIDES
UNITS=GRAMS
SYMNUC=Np-239 U-234 U-235 U-236 U-238 U-239 end
NRANK=6
LIBTYPE=ALL
TIME=SEC
NPOSITION=11 12 13 14 15 16 17 18 19 20 21 22 23 24 25 26 27 28 29 30 31
 32 33 34 35 36 37 38 39 40 41 42 43 44 end
end
#shell
copy ft71f001 "C:\Users\Christopher\Desktop\Christopher's Documents\University of Texas\Research\PIXIE\Analysis\OrigenArp Analysis\N0523.f71"
del ft71f001
end
```

Appendix C

Validity Analysis Using OrigenArp

The following tables show the results of the OrigenArp analysis on the validity of the method of determining FP yields used in this work. Note that the efficiency can be calculated using Equation 4.5, and the half lives and gamma ray yields were taken from the Korea Atomic Energy Research Institute [46]. $*$ These values were taken from the OrigenArp output. $**$ These values were taken from the ENDF-349 library [43].

Nuclide	Half Life (s)	Gamma Energy (keV)	Efficiency at Peak	γ_i	Initial Mass (g)*	Decays From t_d to t_a	Expected Counts	Cumulative χ_i	Expected Cumulative χ_i **	Experimental/ Expected
78Zn	1.5	224.75	0.0923	0.439	9.405E-21	72.67	2.95	3.427E-05	3.580E-05	0.9572
78Ga	5.09	619.40	0.0333	0.77	8.857E-20	684.41	17.56	1.266E-04	1.390E-04	0.9106
78Ge	5220	277.30	0.0750	0.96	2.442E-19	1846.01	132.86	1.915E-04	2.080E-04	0.9207
78As	5443.2	613.80	0.0336	0.54	9.272E-20	698.26	12.67	1.882E-04	2.100E-04	0.8962
79Zn	1	702.20	0.0296	0.312	3.441E-21	26.25	0.24	1.841E-05	1.640E-05	1.1224
79Ga	2.85	464.79	0.0442	0.242	9.493E-20	724.25	7.75	1.951E-04	1.870E-04	1.0433
79Ge	19.1	109.58	0.1637	0.214	2.573E-19	1963.20	68.76	2.636E-04	4.210E-04	0.6262
79As	540	95.50	0.1755	0.0928	4.700E-19	3586.30	58.42	4.145E-04	4.470E-04	0.9272
79Se-m	233.4	95.73	0.1753	0.0962	1.163E-19	887.45	14.97	8.438E-04	4.470E-04	1.8876
79Br-m	4.86	207.20	0.0998	0.764	6.277E-27	4.79E-05	3.65E-06	9.082E-12	1.040E-11	0.8733
80Zn	0.55	712.53	0.0292	0.451	3.526E-22	2.66	3.49E-02	3.385E-06	2.420E-06	1.3988
80Ga	1.68	659.14	0.0314	0.78	3.804E-20	286.57	7.02	1.214E-04	1.190E-04	1.0204
80Ge	29.5	256.36	0.0811	0.27	1.176E-18	8860.60	194.08	1.005E-03	1.150E-03	0.8738
80As	16	666.20	0.0311	0.42	3.727E-19	2808.22	36.65	1.282E-03	1.280E-03	1.0015
81Ga	1.22	216.47	0.0957	0.374	2.113E-20	157.21	5.63	9.058E-05	8.180E-05	1.1073
81Ge	7.6	335.98	0.0616	0.5893	1.050E-18	7813.16	283.75	1.204E-03	1.350E-03	0.8919
81As	33	467.70	0.0440	0.2	1.531E-18	11393.28	100.18	1.574E-03	1.960E-03	0.8031
81Se-m	3438	103.01	0.1692	0.13	1.431E-19	1061.76	23.36	1.110E-04	6.930E-05	1.6014
81Se	1110	275.93	0.0753	0.0067	2.067E-18	15382.83	7.77	1.712E-03	2.040E-03	0.8390
82Ga	0.607	1348.07	0.0162	1	7.992E-21	58.73	0.95	6.782E-05	6.270E-05	1.0816
82Ge	4.6	1091.90	0.0197	1	9.045E-19	6648.27	130.82	1.300E-03	1.320E-03	0.9849
82As-m	13.7	654.40	0.0316	0.151	2.957E-19	2173.59	10.37	2.798E-04	2.710E-04	1.0324
82As	19	654.40	0.0316	0.72	2.140E-18	15730.43	358.00	2.115E-03	2.600E-03	0.8136
83Ge	1.9	306.51	0.0677	1	2.163E-19	1570.59	106.34	5.944E-04	4.800E-04	1.2383
83As	13.4	743.60	0.0280	0.43	3.498E-18	25402.42	305.99	3.287E-03	3.400E-03	0.9667
83Se-m	70.2	356.69	0.0580	0.175	2.473E-18	17960.16	182.15	2.562E-03	2.510E-03	1.0206
83Se	1338	356.70	0.0580	0.7	2.961E-18	21504.25	872.37	2.293E-03	2.650E-03	0.8654
83Br	8640	529.64	0.0388	0.012	2.515E-18	16453.83	7.67	2.348E-03	5.360E-03	0.4380
84As	5.5	1454.55	0.0150	0.89	1.078E-18	7734.77	103.30	1.376E-03	2.260E-03	0.6088
84Se	198	408.20	0.0505	1	1.289E-17	92498.81	4668.68	9.846E-03	9.660E-03	1.0192
84Br-m	360	424.00	0.0486	1	2.010E-19	1442.41	70.04	1.471E-04	1.670E-04	0.8808
84Br	1908	881.60	0.0239	0.416	1.090E-17	78218.13	778.66	1.039E-02	9.850E-03	1.0552
85Ge	0.25	101.90	0.1702	0.05	2.802E-21	19.86	0.17	5.578E-05	2.130E-05	2.6189
85As	2.03	1111.50	0.0194	0.0348	1.089E-18	7721.44	5.20	2.754E-03	2.190E-03	1.2577
85Se	39	345.20	0.0599	0.46	1.169E-17	82896.04	2285.54	9.143E-03	5.560E-03	1.6445
85Br	172.2	802.41	0.0261	0.0256	1.102E-17	78151.05	52.16	1.204E-02	1.280E-02	0.9410
85Kr-m	16128	151.20	0.1313	0.7498	1.557E-17	78396.41	7720.26	1.177E-02	1.290E-02	0.9125
85Kr	3.384E+08	514.00	0.0400	0.0043	3.768E-18	1.58	2.74E-04	2.701E-03	2.830E-03	0.9543
86Se	15	207.50	0.0996	0.0778	1.364E-17	95595.90	741.34	1.211E-02	1.370E-02	0.8842
86Br	55.5	1564.92	0.0139	0.64	1.455E-17	101980.13	909.93	1.594E-02	1.600E-02	0.9960
87Se	5.8	242.50	0.0857	0.37	6.440E-18	44613.30	1415.08	7.723E-03	7.600E-03	1.0162
87Br	55.9	1419.71	0.0154	0.22	2.220E-17	153805.00	520.02	1.870E-02	2.030E-02	0.9211
87Kr	4572	402.59	0.0512	0.496	3.270E-17	223692.72	5679.81	2.397E-02	2.560E-02	0.9362
87Sr-m	10116	388.53	0.0531	0.821	3.070E-24	1.83E-02	7.98E-04	2.149E-09	2.510E-09	0.8563
88Se	1.5	159.20	0.1260	1	1.200E-18	8218.22	1035.32	3.876E-03	3.920E-03	0.9887
88Br	16.4	775.28	0.0269	0.63	1.910E-17	130817.65	2220.60	1.620E-02	1.780E-02	0.9102
88Kr	10224	2392.11	0.0084	0.346	4.690E-17	275666.30	799.04	3.279E-02	3.550E-02	0.9237
88Rb	1062	1836.00	0.0117	0.214	3.760E-18	25756.32	64.70	1.849E-02	3.570E-02	0.5180
89Br	4.37	1097.82	0.0196	0.064	8.680E-18	58780.03	73.66	1.185E-02	1.090E-02	1.0868
89Kr	189	220.95	0.0939	0.201	5.690E-17	385358.66	7270.35	4.112E-02	4.510E-02	0.9118
89Rb	924	1031.92	0.0207	0.629	4.030E-17	272950.60	3557.67	4.857E-02	4.720E-02	1.0291
89Sr	4364928	908.96	0.0233	9.560E-05	6.420E-17	1984.20	4.41E-03	4.402E-02	4.730E-02	0.9308
89Y-m	15.7	908.96	0.0233	0.9916	1.910E-24	1.29E-02	2.99E-04	1.623E-09	4.730E-06	0.0003
90Br	1.9	707.05	0.0294	0.38	2.680E-18	17946.01	200.30	6.792E-03	5.640E-03	1.2042
90Kr	32.3	1118.69	0.0192	0.39	5.870E-17	393119.74	2950.38	4.421E-02	4.860E-02	0.9097
90Rb-m	258	831.69	0.0252	0.966	1.290E-17	86397.11	2107.15	1.157E-02	1.240E-02	0.9330

Nuclide	Half Life (s)	Gamma Energy (keV)	Efficiency at Peak	γ_i	Initial Mass (g)*	Decays From t_d to t_a	Expected Counts	Cumulative χ_i	Expected Cumulative χ_i **	Experimental/ Expected
90Rb	156	831.69	0.0252	0.399	3.990E-17	267228.28	2692.00	4.303E-02	4.500E-02	0.9563
90Y	230688	2186.24	0.0095	1.400E-06	2.052E-20	11.39	1.51E-07	1.141E-01	5.780E-02	1.9738
91Br	0.54	262.70	0.0792	1	3.800E-19	2516.51	199.23	3.267E-03	2.240E-03	1.4584
91Kr	8.6	506.59	0.0406	0.1914	3.390E-17	224524.94	1744.00	3.304E-02	3.550E-02	0.9307
91Rb	58	93.63	0.1770	0.338	5.580E-17	369600.10	22113.82	4.463E-02	5.580E-02	0.7999
91Sr	34200	1024.30	0.0209	0.335	8.150E-17	238712.96	1668.38	5.537E-02	5.830E-02	0.9497
91Y	5054400	1204.77	0.0180	0.0026	7.960E-17	24408.08	1.14	5.549E-02	5.830E-02	0.9519
92Br	0.34	769.00	0.0271	1	4.290E-20	280.99	7.63	5.798E-04	2.680E-04	2.1633
92Kr	1.84	142.31	0.1376	0.641	7.040E-18	46118.41	4068.54	1.798E-02	1.670E-02	1.0768
92Rb	4.48	814.98	0.0257	0.33	3.360E-17	220125.98	1868.71	4.390E-02	4.820E-02	0.9109
92Sr	9756	1383.93	0.0158	0.9	8.480E-17	483809.43	6860.27	5.654E-02	5.940E-02	0.9518
92Y	12744	934.47	0.0227	0.139	3.600E-17	186628.58	588.55	5.388E-02	6.010E-02	0.8965
93Br	0.176	117.00	0.1575	1	3.459E-21	22.41	3.53	9.273E-05	3.090E-05	3.0009
93Kr	1.29	253.42	0.0821	0.4116	1.720E-18	11145.70	376.50	6.110E-03	4.890E-03	1.2494
93Rb	5.85	432.61	0.0476	0.202	3.090E-17	200253.69	1924.41	3.464E-02	3.550E-02	0.9759
93Sr	444	590.24	0.0349	0.68	8.630E-17	559332.80	13279.46	5.967E-02	6.240E-02	0.9562
93Y	36720	266.90	0.0779	0.0732	8.780E-17	238656.96	1361.18	5.781E-02	6.350E-02	0.9104
93Zr	4.73E+13	30.77	0.1540	1	9.276E-17	2.54E-04	3.91E-05	6.072E-02	6.350E-02	0.9563
94Kr	0.21	629.20	0.0328	1	7.790E-20	499.41	16.39	1.721E-03	8.700E-04	1.9779
94Rb	2.71	836.90	0.0251	0.871	1.081E-17	69307.26	1515.36	1.946E-02	1.650E-02	1.1793
94Sr	75	1427.70	0.0153	0.942	7.942E-17	509253.48	7332.07	5.536E-02	6.060E-02	0.9136
94Y	1122	918.74	0.0230	0.56	7.782E-17	499014.03	6439.20	6.085E-02	6.450E-02	0.9434
95Rb	0.377	352.00	0.0587	0.49	7.650E-19	4852.91	139.70	9.028E-03	7.700E-03	1.1725
95Sr	25.1	685.60	0.0302	0.226	6.970E-17	442200.00	3022.03	5.113E-02	5.270E-02	0.9702
95Y	618	954.00	0.0223	0.158	8.350E-17	529788.26	1863.54	6.020E-02	6.380E-02	0.9435
95Zr	5531328	756.73	0.0276	0.5446	9.720E-17	2221.82	33.35	6.237E-02	6.500E-02	0.9595
95Nb-m	311904	204.12	0.1012	0.416	5.120E-20	20.14	0.85	3.834E-04	6.510E-04	0.5890
95Nb	3021408	756.81	0.0276	0.9981	2.150E-17	898.37	24.71	3.509E-02	6.500E-02	0.5398
96Rb	0.199	815.00	0.0257	0.78	1.500E-19	941.58	18.89	3.324E-03	2.060E-03	1.6136
96Sr	1.06	122.28	0.1531	0.765	9.370E-18	58825.22	6890.74	3.893E-02	3.760E-02	1.0355
96Y	5.3	1750.40	0.0124	0.0235	3.490E-17	219116.75	63.76	4.521E-02	6.000E-02	0.7536
97Rb	0.169	167.10	0.1210	0.26	1.750E-20	108.71	3.42	4.522E-04	3.800E-04	1.1900
97Sr	0.42	1905.00	0.0112	0.25	1.820E-18	11307.62	31.80	1.888E-02	1.750E-02	1.0788
97Y	3.76	1103.00	0.0195	0.0507	2.130E-17	132347.37	130.76	2.944E-02	4.890E-02	0.6020
97Zr	60480	743.36	0.0280	0.9306	9.370E-17	163685.24	4268.44	5.888E-02	5.980E-02	0.9846
97Nb-m	58.1	743.40	0.0280	1	8.700E-20	540.63	15.15	4.455E-01	5.630E-02	7.9121
97Nb	4428	657.94	0.0314	0.9823	5.390E-18	33125.17	1023.25	3.543E-02	6.000E-02	0.5905
98Rb	0.114	144.22	0.1362	0.2448	3.810E-21	23.43	0.78	1.447E-04	3.990E-05	3.6275
98Sr	0.65	119.35	0.1555	0.73	1.510E-18	9285.57	1054.17	1.001E-02	8.120E-03	1.2330
98Y	0.59	1223.00	0.0177	0.36	3.190E-18	19617.79	125.13	2.331E-02	1.920E-02	1.2138
98Nb-m	3060	787.36	0.0266	0.934	5.310E-18	32611.34	808.98	3.302E-03	3.860E-04	8.5553
98Nb	2.9	787.40	0.0266	0.13	6.310E-18	38809.82	134.00	1.126E-01	5.750E-02	1.9579
99Sr	0.269	125.12	0.1508	0.161	1.528E-19	930.08	22.59	2.484E-03	1.330E-03	1.8675
99Y	1.47	121.76	0.1535	0.469	8.188E-18	49844.14	3589.41	2.407E-02	2.080E-02	1.1570
99Zr	2.2	469.14	0.0438	0.552	2.591E-17	157739.11	3816.22	5.261E-02	5.630E-02	0.9344
99Nb-m	156	97.79	0.1736	0.0679	3.609E-17	219725.43	2589.99	2.372E-02	2.100E-02	1.1295
99Nb	15	137.72	0.1410	0.906	3.860E-17	235006.97	30025.57	3.405E-02	3.970E-02	0.8576
99Mo	237427	739.50	0.0282	0.1213	7.345E-17	36062.90	123.18	6.048E-02	6.110E-02	0.9899
99Tc-m	21636	322.40	0.0643	0.0262	6.130E-18	22488.61	37.88	9.283E-02	5.380E-02	1.7256
99Tc	6.623E+12	89.50	0.1803	6.500E-06	9.832E-17	1.80E-03	2.11E-09	6.046E-02	6.110E-02	0.9895
100Rb	0.053	129.20	0.1476	1	6.921E-21	41.70	6.15	5.581E-04	3.480E-04	1.6036
100Sr	0.201	963.85	0.0221	0.22	3.648E-20	219.82	1.07	7.683E-04	4.290E-04	1.7909
100Y	0.73	212.53	0.0974	0.73	1.653E-18	9961.56	708.36	9.563E-03	6.100E-03	1.5677
100Zr	7.1	504.25	0.0408	0.31	5.841E-17	352034.53	4449.32	5.570E-02	5.580E-02	0.9982
100Nb-m	3	535.67	0.0384	0.97	1.816E-18	10945.35	407.66	2.836E-03	3.110E-02	0.0912
100Nb	1.5	535.67	0.0384	0.457	1.153E-17	69493.30	1219.42	5.200E-02	3.110E-02	1.6720

Nuclide	Half Life (s)	Gamma Energy (keV)	Efficiency at Peak	γ_i	Initial Mass (g)*	Decays From t_d to t_a	Expected Counts	Cumulative χ_i	Expected Cumulative χ_i **	Experimental/ Expected
100Tc	16	539.59	0.0381	0.07	6.380E-23	0.38	1.03E-03	4.787E-08	5.590E-08	0.8563
101Sr	0.115	128.34	0.1483	0.17	4.563E-21	27.22	0.69	1.760E-04	4.490E-05	3.9202
101Y	0.43	98.21	0.1732	0.3	5.200E-19	3102.58	161.25	5.133E-03	2.830E-03	1.8139
101Zr	2.1	205.70	0.1005	0.061	1.551E-17	92548.72	567.13	3.214E-02	3.070E-02	1.0469
101Nb	7.1	276.10	0.0753	0.21	4.606E-17	274857.68	4346.28	4.477E-02	4.990E-02	0.8973
101Mo	876	505.92	0.0406	0.1162	8.179E-17	488096.01	2304.36	5.068E-02	5.170E-02	0.9803
102Sr	0.068	243.80	0.0853	0.53	6.766E-22	4.00	0.18	4.157E-05	1.730E-06	24.0291
102Y	0.36	151.73	0.1310	79	6.493E-19	3835.92	39686.72	7.474E-03	2.680E-03	2.7888
102Zr	2.9	599.60	0.0344	0.139	1.485E-17	87739.49	419.35	2.333E-02	2.050E-02	1.1382
102Mo	678	211.66	0.0978	0.038	7.289E-17	430715.63	1600.55	4.509E-02	4.280E-02	1.0534
102Tc-m	264	475.00	0.0433	0.0657	1.351E-19	798.33	2.27	8.170E-05	4.290E-02	0.0019
102Tc	5.3	475.20	0.0433	0.87	5.576E-19	3294.96	124.03	3.017E-02	2.240E-03	13.4691
103Y	0.26	149.80	0.1323	0.88	1.253E-20	73.30	8.53	1.979E-04	2.580E-05	7.6707
103Zr	1.3	247.60	0.0840	1	2.504E-18	14650.33	1230.35	7.932E-03	5.010E-03	1.5833
103Nb	1.5	538.50	0.0382	0.34	8.640E-18	50554.33	656.55	2.384E-02	1.910E-02	1.2482
103Mo	67.8	423.91	0.0486	1	4.963E-17	290411.58	14104.28	3.182E-02	2.950E-02	1.0786
103Tc	54	346.38	0.0597	0.175	1.863E-17	109018.32	1139.50	4.235E-02	3.030E-02	1.3977
103Ru	3392928	497.08	0.0414	0.91	5.785E-17	1985.95	74.74	3.420E-02	3.030E-02	1.1288
104Zr	1.2	100.90	0.1710	0.061	1.224E-18	7092.29	73.98	4.158E-03	8.340E-04	4.9853
104Nb	4.8	368.40	0.0561	1	5.332E-18	30899.69	1732.37	5.899E-03	6.550E-03	0.9007
104Mo	60	115.00	0.1591	0.01	3.055E-17	177043.06	281.72	2.125E-02	1.790E-02	1.1873
104Tc	1092	358.00	0.0577	0.89	3.259E-17	188869.45	9705.27	2.315E-02	1.880E-02	1.2314
105Mo	36	85.40	0.1834	0.25	1.827E-17	104865.72	4808.97	1.234E-02	9.160E-03	1.3468
105Tc	456	143.26	0.1369	0.157	1.889E-17	108429.88	2331.11	1.386E-02	9.640E-03	1.4379
105Ru	15984	724.30	0.0287	0.473	2.102E-17	86053.27	1168.69	1.388E-02	9.640E-03	1.4401
106Nb	1	171.55	0.1183	1	2.310E-19	1313.23	155.37	9.209E-04	1.570E-04	5.8657
106Mo	8.4	465.70	0.0442	1	7.519E-18	42749.45	1887.57	6.343E-03	3.750E-03	1.6915
106Tc	36	270.10	0.0770	0.558	6.911E-18	39294.05	1688.06	5.289E-03	4.020E-03	1.3158
130In	0.29	1905.17	0.0112	0.74	7.967E-20	369.27	3.07	8.936E-04	9.720E-04	0.9193
130Sn	222	192.50	0.1068	0.7029	1.314E-17	60908.89	4573.05	6.268E-03	1.180E-02	0.5312
130Sb-m	390	839.40	0.0250	1	9.927E-18	46016.23	1151.96	7.992E-03	1.420E-02	0.5628
130Sb	2304	793.40	0.0264	1	1.448E-17	67109.90	1769.83	7.431E-03	3.330E-03	2.2315
131In	0.28	2434.03	0.0082	0.8645	1.471E-20	67.66	0.48	1.734E-04	2.490E-04	0.6964
131Sn	56	798.50	0.0262	0.86	1.084E-17	49862.52	1124.19	5.355E-03	9.060E-03	0.5911
131Sb	1380	943.40	0.0225	0.462	4.866E-17	223837.76	2325.89	2.383E-02	2.560E-02	0.9309
131Te-m	116640	182.25	0.1122	0.0383	7.726E-18	5590.67	24.03	3.810E-03	4.120E-03	0.9246
131Te	1500	452.32	0.0455	0.1820	1.912E-17	87954.89	727.82	3.562E-02	2.550E-02	1.3967
131I	694656	364.49	0.0567	0.817	5.424E-17	7068.44	327.33	2.597E-02	2.890E-02	0.8985
131Xe-m	1030000	163.93	0.1230	0.0195	2.924E-19	25.82	6.19E-02	2.663E-04	4.050E-04	0.6575
132In	0.2	374.70	0.0551	0.6174	8.041E-21	36.70	1.25	1.289E-04	6.230E-05	2.0694
132Sn	40	340.53	0.0608	0.492	1.529E-17	69798.33	2087.29	7.679E-03	5.980E-03	1.2840
132Sb-m	168	299.20	0.0694	1	2.398E-17	109467.88	7596.75	1.277E-02	1.160E-02	1.1011
132Sb	252	973.90	0.0218	0.99	2.787E-17	127228.81	2751.76	1.303E-02	1.600E-02	0.8143
132Te	281664	228.16	0.0910	0.88	9.360E-17	29236.89	2341.18	4.348E-02	4.300E-02	1.0111
132I	8208	667.72	0.0310	0.987	2.449E-18	10198.20	312.11	1.423E-02	4.310E-02	0.3302
132Cs	559440	667.72	0.0310	0.9938	1.367E-24	2.19E-04	6.74E-06	6.304E-10	7.380E-10	0.8541
133In	0.18	1560.90	0.0140	0.005	3.930E-22	1.78	1.24E-04	6.951E-06	1.710E-06	4.0648
133Sn	1.44	962.18	0.0221	0.12	9.329E-19	4226.42	11.20	2.073E-03	1.380E-03	1.5019
133Sb	150	1096.22	0.0196	0.43	5.366E-17	243117.74	2049.62	2.524E-02	2.400E-02	1.0518
133Te-m	3324	912.67	0.0232	0.5528	6.448E-17	291429.32	3734.45	3.144E-02	3.990E-02	0.7881
133Te	744	312.08	0.0665	0.624	4.803E-17	217616.90	9026.33	2.920E-02	3.060E-02	0.9543
133I	74880	529.87	0.0388	0.87	1.267E-16	134342.66	4536.27	6.510E-02	6.700E-02	0.9716
133Xe-m	189216	223.22	0.0929	0.1	2.274E-18	1031.67	9.59	1.803E-03	1.890E-03	0.9539
133Xe	452995.2	81.00	0.1866	0.38	9.765E-17	19074.75	1352.24	7.072E-02	6.700E-02	1.0556
134Sn	1.04	872.19	0.0242	0.06	1.293E-19	581.39	0.84	3.921E-04	1.770E-04	2.2154
134Sb	0.8	1279.01	0.0170	0.011	1.370E-18	6160.47	1.15	5.397E-03	7.310E-03	0.7383

Nuclide	Half Life (s)	Gamma Energy (keV)	Efficiency at Peak	γ_i	Initial Mass (g)*	Decays From t_d to t_a	Expected Counts	Cumulative χ_i	Expected Cumulative χ_i **	Experimental/ Expected
134Te	2520	767.20	0.0272	0.295	1.487E-16	668461.08	5365.33	6.819E-02	6.970E-02	0.9784
134I-m	222	272.10	0.0764	0.7914	7.652E-18	34411.46	2081.00	3.530E-03	3.640E-03	0.9698
134I	3156	847.03	0.0248	0.954	6.938E-17	311447.01	7376.36	6.097E-02	7.830E-02	0.7787
134Xe-m	0.29	845.90	0.0249	1	1.977E-20	88.91	2.21	2.151E-04	3.190E-04	0.6744
135Sb	1.71	1127.03	0.0191	0.071	1.406E-18	6275.28	8.52	2.616E-03	1.460E-03	1.7915
135Te	19	603.70	0.0342	0.279	6.557E-17	292671.90	2789.22	3.528E-02	3.340E-02	1.0564
135I	23652	1260.41	0.0172	0.287	1.382E-16	351636.55	1738.33	6.259E-02	6.280E-02	0.9966
135Xe-m	918	526.56	0.0391	0.805	3.408E-18	15212.66	478.26	1.543E-03	1.100E-02	0.1402
135Xe	32760	249.79	0.0832	0.9	6.007E-17	122353.10	9167.20	5.110E-02	6.540E-02	0.7813
136Te	17.5	333.99	0.0620	0.188	3.012E-17	133447.99	1555.57	1.632E-02	1.340E-02	1.2182
136I	83.4	1313.02	0.0166	0.667	4.473E-17	198186.18	2190.55	2.677E-02	2.640E-02	1.0139
137Xe	229.2	455.49	0.0452	0.312	1.011E-16	444684.28	6264.59	6.170E-02	6.130E-02	1.0065
137Cs	9.514E+08	661.66	0.0313	0.851	1.372E-16	37.99	1.01	6.095E-02	6.190E-02	0.9847
137Ba-m	153.12	661.66	0.0313	0.9011	2.520E-21	11.08	0.31	1.145E-06	5.850E-02	0.0000
138I	6.5	588.83	0.0350	0.56	2.416E-17	105487.97	2067.30	1.733E-02	1.490E-02	1.1630
138Xe	846	258.41	0.0805	0.315	1.344E-16	586856.21	14878.06	6.100E-02	6.300E-02	0.9682
138Cs-m	174	79.90	0.1873	0.0037	4.329E-18	18902.94	13.08	1.948E-03	2.230E-03	0.8734
138Cs	1932	1436.00	0.0152	1	7.714E-17	336827.32	5118.90	5.838E-02	6.710E-02	0.8700
139I	2.3	527.70	0.0390	1	6.847E-18	29679.55	1156.61	9.529E-03	7.780E-03	1.2248
139Xe	39.7	218.59	0.0948	0.56	9.944E-17	431063.14	22892.55	4.770E-02	5.040E-02	0.9464
139Cs	558	1283.23	0.0169	0.083	1.115E-16	483361.00	679.45	5.562E-02	6.350E-02	0.8759
139Ba	5025.6	165.86	0.1218	0.2372	1.026E-16	436416.89	12606.26	6.800E-02	6.410E-02	1.0608
140I	0.86	376.66	0.0548	0.906	6.964E-19	2996.99	148.81	2.460E-03	1.540E-03	1.5975
140Xe	13.6	805.52	0.0260	0.2	6.758E-17	290853.35	1512.69	3.751E-02	3.650E-02	1.0278
140Cs	63.6	602.35	0.0342	0.525	8.640E-17	371863.15	6683.16	5.497E-02	5.720E-02	0.9611
140Ba	1101600	537.26	0.0383	0.2439	1.399E-16	10813.66	100.97	6.086E-02	6.210E-02	0.9800
140La	144979.2	1596.21	0.0137	0.954	1.253E-17	6937.46	90.41	2.286E-02	6.220E-02	0.3675
141Xe	1.72	909.23	0.0233	0.24	8.361E-18	35727.77	199.47	1.487E-02	1.250E-02	1.1892
141Cs	24.9	561.63	0.0366	0.0466	7.915E-17	338235.28	577.78	4.024E-02	4.170E-02	0.9650
141Ba	1098	190.33	0.1079	0.46	1.195E-16	510685.18	25352.83	5.511E-02	5.830E-02	0.9454
141La	14040	1354.52	0.0161	1.64	1.017E-16	329764.91	8699.13	5.092E-02	5.850E-02	0.8704
141Ce	2808000	145.44	0.1354	0.482	1.282E-16	3881.24	253.23	5.672E-02	5.850E-02	0.9696
142Xe	1.22	571.26	0.0360	1	2.379E-18	10093.97	363.83	5.815E-03	4.390E-03	1.3247
142Cs	1.8	359.60	0.0575	0.272	1.578E-17	66956.23	1046.72	2.662E-02	2.720E-02	0.9786
142Ba	642	255.30	0.0815	0.205	1.264E-16	536358.41	8957.06	5.506E-02	5.750E-02	0.9575
142La	5544	641.29	0.0322	0.474	9.528E-17	393273.50	6007.59	5.946E-02	5.850E-02	1.0164
143Xe	0.51	90.00	0.1799	1	1.677E-19	706.54	127.12	9.831E-04	5.300E-04	1.8550
143Cs	1.78	306.42	0.0677	0.0680	9.512E-18	40077.19	184.68	1.615E-02	1.450E-02	1.1140
143Ba	14.3	211.48	0.0979	0.249	9.299E-17	391815.95	9548.52	4.996E-02	5.550E-02	0.9002
143La	846	620.30	0.0333	0.0234	1.235E-16	520387.29	405.19	5.728E-02	5.920E-02	0.9676
143Ce	119232	293.27	0.0708	0.428	1.272E-16	82629.28	2504.88	5.738E-02	5.960E-02	0.9627
143Pr	1172448	742.10	0.0281	1.200E-06	9.878E-17	7027.11	2.37E-04	5.020E-02	5.960E-02	0.8423
145Pr	21542.4	748.28	0.0279	0.525	3.719E-18	9331.01	136.43	3.896E-02	3.930E-02	0.9913
147Ba	0.892	167.40	0.1208	0.11	7.815E-19	3202.93	42.56	2.517E-03	2.460E-03	1.0231
147La	4.02	117.72	0.1569	0.12	1.275E-17	52257.29	983.70	1.108E-02	8.890E-03	1.2465
147Ce	56	268.80	0.0774	0.072	3.808E-17	156080.75	869.38	1.897E-02	1.890E-02	1.0036
147Pr	804	314.68	0.0659	0.1254	4.370E-17	179120.08	1480.43	2.353E-02	2.250E-02	1.0459
147Nd	948672	531.02	0.0387	0.1309	5.424E-17	4629.47	23.46	2.258E-02	2.250E-02	1.0035
147Pm	82718928	121.22	0.1540	2.850E-05	4.768E-17	47.16	2.07E-04	2.024E-02	2.250E-02	0.8996
148Cs	0.15	141.70	0.1381	1	2.145E-22	0.87	0.12	4.094E-06	1.310E-07	31.2500
148Ba	0.64	56.08	0.1941	0.292	1.109E-19	451.43	25.59	4.944E-04	2.220E-04	2.2268
148La	1.1	158.47	0.1265	0.556	1.777E-18	7233.78	508.60	4.615E-03	3.590E-03	1.2856
148Ce	56	269.52	0.0772	0.1700	3.617E-17	147248.02	1931.41	1.601E-02	1.590E-02	1.0068
148Pr	136.2	301.70	0.0688	0.61	2.166E-17	88179.15	3701.23	1.520E-02	1.670E-02	0.9099
149Ce	5.2	380.00	0.0543	0.337	1.122E-17	45368.71	830.35	8.297E-03	7.780E-03	1.0664
149Pr	138	165.08	0.1222	0.099	2.371E-17	95875.63	1160.26	1.154E-02	1.070E-02	1.0788

Nuclide	Half Life (s)	Gamma Energy (keV)	Efficiency at Peak	γ_i	Initial Mass (g)*	Decays From t_d to t_a	Expected Counts	Cumulative χ_i	Expected Cumulative χ_i **	Experimental/ Expected
149Nd	6192	211.31	0.0979	0.259	2.560E-17	99400.81	2521.55	1.138E-02	1.080E-02	1.0535
149Pm	191116.8	285.95	0.0727	0.031	2.483E-17	9958.74	22.44	1.131E-02	1.080E-02	1.0470
150Pr	6.2	130.23	0.1468	0.32	7.426E-18	29827.43	1400.89	5.175E-03	6.210E-03	0.8333
150Pm	9648	333.92	0.0620	0.68	6.427E-22	2.26	0.10	2.608E-07	3.000E-07	0.8695
151Pr	18.9	484.50	0.0424	0.093	7.744E-18	30898.37	121.93	3.769E-03	3.390E-03	1.1118
151Nd	744	116.80	0.1576	0.3897	1.012E-17	40379.73	2480.37	4.712E-03	4.180E-03	1.1273
151Pm	102211.2	340.08	0.0609	0.225	1.099E-17	7780.14	106.54	4.660E-03	4.190E-03	1.1122
152Ce	1.4	114.80	0.1593	1	7.013E-19	2779.60	442.77	1.401E-03	2.060E-04	6.7989
152Pr	3.2	164.10	0.1229	0.418	2.222E-18	8807.18	452.27	2.177E-03	1.230E-03	1.7697
152Nd	684	278.56	0.0746	0.29	6.919E-18	27425.58	593.54	2.870E-03	2.640E-03	1.0871
152Pm-m	450	244.70	0.0850	0.7835	4.021E-20	159.39	10.61	1.622E-05	1.390E-05	1.1671
152Pm	246	121.80	0.1535	0.157	1.442E-18	5715.85	137.76	4.845E-03	2.660E-03	1.8214
152Eu-m	33480	344.28	0.0601	0.6854	3.896E-27	6.94E-06	2.86E-07	1.560E-12	1.360E-12	1.1473
153Pr	4.3	191.70	0.1072	0.5	9.140E-19	3599.02	192.95	7.321E-04	3.850E-04	1.9016
153Nd	32	418.34	0.0492	0.0685	3.813E-18	15014.86	50.63	2.095E-03	1.490E-03	1.4058
153Pm	324	127.30	0.1491	0.18	3.102E-18	12215.37	327.80	1.719E-03	1.580E-03	1.0879
153Sm	166665.6	103.18	0.1691	0.298	4.716E-18	2096.36	105.63	1.899E-03	1.580E-03	1.2021
154Pr	2.3	162.40	0.1239	0.152	6.572E-20	257.10	4.84	8.232E-05	5.110E-05	1.6110
154Nd	25.9	151.70	0.1310	0.13	1.832E-18	7167.12	122.04	8.317E-04	6.310E-04	1.3181
154Pm-m	162	1439.94	0.0152	0.1159	1.268E-19	496.07	0.87	5.119E-05	5.410E-05	0.9462
154Pm	102	839.36	0.0250	0.088	1.182E-18	4624.29	10.19	9.532E-04	6.860E-04	1.3895
154Eu	2.712E+08	723.31	0.0287	0.2011	4.224E-24	1.22E-06	7.03E-09	1.670E-09	1.940E-09	0.8606
155Nd	8.9	180.57	0.1131	1	6.581E-19	2557.94	289.39	3.720E-04	1.820E-04	2.0438
155Pm	42	778.60	0.0268	1	4.900E-19	1904.61	51.11	2.193E-04	3.080E-04	0.7119
155Sm	1332	104.32	0.1681	0.746	1.028E-18	3995.89	501.14	4.730E-04	3.210E-04	1.4735
155Eu	1.498E+08	86.55	0.1826	0.307	1.174E-18	0.61	3.41E-02	4.611E-04	3.210E-04	1.4364

Appendix D

Maple™15 Worksheets

D.1 Normalizing Flux to ^{131}I

The following is the Maple™15 worksheet used to calculate the flux normalized to ^{131}I.

```
> restart;
> with(inttrans);
>
#Solve for FP yields (chi1, chi2, chi3). For FPs that are too short-lived to be determined, use values for chi from ENDF library;
> ti := 10;
> td := 86220;
> ta := 28800;
>
> NULL;
> sigma := 0.272841e-21;
> N25 := 1.856157129*10^18;
>
#131 Decay Chain (131Sb -> 131Te-m & 131Te -> 131I). chi_Sb, chi_Te-m, chi_Te taken from ENDF library;
> lambda1 := 0.502281e-3;
> `&lambda;2m` := 0.594262e-5;
> lambda2 := 0.462098e-3;
> lambda3 := 0.997828e-6;
>
#Probabilities taken from JEFF 3.1.1 (2007);
> P := 0.801e-1;
> Q := .21;
>
> chi1 := 0.256e-1;
> `&chi;2m` := 0.412e-2;
> chi2 := 0.255e-1;
> chi3 := 0.289e-1;
>
> epsilon3 := 0.45463803e-1;
> gamma3 := .817;
>
#During irradiation;
#P is the probability that FP3 will decay to the metastable state of FP4;
#Q is the probability that FP4m will decay to the ground state of FP4;
> ode1 := diff(N1i(t), t) = phi*sigma*N25*chi1-lambda1*N1i(t);
> ode2m := diff(N2mi(t), t) = phi*sigma*N25*`&chi;2m`+P*lambda1*N1i(t)-`&lambda;2m`*N2mi(t);
> ode2 := diff(N2i(t), t) = phi*sigma*N25*chi2+(1-P)*lambda1*N1i(t)+Q*`&lambda;2m`*N2mi(t)-lambda2*N2i(t);
> ode3 := diff(N3i(t), t) = phi*sigma*N25*chi3+lambda2*N2i(t)+(1-Q)*`&lambda;2m`*N2mi(t)-lambda3*N3i(t);
>
#Laplace transform;
> L1 := laplace(ode1, t, s);
> Lp1 := subs(laplace(N1i(t), t, s) = N1i(s), L1);
> L2m := laplace(ode2m, t, s);
> Lp2m := subs(laplace(N2mi(t), t, s) = N2mi(s), L2m);
> L2 := laplace(ode2, t, s);
> Lp2 := subs(laplace(N2i(t), t, s) = N2i(s), L2);
> L3 := laplace(ode3, t, s);
> Lp3 := subs(laplace(N3i(t), t, s) = N3i(s), L3);
>
> solve(Lp1, N1i(s));
> solve(Lp2m, N2mi(s));
> solve(Lp2, N2i(s));
> solve(Lp3, N3i(s));
>
#No FP present prior to irradiation;
> N1i(0) := 0;
> N2mi(0) := 0;
> N2i(0) := 0;
> N3i(0) := 0;
```

```
>
#Convert back to time domain;
> N1i(t):=invlaplace(solve(Lp1,N1i(s)),s,t):
> N2mi(t):=invlaplace(solve(Lp2m,N2mi(s)),s,t):
> N2i(t):=invlaplace(solve(Lp2,N2i(s)),s,t):
> N3i(t):=invlaplace(solve(Lp3,N3i(s)),s,t):
>
#After irradiation, t=ti;
> N1(0) := 0.2581175804e-1*phi*(1.-1.*exp(-0.5022810000e-3*ti));
> N2m(0) := 1.754974371*10^(-22)*phi*(2.996402915*10^21+1.192197520*10^19*exp(-0.5022810000e-3*ti)
-3.008324890*10^21*exp(-0.5942620000e-5*ti));
> N2(0) := 2.154839214*10^(-37)*phi*(2.560554231*10^35-1.626411763*10^36*exp(-0.4620980000e-3*ti)
+1.377059276*10^36*exp(-0.5022810000e-3*ti)-6.702936365*10^33*exp(-0.5942620000e-5*ti));
> N3(0) := 1.886415335*10^(-63)*phi*(2.263240100*10^64-2.301083977*10^64*exp(-9.978280000*10^(-7)*ti)
+1.861859321*10^62*exp(-0.4620980000e-3*ti)-1.450147772*10^62*exp(-0.5022810000e-3*ti)+3.372676191*10^62*exp(-0.5942620000e-5*ti));
>
#Post irradiation FP decay & buildup;
> ode1 := diff(N1(t), t) = -lambda1*N1(t);
> ode2m := diff(N2m(t), t) = P*lambda1*N1(t)-`&lambda;2m`*N2m(t);
> ode2 := diff(N2(t), t) = (1-P)*lambda1*N1(t)+Q*`&lambda;2m`*N2m(t)-lambda2*N2(t);
> ode3 := diff(N3(t), t) = lambda2*N2(t)+(1-Q)*`&lambda;2m`*N2m(t)-lambda3*N3(t);
>
#Laplace transform;
> L1 := laplace(ode1, t, s);
> Lp1 := subs(laplace(N1(t), t, s) = N1(s), L1);
> L2m := laplace(ode2m, t, s);
> Lp2m := subs(laplace(N2m(t), t, s) = N2m(s), L2m);
> L2 := laplace(ode2, t, s);
> Lp2 := subs(laplace(N2(t), t, s) = N2(s), L2);
> L3 := laplace(ode3, t, s);
> Lp3 := subs(laplace(N3(t), t, s) = N3(s), L3);
>
#Convert back to time domain;
> N1(t):=invlaplace(solve(Lp1,N1(s)),s,t):
> N2m(t):=invlaplace(solve(Lp2m,N2m(s)),s,t):
> N2(t):=invlaplace(solve(Lp2,N2(s)),s,t):
> N3(t):=invlaplace(solve(Lp3,N3(s)),s,t):
>
#Define Activity (A_i=lambda_i*N_i). Calculate for FP5 because that is the only one that can be seen in the spectra;
> A3 := lambda3*N3(t);

>
#Calculate decays during acquisition from td to (td+ta). Integrate activity over acquisition period;
> Decays3 := int(A3, t = td .. td+ta);
>
#Calculate counts (Counts_i=epsilon_i*gamma_i*Decays_i);
> Counts3 := epsilon3*gamma3*Decays3;

>
#Solve for chi_5 using counts from spectra;
> phi := 'phi';
> phi := solve(Counts3 = 157824, phi);
```

D.2 ^{95}Zr

The following is the Maple™15 worksheet used to calculate the FP yield of ^{95}Zr.

```
> restart;
> with(inttrans);
>
#Solve for FP yields (chi1, chi2, chi3). For FPs that are too short-lived to be determined, use values for chi from ENDF library;
#95 decaychain (95Sr -> 95Y -> 95Zr). chi_Sr, chi_Y taken from ENDF library;
> ti := 10;
> td := 435960;
> ta := 86400;
>
> phi := 3.985675764*10^11;
> sigma := 0.272841e-21;
> N25 := 1.856157129*10^18;
>
> lambda1 := 0.27615426e-1;
> lambda2 := 0.1121597e-2;
> lambda3 := 0.125313e-6;
>
> chi1 := 0.527e-1;
> chi2 := 0.638e-1;
>
> epsilon3 := 0.26442698e-1;
> gamma3 := .5446;
>
#During irradiation
NULL;
> ode1 := diff(N1i(t), t) = phi*sigma*N25*chi1-lambda1*N1i(t);
> ode2 := diff(N2i(t), t) = phi*sigma*N25*chi2+lambda1*N1i(t)-lambda2*N2i(t);
> ode3 := diff(N3i(t), t) = phi*sigma*N25*chi3+lambda2*N2i(t)-lambda3*N3i(t);
>
#Laplace transform;
> L1 := laplace(ode1, t, s);
> Lp1 := subs(laplace(N1i(t), t, s) = N1i(s), L1);
> L2 := laplace(ode2, t, s);
> Lp2 := subs(laplace(N2i(t), t, s) = N2i(s), L2);
> L3 := laplace(ode3, t, s);
> Lp3 := subs(laplace(N3i(t), t, s) = N3i(s), L3);
>
#No FP present prior to irradiation;
> N1i(0) := 0;
> N2i(0) := 0;
> N3i(0) := 0;
>
#Convert back to time domain;
> N1i(t):=invlaplace(solve(Lp1,N1i(s)),s,t):
> N2i(t):=invlaplace(solve(Lp2,N2i(s)),s,t):
> N3i(t):=invlaplace(solve(Lp3,N3i(s)),s,t):
>
#After irradiation, t=ti;
> N1(0) := 3.851990471*10^8-3.851990471*10^8*exp(-0.2761542600e-1*ti);
> N2(0) := 4.015061689*10^8*exp(-0.2761542600e-1*ti)-2.136749849*10^10*exp(-0.1121597000e-2*ti)+2.096599232*10^10;
> N3(0) := 1.876532689*10^14+1.610757673*10^15*chi3-9.898827206*10^(-17)*exp(-0.2761542600e-1*ti)*(4.891363918*10^16*chi3
+1.647386648*10^23)+1.500376049*10^(-14)*exp(-0.1121597000e-2*ti)*(3.258638405*10^15*chi3+1.424302001*10^24)
-1.288355711*10^(-16)*exp(-1.253130000*10^(-7)*ti)*(1.250242972*10^31*chi3+1.456698805*10^30);
>
#Post irradiation FP decay & buildup;
> ode1 := diff(N1(t), t) = -lambda1*N1(t);
> ode2 := diff(N2(t), t) = lambda1*N1(t)-lambda2*N2(t);
> ode3 := diff(N3(t), t) = lambda2*N2(t)-lambda3*N3(t);
>
#Laplace transform;
> L1 := laplace(ode1, t, s);
> Lp1 := subs(laplace(N1(t), t, s) = N1(s), L1);
> L2 := laplace(ode2, t, s);
> Lp2 := subs(laplace(N2(t), t, s) = N2(s), L2);
> L3 := laplace(ode3, t, s);
> Lp3 := subs(laplace(N3(t), t, s) = N3(s), L3);
>
#Convert back to time domain;
> N1(t):=invlaplace(solve(Lp1,N1(s)),s,t):
> N2(t):=invlaplace(solve(Lp2,N2(s)),s,t):
> N3(t):=invlaplace(solve(Lp3,N3(s)),s,t):
>
#Define Activity (A_i=lambda_i*N_i). Calculate only for FP5 because that is what is being measured;
> A3 := lambda3*N3(t);

>
#Calculate decays during acquisition from td to (td+ta). Integrate activity over acquisition period;
```

```
> Decays3 := int(A3, t = td .. td+ta);
>
#Calculate counts (Counts_i=epsilon_i*gamma_i*Decays_i);
> Counts3 := epsilon3*gamma3*Decays3;
>
> chi3 := 'chi3';
> chi3 := solve(Counts3 = 54493, chi3);
>
> Ratio3 := chi3/(0.65e-1);
```

D.3 ^{97}Zr

The following is the Maple™15 worksheet used to calculate the FP yield of ^{97}Zr.

```
> restart;
> with(inttrans);
>
#Solve for FP yields (chi1, chi2, chi3). For FPs that are too short-lived to be determined, use values for chi from ENDF library;
#97 decaychain (97Sr -> 97Y -> 97Zr). chi_Sr, chi_Y taken from ENDF library;
> ti := 10;
> td := 435960;
> ta := 86400;
>
> phi := 3.985675764*10^11;
> sigma := 0.272841e-21;
> N25 := 1.856157129*10^18;
>
> lambda1 := 1.65035043;
> lambda2 := .184347654;
> lambda3 := 0.114608e-4;
>
> chi1 := 0.175e-1;
> chi2 := 0.489e-1;
>
> epsilon3 := 0.26805241e-1;
> gamma3 := .9306;
>
#During irradiation
NULL;
> ode1 := diff(N1i(t), t) = phi*sigma*N25*chi1-lambda1*N1i(t);
> ode2 := diff(N2i(t), t) = phi*sigma*N25*chi2+lambda1*N1i(t)-lambda2*N2i(t);
> ode3 := diff(N3i(t), t) = phi*sigma*N25*chi3+lambda2*N2i(t)-lambda3*N3i(t);
>
#Laplace transform;
> L1 := laplace(ode1, t, s);
> Lp1 := subs(laplace(N1i(t), t, s) = N1i(s), L1);
> L2 := laplace(ode2, t, s);
> Lp2 := subs(laplace(N2i(t), t, s) = N2i(s), L2);
> L3 := laplace(ode3, t, s);
> Lp3 := subs(laplace(N3i(t), t, s) = N3i(s), L3);
>
> solve(Lp1, N1i(s));
> solve(Lp2, N2i(s));
> solve(Lp3, N3i(s));
>
#No FP present prior to irradiation;
> N1i(0) := 0;
> N2i(0) := 0;
> N3i(0) := 0;
>
#Convert back to time domain;
> N1i(t):=invlaplace(solve(Lp1,N1i(s)),s,t):
> N2i(t):=invlaplace(solve(Lp2,N2i(s)),s,t):
> N3i(t):=invlaplace(solve(Lp3,N3i(s)),s,t):
>
#After irradiation, t=ti;
> N1(0) := 2.140366840*10^6-2.140366840*10^6*exp(-1.650350430*ti);
> N2(0) := 7.270374803*10^7-7.511326280*10^7*exp(-.1843476540*ti)+2.409514766*10^6*exp(-1.650350430*ti);
> N3(0) := 1.169444139*10^12+1.761211052*10^13*chi3-2.003576222*10^(-20)*exp(-1.650350430*ti)*(3.476472078*10^18*chi3
+1.343346919*10^25)+6.423429413*10^(-20)*exp(-.1843476540*ti)*(4.942287523*10^17*chi3+1.169436574*10^27)
-5.873963578*10^(-16)*exp(-0.1146080000e-4*ti)*(2.998334990*10^28*chi3+1.991021858*10^27);
>
#Post irradiation FP decay & buildup;
> ode1 := diff(N1(t), t) = -lambda1*N1(t);
> ode2 := diff(N2(t), t) = lambda1*N1(t)-lambda2*N2(t);
> ode3 := diff(N3(t), t) = lambda2*N2(t)-lambda3*N3(t);
>
#Laplace transform;
> L1 := laplace(ode1, t, s);
> Lp1 := subs(laplace(N1(t), t, s) = N1(s), L1);
> L2 := laplace(ode2, t, s);
> Lp2 := subs(laplace(N2(t), t, s) = N2(s), L2);
> L3 := laplace(ode3, t, s);
> Lp3 := subs(laplace(N3(t), t, s) = N3(s), L3);
>
#Convert back to time domain;
> N1(t):=invlaplace(solve(Lp1,N1(s)),s,t):
> N2(t):=invlaplace(solve(Lp2,N2(s)),s,t):
> N3(t):=invlaplace(solve(Lp3,N3(s)),s,t):
>
#Define Activity (A_i=lambda_i*N_i). Calculate only for FP5 because that is what is being measured;
```

```
> A3 := lambda3*N3(t);

>
#Calculate decays during acquisition from td to (td+ta). Integrate activity over acquisition period;
> Decays3 := int(A3, t = td .. td+ta);
>
#Calculate counts (Counts_i=epsilon_i*gamma_i*Decays_i);
> Counts3 := epsilon3*gamma3*Decays3;
>
> chi3 := 'chi3';
> chi3 := solve(Counts3 = 27842, chi3);
>
> Ratio3 := chi3/(0.598e-1);
```

D.4 ^{99}Mo

The following is the Maple™15 worksheet used to calculate the FP yield of ^{99}Mo.

```
> restart;
> with(inttrans);
>
#Solve for FP yields (chi1, chi2, chi3). For FPs that are too short-lived to be determined, use values for chi from ENDF library;
> ti := 10;
> td := 775200;
> ta := 259200;
>
> phi := 3.985675764*10^11;
> sigma := 0.272841e-21;
> N25 := 1.856157129*10^18;
>
#99 Decay Chain (99Zr -> 99Nb-m & 99Nb -> 99Mo). chi_Zr, chi_Nb-m, chi_Mo taken from ENDF library;
> lambda1 := .3150669;
> `&lambda;2m` := 0.4443251e-2;
> lambda2 := 0.46209812e-1;
> lambda3 := 0.291941e-5;
>
#P is the probability that FP1 will decay to the metastable state of FP2;
#Q is the probability that FP2m will decay to the ground state of FP2;
#Probabilities taken from JEFF 3.1.1 (2007);
> P := .368;
> Q := 0.2e-1;
>
> chi1 := 0.563e-1;
> `&chi;2m` := 0.21e-1;
> chi2 := 0.397e-1;
>
> epsilon3 := 0.26911889e-1;
> gamma3 := .1213;
>
#During irradiation;
> ode1 := diff(N1i(t), t) = phi*sigma*N25*chi1-lambda1*N1i(t);
> ode2m := diff(N2mi(t), t) = phi*sigma*N25*`&chi;2m`+P*lambda1*N1i(t)-`&lambda;2m`*N2mi(t);
> ode2 := diff(N2i(t), t) = phi*sigma*N25*chi2+(1-P)*lambda1*N1i(t)+Q*`&lambda;2m`*N2mi(t)-lambda2*N2i(t);
> ode3 := diff(N3i(t), t) = phi*sigma*N25*chi3+lambda2*N2i(t)+(1-Q)*`&lambda;2m`*N2mi(t)-lambda3*N3i(t);
>
#Laplace transform;
> L1 := laplace(ode1, t, s);
> Lp1 := subs(laplace(N1i(t), t, s) = N1i(s), L1);
> L2m := laplace(ode2m, t, s);
> Lp2m := subs(laplace(N2mi(t), t, s) = N2mi(s), L2m);
> L2 := laplace(ode2, t, s);
> Lp2 := subs(laplace(N2i(t), t, s) = N2i(s), L2);
> L3 := laplace(ode3, t, s);
> Lp3 := subs(laplace(N3i(t), t, s) = N3i(s), L3);
>
> solve(Lp1, N1i(s));
> solve(Lp2m, N2mi(s));
> solve(Lp2, N2i(s));
> solve(Lp3, N3i(s));
>
#No FP present prior to irradiation;
> N1i(0) := 0;
> N2mi(0) := 0;
> N2i(0) := 0;
> N3i(0) := 0;
>
#Convert back to time domain;
> N1i(t):=invlaplace(solve(Lp1,N1i(s)),s,t):
> N2mi(t):=invlaplace(solve(Lp2m,N2mi(s)),s,t):
> N2i(t):=invlaplace(solve(Lp2,N2i(s)),s,t):
> N3i(t):=invlaplace(solve(Lp3,N3i(s)),s,t):
>
#After irradiation, t=ti;
> N1(0) := 3.606882138*10^7-3.606882138*10^7*exp(-.3150669000*ti);
> N2m(0) := 1.895191643*10^9-1.908654835*10^9*exp(-0.4443251000e-2*ti)+1.346319179*10^7*exp(-.3150669000*ti);
> N2(0) := 3.324818247*10^8-4.060967623*10^6*exp(-0.4443251000e-2*ti)-3.551298779*10^8*exp(-0.4620981200e-1*ti)
+2.670902085*10^7*exp(-.3150669000*ti);
> N3(0) := 8.089414824*10^12+6.914029763*10^13*chi3+1.067698893*10^(-23)*exp(-0.4620981200e-1*ti)*(7.657106684*10^22*chi3
+3.326334024*10^31)+1.562717610*10^(-23)*exp(-0.4443251000e-2*ti)*(3.739192889*10^23*chi3+1.224772380*10^32)
-4.825056999*10^(-22)*exp(-.3150669000*ti)*(4.426814218*10^20*chi3+8.504416198*10^27)-2.119551523*10^(-26)
*exp(-0.2919410000e-5*ti)*(3.262024862*10^39*chi3+3.817637721*10^38);
>
#Post irradiation FP decay & buildup;
> ode1 := diff(N1(t), t) = -lambda1*N1(t);
> ode2m := diff(N2m(t), t) = P*lambda1*N1(t)-`&lambda;2m`*N2m(t);
```

```
> ode2 := diff(N2(t), t) = (1-P)*lambda1*N1(t)+Q*`&lambda;2m`*N2m(t)-lambda2*N2(t);
> ode3 := diff(N3(t), t) = lambda2*N2(t)+(1-Q)*`&lambda;2m`*N2m(t)-lambda3*N3(t);
>
#Laplace transform;
> L1 := laplace(ode1, t, s);
> Lp1 := subs(laplace(N1(t), t, s) = N1(s), L1);
> L2m := laplace(ode2m, t, s);
> Lp2m := subs(laplace(N2m(t), t, s) = N2m(s), L2m);
> L2 := laplace(ode2, t, s);
> Lp2 := subs(laplace(N2(t), t, s) = N2(s), L2);
> L3 := laplace(ode3, t, s);
> Lp3 := subs(laplace(N3(t), t, s) = N3(s), L3);
>
#Convert back to time domain;
> N1(t):=invlaplace(solve(Lp1,N1(s)),s,t):
> N2m(t):=invlaplace(solve(Lp2m,N2m(s)),s,t):
> N2(t):=invlaplace(solve(Lp2,N2(s)),s,t):
> N3(t):=invlaplace(solve(Lp3,N3(s)),s,t):
>
#Define Activity (A_i=lambda_i*N_i). Calculate for FP5 because that is the only one that can be seen in the spectra;
> A3 := lambda3*N3(t);

>
#Calculate decays during acquisition from td to (td+ta). Integrate activity over acquisition period;
> Decays3 := int(A3, t = td .. td+ta);
>
#Calculate counts (Counts_i=epsilon_i*gamma_i*Decays_i);
> Counts3 := epsilon3*gamma3*Decays3;

>
#Solve for chi_3 using counts from spectra;
> chi3 := 'chi3';
> chi3 := solve(Counts3 = 63566, chi3);
>
> Ratio3 := chi3/(0.611e-1);
```

D.5 ^{103}Ru

The following is the Maple™15 worksheet used to calculate the FP yield of ^{103}Ru.

```
> restart;
> with(inttrans);
>
#Solve for FP yields (chi1, chi2, chi3). For FPs that are too short-lived to be determined, use values for chi from ENDF library;
#103 decaychain (103Mo -> 103Tc -> 103Ru). chi_Mo, chi_Tc taken from ENDF library;
> ti := 10;
> td := 435960;
> ta := 86400;
>
> phi := 3.985675764*10^11;
> sigma := 0.272841e-21;
> N25 := 1.856157129*10^18;
>
> lambda1 := 0.1022341e-1;
> lambda2 := 0.12836059e-1;
> lambda3 := 0.204292e-6;
>
> chi1 := 0.295e-1;
> chi2 := 0.303e-1;
>
> epsilon3 := 0.36177727e-1;
> gamma3 := .91;
>
#During irradiation
NULL;
> ode1 := diff(N1i(t), t) = phi*sigma*N25*chi1-lambda1*N1i(t);
> ode2 := diff(N2i(t), t) = phi*sigma*N25*chi2+lambda1*N1i(t)-lambda2*N2i(t);
> ode3 := diff(N3i(t), t) = phi*sigma*N25*chi3+lambda2*N2i(t)-lambda3*N3i(t);
>
#Laplace transform;
> L1 := laplace(ode1, t, s);
> Lp1 := subs(laplace(N1i(t), t, s) = N1i(s), L1);
> L2 := laplace(ode2, t, s);
> Lp2 := subs(laplace(N2i(t), t, s) = N2i(s), L2);
> L3 := laplace(ode3, t, s);
> Lp3 := subs(laplace(N3i(t), t, s) = N3i(s), L3);
>
> solve(Lp1, N1i(s));
> solve(Lp2, N2i(s));
> solve(Lp3, N3i(s));
>
#No FP present prior to irradiation;
> N1i(0) := 0;
> N2i(0) := 0;
> N3i(0) := 0;
>
#Convert back to time domain;
> N1i(t):=invlaplace(solve(Lp1,N1i(s)),s,t):
> N2i(t):=invlaplace(solve(Lp2,N2i(s)),s,t):
> N3i(t):=invlaplace(solve(Lp3,N3i(s)),s,t):
>
#After irradiation, t=ti;
> N1(0) := 5.824418517*10^8-5.824418517*10^8*exp(-0.1022341000e-1*ti);
> N2(0) := -2.279120484*10^9*exp(-0.1022341000e-1*ti)+1.338756872*10^9*exp(-0.1283605900e-1*ti)+9.403636119*10^8;
> N3(0) := 5.908485305*10^13+9.880410212*10^14*chi3+2.323070742*10^(-13)*exp(-0.1283605900e-1*ti)*(4.329263219*10^13*chi3
-5.762967761*10^21)-3.662149373*10^(-11)*exp(-0.1022341000e-1*ti)*(3.609960976*10^11*chi3-7.814043684*10^19)
-5.968383627*10^(-14)*exp(-2.042920000*10^(-7)*ti)*(1.655458300*10^28*chi3+9.899895781*10^26);
>
#Post irradiation FP decay & buildup;
> ode1 := diff(N1(t), t) = -lambda1*N1(t);
> ode2 := diff(N2(t), t) = lambda1*N1(t)-lambda2*N2(t);
> ode3 := diff(N3(t), t) = lambda2*N2(t)-lambda3*N3(t);
>
#Laplace transform;
> L1 := laplace(ode1, t, s);
> Lp1 := subs(laplace(N1(t), t, s) = N1(s), L1);
> L2 := laplace(ode2, t, s);
> Lp2 := subs(laplace(N2(t), t, s) = N2(s), L2);
> L3 := laplace(ode3, t, s);
> Lp3 := subs(laplace(N3(t), t, s) = N3(s), L3);
>
#Convert back to time domain;
> N1(t):=invlaplace(solve(Lp1,N1(s)),s,t):
> N2(t):=invlaplace(solve(Lp2,N2(s)),s,t):
> N3(t):=invlaplace(solve(Lp3,N3(s)),s,t):
>
#Define Activity (A_i=lambda_i*N_i). Calculate only for FP5 because that is what is being measured;
```

```
> A3 := lambda3*N3(t);

>
#Calculate decays during acquisition from td to (td+ta). Integrate activity over acquisition period;
> Decays3 := int(A3, t = td .. td+ta);
>
#Calculate counts (Counts_i=epsilon_i*gamma_i*Decays_i);
> Counts3 := epsilon3*gamma3*Decays3;
>
> chi3 := 'chi3';
> chi3 := solve(Counts3 = 95026, chi3);
>
> Ratio3 := chi3/(0.303e-1);
```

D.6 ^{131}I

The following is the Maple™15 worksheet used to calculate the FP yield of ^{131}I.

```
> restart;
> with(inttrans);
>
#Solve for FP yields (chi1, chi2, chi3). For FPs that are too short-lived to be determined, use values for chi from ENDF library;
> ti := 10;
> td := 86220;
> ta := 28800;
>
> phi := 3.985675764*10^11;
> sigma := 0.272841e-21;
> N25 := 1.856157129*10^18;
>
#131 Decay Chain (131Sb -> 131Te-m & 131Te -> 131I). chi_Sb, chi_Te-m, chi_Te taken from ENDF library;
> lambda1 := 0.502281e-3;
> `&lambda;2m` := 0.594262e-5;
> lambda2 := 0.462098e-3;
> lambda3 := 0.997828e-6;
>
#Probabilities taken from JEFF 3.1.1 (2007);
> P := 0.801e-1;
> Q := .21;
>
> chi1 := 0.256e-1;
> `&chi;2m` := 0.412e-2;
> chi2 := 0.255e-1;
>
> epsilon3 := 0.45463803e-1;
> gamma3 := .817;
>
#During irradiation;
#P is the probability that FP3 will decay to the metastable state of FP4;
#Q is the probability that FP4m will decay to the ground state of FP4;
> ode1 := diff(N1i(t), t) = phi*sigma*N25*chi1-lambda1*N1i(t);
> ode2m := diff(N2mi(t), t) = phi*sigma*N25*`&chi;2m`+P*lambda1*N1i(t)-`&lambda;2m`*N2mi(t);
> ode2 := diff(N2i(t), t) = phi*sigma*N25*chi2+(1-P)*lambda1*N1i(t)+Q*`&lambda;2m`*N2mi(t)-lambda2*N2i(t);
> ode3 := diff(N3i(t), t) = phi*sigma*N25*chi3+lambda2*N2i(t)+(1-Q)*`&lambda;2m`*N2mi(t)-lambda3*N3i(t);
>
#Laplace transform;
> L1 := laplace(ode1, t, s);
> Lp1 := subs(laplace(N1i(t), t, s) = N1i(s), L1);
> L2m := laplace(ode2m, t, s);
> Lp2m := subs(laplace(N2mi(t), t, s) = N2mi(s), L2m);
> L2 := laplace(ode2, t, s);
> Lp2 := subs(laplace(N2i(t), t, s) = N2i(s), L2);
> L3 := laplace(ode3, t, s);
> Lp3 := subs(laplace(N3i(t), t, s) = N3i(s), L3);
>
> solve(Lp1, N1i(s));
> solve(Lp2m, N2mi(s));
> solve(Lp2, N2i(s));
> solve(Lp3, N3i(s));
>
#No FP present prior to irradiation;
> N1i(0) := 0;
> N2mi(0) := 0;
> N2i(0) := 0;
> N3i(0) := 0;
>
#Convert back to time domain;
> N1i(t):=invlaplace(solve(Lp1,N1i(s)),s,t):
> N2mi(t):=invlaplace(solve(Lp2m,N2mi(s)),s,t):
> N2i(t):=invlaplace(solve(Lp2,N2i(s)),s,t):
> N3i(t):=invlaplace(solve(Lp3,N3i(s)),s,t):
>
#After irradiation, t=ti;
> N1(0) := 1.028772984*10^10-1.028772984*10^10*exp(-0.5022810000e-3*ti);
> N2m(0) := 8.339134114*10^8*exp(-0.5022810000e-3*ti)-2.104250705*10^11*exp(-0.5942620000e-5*ti)+2.095911571*10^11;
> N2(0) := -1.396842185*10^11*exp(-0.4620980000e-3*ti)+1.182686041*10^11*exp(-0.5022810000e-3*ti)
-5.756810532*10^8*exp(-0.5942620000e-5*ti)+2.199129551*10^10;
> N3(0) := 1.117035697*10^13+2.022882464*10^14*chi3-1.991360590*10^(-16)*exp(-0.5022810000e-3*ti)*(9.475213770*10^18*chi3
+5.475220770*10^26)+1.202467476*10^(-18)*exp(-0.5942620000e-5*ti)*(1.379600465*10^22*chi3+2.108825274*10^29)
-5.611743984*10^(-20)*exp(-9.978280000*10^(-7)*ti)*(3.604730490*10^33*chi3+2.041235574*10^32)+2.048356079*10^(-15)
*exp(-0.4620980000e-3*ti)*(8.499638448*10^17*chi3+6.834089963*10^25);
>
#Post irradiation FP decay & buildup;
> ode1 := diff(N1(t), t) = -lambda1*N1(t);
> ode2m := diff(N2m(t), t) = P*lambda1*N1(t)-`&lambda;2m`*N2m(t);
```

```
> ode2 := diff(N2(t), t) = (1-P)*lambda1*N1(t)+Q*`&lambda;2m`*N2m(t)-lambda2*N2(t);
> ode3 := diff(N3(t), t) = lambda2*N2(t)+(1-Q)*`&lambda;2m`*N2m(t)-lambda3*N3(t);
>
#Laplace transform;
> L1 := laplace(ode1, t, s);
> Lp1 := subs(laplace(N1(t), t, s) = N1(s), L1);
> L2m := laplace(ode2m, t, s);
> Lp2m := subs(laplace(N2m(t), t, s) = N2m(s), L2m);
> L2 := laplace(ode2, t, s);
> Lp2 := subs(laplace(N2(t), t, s) = N2(s), L2);
> L3 := laplace(ode3, t, s);
> Lp3 := subs(laplace(N3(t), t, s) = N3(s), L3);
>
#Convert back to time domain;
> N1(t):=invlaplace(solve(Lp1,N1(s)),s,t):
> N2m(t):=invlaplace(solve(Lp2m,N2m(s)),s,t):
> N2(t):=invlaplace(solve(Lp2,N2(s)),s,t):
> N3(t):=invlaplace(solve(Lp3,N3(s)),s,t):
>
#Define Activity (A_i=lambda_i*N_i). Calculate for FP5 because that is the only one that can be seen in the spectra;
> A3 := lambda3*N3(t);

>
#Calculate decays during acquisition from td to (td+ta). Integrate activity over acquisition period;
> Decays3 := int(A3, t = td .. td+ta);
>
#Calculate counts (Counts_i=epsilon_i*gamma_i*Decays_i);
> Counts3 := epsilon3*gamma3*Decays3;

>
#Solve for chi_5 using counts from spectra;
> chi3 := 'chi3';
> chi3 := solve(Counts3 = 157824, chi3);
>
> Ratio3 := chi3/(0.289e-1);
```

D.7 ^{140}Ba

The following is the Maple™15 worksheet used to calculate the FP yield of ^{140}Ba.

```
> restart;
> with(inttrans);
>
#Solve for FP yields (chi1, chi2, chi3). For FPs that are too short-lived to be determined, use values for chi from ENDF library;
#140 decaychain (140Xe -> 140Cs -> 140Ba). chi_Xe, chi_Cs taken from ENDF library;
> ti := 10;
> td := 86220;
> ta := 28800;
>
> phi := 3.985675764*10^11;
> sigma := 0.272841e-21;
> N25 := 1.856157129*10^18;
>
> lambda1 := 0.50966704e-1;
> lambda2 := 0.10898541e-1;
> lambda3 := 0.629219e-6;
>
> chi1 := 0.365e-1;
> chi2 := 0.572e-1;
>
> epsilon3 := 0.3416916e-1;
> gamma3 := .2439;
>
#During irradiation
NULL;
> ode1 := diff(N1i(t), t) = phi*sigma*N25*chi1-lambda1*N1i(t);
> ode2 := diff(N2i(t), t) = phi*sigma*N25*chi2+lambda1*N1i(t)-lambda2*N2i(t);
> ode3 := diff(N3i(t), t) = phi*sigma*N25*chi3+lambda2*N2i(t)-lambda3*N3i(t);
>
#Laplace transform;
> L1 := laplace(ode1, t, s);
> Lp1 := subs(laplace(N1i(t), t, s) = N1i(s), L1);
> L2 := laplace(ode2, t, s);
> Lp2 := subs(laplace(N2i(t), t, s) = N2i(s), L2);
> L3 := laplace(ode3, t, s);
> Lp3 := subs(laplace(N3i(t), t, s) = N3i(s), L3);
>
#No FP present prior to irradiation;
> N1i(0) := 0;
> N2i(0) := 0;
> N3i(0) := 0;
>
#Convert back to time domain;
> N1i(t):=invlaplace(solve(Lp1,N1i(s)),s,t):
> N2i(t):=invlaplace(solve(Lp2,N2i(s)),s,t):
> N3i(t):=invlaplace(solve(Lp3,N3i(s)),s,t):
>
#After irradiation, t=ti;
> N1(0) := 1.445548448*10^8-1.445548448*10^8*exp(-0.5096670400e-1*ti);
> N2(0) := -1.919265659*10^9*exp(-0.1089854100e-1*ti)+1.735391894*10^9+1.838737651*10^8*exp(-0.5096670400e-1*ti);
> N3(0) := 3.005827814*10^13+3.207927229*10^14*chi3-1.681043319*10^(-15)*exp(-0.1089854100e-1*ti)*(3.597688613*10^14*chi3
-1.141776926*10^24)-1.967717665*10^(-14)*exp(-0.5096670400e-1*ti)*(1.642769315*10^13*chi3+1.998223949*10^21)
-2.289094299*10^(-17)*exp(-6.292190000*10^(-7)*ti)*(1.401395840*10^31*chi3+1.313190034*10^30);
>
#Post irradiation FP decay & buildup;
> ode1 := diff(N1(t), t) = -lambda1*N1(t);
> ode2 := diff(N2(t), t) = lambda1*N1(t)-lambda2*N2(t);
> ode3 := diff(N3(t), t) = lambda2*N2(t)-lambda3*N3(t);
>
#Laplace transform;
> L1 := laplace(ode1, t, s);
> Lp1 := subs(laplace(N1(t), t, s) = N1(s), L1);
> L2 := laplace(ode2, t, s);
> Lp2 := subs(laplace(N2(t), t, s) = N2(s), L2);
> L3 := laplace(ode3, t, s);
> Lp3 := subs(laplace(N3(t), t, s) = N3(s), L3);
>
#Convert back to time domain;
> N1(t):=invlaplace(solve(Lp1,N1(s)),s,t):
> N2(t):=invlaplace(solve(Lp2,N2(s)),s,t):
> N3(t):=invlaplace(solve(Lp3,N3(s)),s,t):
>
#Define Activity (A_i=lambda_i*N_i). Calculate only for FP5 because that is what is being measured;
> A3 := lambda3*N3(t);

>
#Calculate decays during acquisition from td to (td+ta). Integrate activity over acquisition period;
```

```
> Decays3 := int(A3, t = td .. td+ta);
>
#Calculate counts (Counts_i=epsilon_i*gamma_i*Decays_i);
> Counts3 := epsilon3*gamma3*Decays3;
>
> chi3 := 'chi3';
> chi3 := solve(Counts3 = 43968, chi3);
>
> Ratio3 := chi3/(0.621e-1);
```

D.8 ^{143}Ce

The following is the Maple™15 worksheet used to calculate the FP yield of ^{143}Ce.

```
> restart;
> with(inttrans);
>
#Solve for FP yields (chi1, chi2, chi3). For FPs that are too short-lived to be determined, use values for chi from ENDF library;
#143 decaychain (14Ba -> 143La -> 143Ce). chi_Ba, chi_La taken from ENDF library;
> ti := 10;
> td := 435960;
> ta := 86400;
>
> phi := 3.985675764*10^11;
> sigma := 0.272841e-21;
> N25 := 1.856157129*10^18;
>
> lambda1 := 0.48471831e-1;
> lambda2 := 0.819323e-3;
> lambda3 := 0.581343e-5;
>
> chi1 := 0.555e-1;
> chi2 := 0.592e-1;
>
> epsilon3 := 0.53494008e-1;
> gamma3 := .428;
>
#During irradiation
NULL;
> ode1 := diff(N1i(t), t) = phi*sigma*N25*chi1-lambda1*N1i(t);
> ode2 := diff(N2i(t), t) = phi*sigma*N25*chi2+lambda1*N1i(t)-lambda2*N2i(t);
> ode3 := diff(N3i(t), t) = phi*sigma*N25*chi3+lambda2*N2i(t)-lambda3*N3i(t);
>
#Laplace transform;
> L1 := laplace(ode1, t, s);
> Lp1 := subs(laplace(N1i(t), t, s) = N1i(s), L1);
> L2 := laplace(ode2, t, s);
> Lp2 := subs(laplace(N2i(t), t, s) = N2i(s), L2);
> L3 := laplace(ode3, t, s);
> Lp3 := subs(laplace(N3i(t), t, s) = N3i(s), L3);
>
#No FP present prior to irradiation;
> N1i(0) := 0;
> N2i(0) := 0;
> N3i(0) := 0;
>
#Convert back to time domain;
> N1i(t):=invlaplace(solve(Lp1,N1i(s)),s,t):
> N2i(t):=invlaplace(solve(Lp2,N2i(s)),s,t):
> N3i(t):=invlaplace(solve(Lp3,N3i(s)),s,t):
>
#After irradiation, t=ti;
> N1(0) := 2.311159368*10^8-2.311159368*10^8*exp(-0.4847183100e-1*ti);
> N2(0) := 2.825755668*10^10+2.350896753*10^8*exp(-0.4847183100e-1*ti)-2.849264636*10^10*exp(-0.8193230000e-3*ti);
> N3(0) := 3.982513956*10^12+3.472113301*10^13*chi3-1.786559448*10^(-17)*exp(-0.4847183100e-1*ti)*(1.020428918*10^16*chi3
+2.224507606*10^23)-6.296894541*10^(-14)*exp(-0.8193230000e-3*ti)*(4.696136915*10^13*chi3-4.557207968*10^23)
-8.725645133*10^(-16)*exp(-0.5813430000e-5*ti)*(3.979205260*10^28*chi3+4.597031141*10^27);
>
#Post irradiation FP decay & buildup;
> ode1 := diff(N1(t), t) = -lambda1*N1(t);
> ode2 := diff(N2(t), t) = lambda1*N1(t)-lambda2*N2(t);
> ode3 := diff(N3(t), t) = lambda2*N2(t)-lambda3*N3(t);
>
#Laplace transform;
> L1 := laplace(ode1, t, s);
> Lp1 := subs(laplace(N1(t), t, s) = N1(s), L1);
> L2 := laplace(ode2, t, s);
> Lp2 := subs(laplace(N2(t), t, s) = N2(s), L2);
> L3 := laplace(ode3, t, s);
> Lp3 := subs(laplace(N3(t), t, s) = N3(s), L3);
>
#Convert back to time domain;
> N1(t):=invlaplace(solve(Lp1,N1(s)),s,t):
> N2(t):=invlaplace(solve(Lp2,N2(s)),s,t):
> N3(t):=invlaplace(solve(Lp3,N3(s)),s,t):
>
#Define Activity (A_i=lambda_i*N_i). Calculate only for FP5 because that is what is being measured;
> A3 := lambda3*N3(t);

>
#Calculate decays during acquisition from td to (td+ta). Integrate activity over acquisition period;
```

```
> Decays3 := int(A3, t = td .. td+ta);
>
#Calculate counts (Counts_i=epsilon_i*gamma_i*Decays_i);
> Counts3 := epsilon3*gamma3*Decays3;
>
> chi3 := 'chi3';
> chi3 := solve(Counts3 = 250275, chi3);
>
> Ratio3 := chi3/(0.596e-1);
```

D.9 ^{144}Ce

The following is the Maple™15 worksheet used to calculate the FP yield of ^{144}Ce.

```
> restart;
> with(inttrans);
>
#Solve for FP yields (chi1, chi2, chi3). For FPs that are too short-lived to be determined, use values for chi from ENDF library;
#144 decaychain (144Ba -> 144La -> 144Ce). chi_Ba, chi_La taken from ENDF library;
> ti := 10;
> td := 775200;
> ta := 259200;
>
> phi := 3.985675764*10^11;
> sigma := 0.272841e-21;
> N25 := 1.856157129*10^18;
>
> lambda1 := 0.60802384e-1;
> lambda2 := 0.17030643e-1;
> lambda3 := 0.281888e-7;
>
> chi1 := 0.44e-1;
> chi2 := 0.547e-1;
>
> epsilon3 := 0.93516338e-1;
> gamma3 := .1109;
>
#During irradiation
NULL;
> ode1 := diff(N1i(t), t) = phi*sigma*N25*chi1-lambda1*N1i(t);
> ode2 := diff(N2i(t), t) = phi*sigma*N25*chi2+lambda1*N1i(t)-lambda2*N2i(t);
> ode3 := diff(N3i(t), t) = phi*sigma*N25*chi3+lambda2*N2i(t)-lambda3*N3i(t);
>
#Laplace transform;
> L1 := laplace(ode1, t, s);
> Lp1 := subs(laplace(N1i(t), t, s) = N1i(s), L1);
> L2 := laplace(ode2, t, s);
> Lp2 := subs(laplace(N2i(t), t, s) = N2i(s), L2);
> L3 := laplace(ode3, t, s);
> Lp3 := subs(laplace(N3i(t), t, s) = N3i(s), L3);
>
#No FP present prior to irradiation;
> N1i(0) := 0;
> N2i(0) := 0;
> N3i(0) := 0;
>
#Convert back to time domain;
> N1i(t):=invlaplace(solve(Lp1,N1i(s)),s,t):
> N2i(t):=invlaplace(solve(Lp2,N2i(s)),s,t):
> N3i(t):=invlaplace(solve(Lp3,N3i(s)),s,t):
>
#After irradiation, t=ti;
> N1(0) := 1.460691172*10^8-1.460691172*10^8*exp(-0.6080238400e-1*ti);
> N2(0) := -1.372703695*10^9*exp(-0.1703064300e-1*ti)+2.029014691*10^8*exp(-0.6080238400e-1*ti)+1.169802226*10^9;
> N3(0) := 7.067517630*10^14+7.160605498*10^15*chi3-3.150683647*10^(-16)*exp(-0.1703064300e-1*ti)*(9.007657717*10^15*chi3
-4.356851151*10^24)-6.327980344*10^(-15)*exp(-0.6080238400e-1*ti)*(5.604289280*10^13*chi3+8.981124340*10^21)
-1.403242167*10^(-15)*exp(-2.818880000*10^(-8)*ti)*(5.102900743*10^30*chi3+5.036572413*10^29);
>
#Post irradiation FP decay & buildup;
> ode1 := diff(N1(t), t) = -lambda1*N1(t);
> ode2 := diff(N2(t), t) = lambda1*N1(t)-lambda2*N2(t);
> ode3 := diff(N3(t), t) = lambda2*N2(t)-lambda3*N3(t);
>
#Laplace transform;
> L1 := laplace(ode1, t, s);
> Lp1 := subs(laplace(N1(t), t, s) = N1(s), L1);
> L2 := laplace(ode2, t, s);
> Lp2 := subs(laplace(N2(t), t, s) = N2(s), L2);
> L3 := laplace(ode3, t, s);
> Lp3 := subs(laplace(N3(t), t, s) = N3(s), L3);
>
#Convert back to time domain;
> N1(t):=invlaplace(solve(Lp1,N1(s)),s,t):
> N2(t):=invlaplace(solve(Lp2,N2(s)),s,t):
> N3(t):=invlaplace(solve(Lp3,N3(s)),s,t):
>
#Define Activity (A_i=lambda_i*N_i). Calculate only for FP5 because that is what is being measured;
> A3 := lambda3*N3(t);

>
#Calculate decays during acquisition from td to (td+ta). Integrate activity over acquisition period;
```

```
> Decays3 := int(A3, t = td .. td+ta);
>
#Calculate counts (Counts_i=epsilon_i*gamma_i*Decays_i);
> Counts3 := epsilon3*gamma3*Decays3;
> chi3 := 'chi3';
> chi3 := solve(Counts3 = 22230, chi3);
>
> Ratio3 := chi3/(0.55e-1);
```

D.10 ^{145}Pr

The following is the Maple™15 worksheet used to calculate the FP yield of ^{145}Pr.

```
> restart;
> with(inttrans);
>
#Solve for FP yields (chi1, chi2, chi3). For FPs that are too short-lived to be determined, use values for chi from ENDF library;
#145 decaychain (145La -> 145Ce -> 145Pr). chi_La, chi_Ce taken from ENDF library;
> ti := 10;
> td := 86220;
> ta := 28800;
>
> phi := 3.985675764*10^11;
> sigma := 0.272841e-21;
> N25 := 1.856157129*10^18;
>
> lambda1 := 0.28881133e-1;
> lambda2 := 0.3850818e-2;
> lambda3 := 0.321975e-4;
>
> chi1 := 0.385e-1;
> chi2 := 0.393e-1;
>
> epsilon3 := 0.26670653e-1;
> gamma3 := .525;
>
#During irradiation
NULL;
> ode1 := diff(N1i(t), t) = phi*sigma*N25*chi1-lambda1*N1i(t);
> ode2 := diff(N2i(t), t) = phi*sigma*N25*chi2+lambda1*N1i(t)-lambda2*N2i(t);
> ode3 := diff(N3i(t), t) = phi*sigma*N25*chi3+lambda2*N2i(t)-lambda3*N3i(t);
>
#Laplace transform;
> L1 := laplace(ode1, t, s);
> Lp1 := subs(laplace(N1i(t), t, s) = N1i(s), L1);
> L2 := laplace(ode2, t, s);
> Lp2 := subs(laplace(N2i(t), t, s) = N2i(s), L2);
> L3 := laplace(ode3, t, s);
> Lp3 := subs(laplace(N3i(t), t, s) = N3i(s), L3);
>
#No FP present prior to irradiation;
> N1i(0) := 0;
> N2i(0) := 0;
> N3i(0) := 0;
>
#Convert back to time domain;
> N1i(t):=invlaplace(solve(Lp1,N1i(s)),s,t):
> N2i(t):=invlaplace(solve(Lp2,N2i(s)),s,t):
> N3i(t):=invlaplace(solve(Lp3,N3i(s)),s,t):
>
#After irradiation, t=ti;
> N1(0) := 2.690746841*10^8-2.690746841*10^8*exp(-0.2888113300e-1*ti);
> N2(0) := -4.388524488*10^9*exp(-0.3850818000e-2*ti)+4.078053695*10^9+3.104707925*10^8*exp(-0.2888113300e-1*ti);
> N3(0) := 4.877348418*10^11+6.269085372*10^12*chi3-1.918004656*10^(-16)*exp(-0.2888113300e-1*ti)*(2.275884930*10^16*chi3
+2.160699113*10^23)-4.347045387*10^(-14)*exp(-0.3850818000e-2*ti)*(1.452552117*10^14*chi3-1.018054071*10^23)
-7.048254291*10^(-12)*exp(-0.3219750000e-4*ti)*(8.894522123*10^23*chi3+6.982139215*10^22);
>
#Post irradiation FP decay & buildup;
> ode1 := diff(N1(t), t) = -lambda1*N1(t);
> ode2 := diff(N2(t), t) = lambda1*N1(t)-lambda2*N2(t);
> ode3 := diff(N3(t), t) = lambda2*N2(t)-lambda3*N3(t);
>
#Laplace transform;
> L1 := laplace(ode1, t, s);
> Lp1 := subs(laplace(N1(t), t, s) = N1(s), L1);
> L2 := laplace(ode2, t, s);
> Lp2 := subs(laplace(N2(t), t, s) = N2(s), L2);
> L3 := laplace(ode3, t, s);
> Lp3 := subs(laplace(N3(t), t, s) = N3(s), L3);
>
#Convert back to time domain;
> N1(t):=invlaplace(solve(Lp1,N1(s)),s,t):
> N2(t):=invlaplace(solve(Lp2,N2(s)),s,t):
> N3(t):=invlaplace(solve(Lp3,N3(s)),s,t):
>
#Define Activity (A_i=lambda_i*N_i). Calculate only for FP5 because that is what is being measured;
> A3 := lambda3*N3(t);

>
#Calculate decays during acquisition from td to (td+ta). Integrate activity over acquisition period;
```

```
> Decays3 := int(A3, t = td .. td+ta);
>
#Calculate counts (Counts_i=epsilon_i*gamma_i*Decays_i);
> Counts3 := epsilon3*gamma3*Decays3;
>
> chi3 := 'chi3';
> chi3 := solve(Counts3 = 122347, chi3);
> Ratio3 := chi3/(0.393e-1);
```

D.11 ^{147}Nd

The following is the Maple™15 worksheet used to calculate the FP yield of ^{147}Nd.

```
> restart;
> with(inttrans);
>
#Solve for FP yields (chi1, chi2, chi3). For FPs that are too short-lived to be determined, use values for chi from ENDF library;
#147 decaychain (147Ce -> 147Pr -> 147Nd). chi_Ce, chi_Pr taken from ENDF library;
> ti := 10;
> td := 775200;
> ta := 259200;
>
> phi := 3.985675764*10^11;
> sigma := 0.272841e-21;
> N25 := 1.856157129*10^18;
>
> lambda1 := 0.12377628e-1;
> lambda2 := 0.862123e-3;
> lambda3 := 0.73065e-6;
>
> chi1 := 0.225e-1;
> chi2 := 0.225e-1;
>
> epsilon3 := 0.34464409e-1;
> gamma3 := .130851;
>
#During irradiation
NULL;
> ode1 := diff(N1i(t), t) = phi*sigma*N25*chi1-lambda1*N1i(t);
> ode2 := diff(N2i(t), t) = phi*sigma*N25*chi2+lambda1*N1i(t)-lambda2*N2i(t);
> ode3 := diff(N3i(t), t) = phi*sigma*N25*chi3+lambda2*N2i(t)-lambda3*N3i(t);
>
#Laplace transform;
> L1 := laplace(ode1, t, s);
> Lp1 := subs(laplace(N1i(t), t, s) = N1i(s), L1);
> L2 := laplace(ode2, t, s);
> Lp2 := subs(laplace(N2i(t), t, s) = N2i(s), L2);
> L3 := laplace(ode3, t, s);
> Lp3 := subs(laplace(N3i(t), t, s) = N3i(s), L3);
>
> solve(Lp1, N1i(s));
> solve(Lp2, N2i(s));
> solve(Lp3, N3i(s));
>
#No FP present prior to irradiation;
> N1i(0) := 0;
> N2i(0) := 0;
> N3i(0) := 0;
>
#Convert back to time domain;
> N1i(t):=invlaplace(solve(Lp1,N1i(s)),s,t):
> N2i(t):=invlaplace(solve(Lp2,N2i(s)),s,t):
> N3i(t):=invlaplace(solve(Lp3,N3i(s)),s,t):
>
#After irradiation, t=ti;
> N1(0) := 3.669200365*10^8-3.669200365*10^8*exp(-0.1237762800e-1*ti);
> N2(0) := 3.943899740*10^8*exp(-0.1237762800e-1*ti)+1.053585096*10^10-1.093024093*10^10*exp(-0.8621230000e-3*ti);
> N3(0) := 1.243166966*10^13+2.762593257*10^14*chi3-7.618457782*10^(-14)*exp(-0.1237762800e-1*ti)*(7.451604125*10^12*chi3
+3.605921295*10^20)-4.677424231*10^(-14)*exp(-0.8621230000e-3*ti)*(5.650371538*10^14*chi3-2.338789820*10^23)
-3.851226547*10^(-13)*exp(-7.306500000*10^(-7)*ti)*(7.173281611*10^26*chi3+3.230810120*10^25);
>
#Post irradiation FP decay & buildup;
> ode1 := diff(N1(t), t) = -lambda1*N1(t);
> ode2 := diff(N2(t), t) = lambda1*N1(t)-lambda2*N2(t);
> ode3 := diff(N3(t), t) = lambda2*N2(t)-lambda3*N3(t);
>
#Laplace transform;
> L1 := laplace(ode1, t, s);
> Lp1 := subs(laplace(N1(t), t, s) = N1(s), L1);
> L2 := laplace(ode2, t, s);
> Lp2 := subs(laplace(N2(t), t, s) = N2(s), L2);
> L3 := laplace(ode3, t, s);
> Lp3 := subs(laplace(N3(t), t, s) = N3(s), L3);
>
#Convert back to time domain;
> N1(t):=invlaplace(solve(Lp1,N1(s)),s,t):
> N2(t):=invlaplace(solve(Lp2,N2(s)),s,t):
> N3(t):=invlaplace(solve(Lp3,N3(s)),s,t):
>
#Define Activity (A_i=lambda_i*N_i). Calculate only for FP5 because that is what is being measured;
```

```
> A3 := lambda3*N3(t);

>
#Calculate decays during acquisition from td to (td+ta). Integrate activity over acquisition period;
> Decays3 := int(A3, t = td .. td+ta);
>
#Calculate counts (Counts_i=epsilon_i*gamma_i*Decays_i);
> Counts3 := epsilon3*gamma3*Decays3;
>
> chi3 := 'chi3';
> chi3 := solve(Counts3 = 58193, chi3);
> Ratio3 := chi3/(0.225e-1);
```

References

[1] Matthew Bunn and Anthony Weir. The seven myths of nuclear terrorism. *Current History*, 104(681):153–161, May 2005.

[2] Devabhaktuni Srikrishna, Amalavoyal Narasimha Chari, and Thomas Tisch. Nuclear detection: History and facts. Technical report, January 2008.

[3] Jonathan Medalia. *Nuclear Terrorism: A Brief Review of Threats and Responses*. Congressional Research Service, February 2005.

[4] Department of Homeland Security. National technical nuclear forensics center. http://www.dhs.gov/national-technical-nuclear-forensics-center.

[5] J. Miller. *Analytical Inverse Model for Post-Event Attribution of Plutonium*. PhD thesis, Texas A & M University, Colle, December 2008.

[6] Nuclear forensics and attribution. http://www.dtra.mil/missions/NuclearDetectionForensics/Forensics.aspx.

[7] Dr. Y. Nuclear forensics | ScienceWonk. https://www.fas.org/blogs/sciencewonk/2012/04/nuclear-forensics/, April 2012.

[8] 111th Congress. Public law 111-140, February 2010.

[9] M.R. Scott. *Nuclear forensics: attributing the source of spent fuel used in an RDD event*. PhD thesis, Texas A & M University, College Station, TX, May 2005.

[10] William Dunlop and Harold Smith. Who did it? using international forensics to detect and deter nuclear terrorism. *Arms Control Today*, 36(8):6–10, October 2006.

[11] Matthew Allen. Nuclear forensics: How strong is the new foundation of nuclear deterrence?, 2007.

[12] Gene Aloise. Nuclear forensics: Comprehensive interagency plan needed to address human capital issues. Technical Report GAO-09-527R, Government Accountability Office, Washington, DC, April 2009.

[13] Chemical Office of the Assistant Secretary of Defense for Nuclear and Biological Defense Programs. *The Nuclear Matters Handbook*. Office of the Assistant Secretary of Defense for Nuclear, Chemical, and Biological Defense Programs, Washington, DC, 2011.

[14] Alexander Glaser and Tom Bielefeld. Nuclear forensics capabilities, limits, and the "CSI effect", July 2008.

[15] Michael May, Reza Abedin-Zadeh, Donald Barr, Albert Carnesale, Philip E. Coyle, Jay Davis, William Dorland, William Dunlop, Steve Fetter, Alexander Glaser, Ian D. Hutcheson, Francis Slakey, and Benn Tannenbaum. *Nuclear Forensics Role, State of the Art, and Program Needs*. American Association for the Advancement of Science, Washington, DC, 2008.

[16] Committee on Nuclear Forensics; National Research Council. *Nuclear Forensics:A Capability at Risk (Abbreviated Version)*. The National Academies Press, Washington, DC, 2010.

[17] Iulia Iliut. Nuclear forensics: Key to ensuring nuclear security. http://www.iaea.org/newscenter/news/2012/nuclearforensics.html, April 2012.

[18] Preventing Nuclear Smuggling Program. Nuclear forensics attribution terms, 2012.

[19] A.W. Ajlouni, Y.S. Almasa'efa, and M. Abdelsalam. Nuclear fission products: From source to environment. *Journal of Environmental Science and Technology*, 3(4):182–194, April 2010.

[20] A. J. Fahey, C. J. Zeissler, D. E. Newbury, J. Davis, and R. M. Lindstrom. Postdetonation nuclear debris for attribution. *Proceedings of the National Academy of Sciences*, November 2010.

[21] Suraya Omar. Nuclear forensics and attribution. Technical report, Stanford University, Stanford, CA, March 2012.

[22] G. Nicolaou. Identification of unknown irradiated nuclear fuel through its fission product content. *Journal of Radioanalytical and Nuclear Chemistry*, 279(2):503–508, February 2009.

[23] Kenton J. Moody, Ian D. Hutcheon, and Patrick M. Grant. *Nuclear Forensic Analysis*. CRC Press, Boca Raton, FL, 2005.

[24] Reza Abedin-Zadeh. *Nuclear Forensics Support*. Vienna, Austria, 2006.

[25] K. Mayer, M. Wallenius, and T. Fanghnel. Nuclear forensic scienceFrom cradle to maturity. *Journal of Alloys and Compounds*, 444445:50–56, October 2007.

[26] W.E. Grummitt and G. Wilkinson. Fission products of u^{235} : Abstract : Nature. *Nature*, 158:163, August 1946.

[27] U.S. Department of Energy. Uranium-235 fission yield vs. mass number. http://nuclearpowertraining.tpub.com/h1019v1/css/h1019v1_81.htm.

[28] Rod Adams. Another isotope has been found at minute concentrations at the vermont yankee leak site. http://atomicinsights.com/2010/04/another-isotope-has-been-found-at-minute-concentrations-at-the-vermont-yankee-leak-site.html, April 2010.

[29] G. P. Ford, J. S. Gilmore, D. P. Ames, J. P. Balagna, J. W. Barnes, A. A. Comstock, G. A. Cowan, P. B. Elkin, D. C. Hoffman, G. W. Knobeloch, E. J. Lang, M. A. Melnick, C. O. Minkkinen, B. D. Pollock, J. E. Sattizshn, C. W. Stanley, and B. Warren. Mass yields from fission by neutrons between thermal and 14.7 MeV. Technical report, Los Alamos National Laboratory, Los Alamos, NM, February 1956.

[30] Bin Li. Analysis of fission products a method for verification of a CTBT during OnSite inspections. *Science & Global Security*, 7(2):195–207, 1998.

[31] David Hamilton. Case study: Fission yield module and the oklo nuclear geyser, September 2006.

[32] J. H. Warren. Fission product security problem. Technical report, U.S. Atomic Energy Commission, Richland, WA, February 1964.

[33] Carl R. Nave. Nuclear fission fragments. http://hyperphysics.phy-astr.gsu.edu/hbase/nucene/fisfrag.html, 2012.

[34] G. F. Knoll. *G. F. Knoll's Radiation Detection 3rd (Third) edition(Radiation Detection and Measurement [Hardcover].* John Wiley & Sons, Inc., Hoboken, NJ, 3rd edition edition, 2000.

[35] E. T. Jurney, P. J. Bendt, and T. R. England. Fission product gamma spectra. Informal Report LA-7620-MS, January 1979.

[36] K. Way, E. P. Wigner, and U.S. Atomic Energy Commission. *Radiation from fission products.* United States Atomic Energy Commission. MDDC-48. Technical Information Division, Atomic Energy Commission, Oak Ridge, TN, 1946.

[37] R.E. Marrs, E.B. Norman, J.T. Burke, R.A. Macri, H.A. Shugart, E. Browne, and A.R. Smith. Fission-product gamma-ray line pairs sensitive to fissile material and neutron energy. *Nuclear Instruments and Methods in Physics Research Section A: Accelerators, Spectrometers, Detectors and Associated Equipment*, 592(3):463–471, 2008.

[38] European Atomic Energy Community. Nuclide explorer. http://www.nucleonica.net/Application/NuclideExplorerForm.aspx, 2012.

[39] International Atomic Energy Agency. Compilation and evaluation of fission yield nuclear data. Technical Report IAEA-TECDOC-1168, International Atomic Energy Agency, Vienna, Austria, December 2000.

[40] John R. Lamarsh and Anthony J. Baratta. *Introduction to Nuclear Engineering.* Prentice-Hall, Inc., Upper Saddle River, NJ, 3rd edition edition, 2001.

[41] Kaye & Laby Online. Nuclear fission 4.7.1. http://www.kayelaby.npl.co.uk/atomic_and_nuclear_physics/4_7/4_7_1.html, 2012.

[42] Ian Rittersdorf. Gamma ray spectroscopy. Technical report, University of Michigan, Ann Arbor, MI, May 2007.

[43] T.R. England and B.F. Rider. ENDF-349 evaluation and compilation of fission product yields 1993, October 1994.

[44] W. Meinke. Certificate of analysis standard reference material 953 neutron density monitor wire (Cobalt in aluminum), March 1969.

[45] John Neuhoff. Certificate of analysis CRM 129-a uranium oxide (U_3O_8) assay and isotopic standard, November 2003.

[46] Nuclear Data Center. Table of nuclides. http://atom.kaeri.re.kr/, 2000.

[47] Faculty Innovation Center. TRIGA reactor. http://nuclear.engr.utexas.edu/index.php?option=com_content&view=article&id=49&Itemid=55, 2010.

[48] W.B. Wilson, T.R. England, and K.A. Van Riper. Status of CINDER'90 codes and data, 1999.

[49] M.A. Kellett, O. Bersillon, and R.W. Mills. *The JEFF-3.1/-3.1.1 radioactive decay data and fission yields sub-libraries.* Organisation for Economic Co-operation and Development, Issy-les-Moulineaux, France, 2009.

[50] M.I. Taskaeva. Certificate of calibration standard radionuclide source 84310-598 point source in tape on 2 inch aluminum ring, May 2011.

Vita

Christopher Hing Lu was born in Wheat Ridge, Colorado, the son of David Trunghuu Lu and Hazel Jean Lu and brother of Desiree Yun Alvarado (née Lu). He enlisted in the United States Navy after high school in the Naval Nuclear Propulsion Program. Having been selected for the Seaman to Admiral-21 commissioning program, he received a Bachelor of Science in Physics with a concentration in Nuclear and Radiation Physics from The University of Texas at Austin (UT) in 2010, and subsequently received a commission as a U.S. Naval Officer. Christopher continued in the nuclear propulsion pipeline until he was honorably discharged from the Navy in 2011, at which point he went back to UT to pursue a graduate degree in Nuclear Engineering.

Email address: christopher.h.lu@gmail.com

This thesis was typeset with LaTeX[†] by the author.

[†] LaTeX is a document preparation system developed by Leslie Lamport as a special version of Donald Knuth's TeX Program.